
Final Report

2019 Update to the Site-Specific Seismic Hazard Analyses and Development of Seismic Design Ground Motions for Stanford University



Prepared for:

Stanford University
Land, Buildings and Real Estate
415 Broadway, Third Floor
Redwood City, CA 94063

Prepared by:

Lettis Consultants International, Inc.
Patricia Thomas and Ivan Wong
1000 Burnett Ave., Suite 350
Concord, CA 94520

and

Pacific Engineering and Analysis
Walt Silva and Robert Darragh
856 Seaview Dr.
El Cerrito, CA 94530



15 January 2020



EARTH SCIENCE CONSULTANTS

Lettis Consultants International, Inc.
1000 Burnett Avenue, Suite 350
Concord, CA 94520
(925) 482-0360; fax (925) 482-0361

15 January 2020

Ms. Michelle DeWan
Associate Director, Project Manager
Stanford University
Land, Buildings and Real Estate
Redwood City, CA 94063

Mr. Harry Jones, II, SE
Stanford Seismic Advisory Committee
DCI Engineers
131 17th St., Suite 605
Denver, CO 80202

**SUBJECT: 2019 Update of the Site-Specific Seismic Hazard Analyses and Seismic Design
Ground Motions for Stanford University, Stanford, California**
LCI Project No. 1834.0000

Dear Ms. DeWan and Mr. Jones,

Lettis Consultants International, Inc. (LCI) is pleased to submit this report that presents our final site-specific seismic hazard results and seismic design ground motions for the Stanford campus. It has been our pleasure to work with the Stanford Seismic Advisory Committee and Stanford University on this project. Please do not hesitate to contact us with any questions or comments that you may have regarding this report. You may contact us directly at (925) 482-0360.

Respectfully,

Patricia Thomas, Ph.D., Senior Engineering Seismologist
thomas@lettisci.com

Ivan Wong, Senior Principal Seismologist
wong@lettisci.com



TABLE OF CONTENTS

EXECUTIVE SUMMARY

1.0	Introduction	9
1.1	Background and Purpose.....	9
1.2	Acknowledgements.....	9
2.0	Inputs to Hazard Analyses.....	10
2.1	Seismic Sources	10
2.1.1	Fault Sources.....	10
2.1.2	Crustal Background Earthquakes.....	11
2.2	Ground Motion Models.....	12
3.0	Reference Rock Seismic Hazard Results	14
3.1	PSHA Results	14
3.2	DSHA Results.....	15
4.0	Site Response Analysis.....	16
4.1	Site Response Methodology	16
4.2	Site Response Inputs.....	17
4.3	Site Response Results.....	18
5.0	Site-Specific Design Ground Motions	21
5.1	Site-Specific Horizontal MCE_R and DE Spectra.....	21
5.2	Site-Specific Vertical MCE_R and DE Spectra.....	23
5.3	Comparison with ASCE 7-16 MCE_R and DE Spectra	24
5.4	Comparison with 2013 Site-Specific Spectra.....	24
6.0	Recommendations for Time Histories.....	25
7.0	References Cited.....	26



LIST OF TABLES

Table ES-1. Site-Specific Horizontal and Vertical $MCE_R/BSE-2N$ and $DE/BSE-1N$ Spectra for Zone 0.....	3
Table ES-2. Site-Specific Horizontal and Vertical $MCE_R/BSE-2N$ and $DE/BSE-1N$ Spectra for Zone 1.....	4
Table ES-3. Site-Specific Horizontal and Vertical $MCE_R/BSE-2N$ and $DE/BSE-1N$ Spectra for Zone 2.....	5
Table ES-4. Site-Specific Horizontal and Vertical $MCE_R/BSE-2N$ and $DE/BSE-1N$ Spectra for Zone 3.....	6
Table ES-5. Site-Specific Spectral Acceleration Parameters.....	6
Table 1. Magnitude and Distance Deaggregation.....	29
Table 2. Inputs for DSHA	30

LIST OF FIGURES

Figure ES-1. Site-Specific Horizontal and Vertical $MCE_R/BSE-2N$ Response Spectra for Zones 0, 1, 2 and 3	
Figure ES-2. Site-Specific Horizontal and Vertical $DE/BSE-1N$ Response Spectra for Zones 0, 1, 2 and 3	
Figure 1. Historical Seismicity ($M > 3.0$, 1800 – 2019) and Quaternary Faults in the San Francisco Bay Region	
Figure 2. Design Ground Motion Zones	
Figure 3. Seismic Hazard Curves for Peak Horizontal Acceleration for Zone 0 and $V_{S30} 760$ m/sec	
Figure 4. Seismic Hazard Curves for 0.2 Sec Horizontal Spectral Acceleration for Zone 0 and $V_{S30} 760$ m/sec	
Figure 5. Seismic Hazard Curves for 1.0 Sec Horizontal Spectral Acceleration for Zone 0 and $V_{S30} 760$ m/sec	
Figure 6. Seismic Source Contributions to Peak Horizontal Acceleration for Zone 0 and $V_{S30} 760$ m/sec	
Figure 7. Seismic Source Fractional Contributions to Peak Horizontal Acceleration for Zone 0 and $V_{S30} 760$ m/sec	
Figure 8. Seismic Source Contributions to 0.2 Sec Horizontal Spectral Acceleration for Zone 0 and $V_{S30} 760$ m/sec	
Figure 9. Seismic Source Fractional Contributions to 0.2 Sec Horizontal Spectral Acceleration for Zone 0 and $V_{S30} 760$ m/sec	
Figure 10. Seismic Source Contributions to 1.0 Sec Horizontal Spectral Acceleration for Zone 0 and $V_{S30} 760$ m/sec	
Figure 11. Seismic Source Fractional Contributions to 1.0 Sec Horizontal Spectral Acceleration for Zone 0 and $V_{S30} 760$ m/sec	

- Figure 12. Magnitude, Distance, and Epsilon Contributions to the Mean Peak Horizontal Acceleration Hazard at 2,475-Year Return Period for Zone 0 and V_{S30} 760 m/sec
- Figure 13. Magnitude, Distance, and Epsilon Contributions to the Mean 0.2 Sec Horizontal Spectral Acceleration Hazard at 2,475-Year Return Period for Zone 0 and V_{S30} 760 m/sec
- Figure 14. Magnitude, Distance, and Epsilon Contributions to the Mean 1.0 Sec Horizontal Spectral Acceleration Hazard at 2,475-Year Return Period for Zone 0 and V_{S30} 760 m/sec
- Figure 15. Uniform Hazard Response Spectra at a 2,475-Year Return Period for Zones 0, 1, 2 and 3 and V_{S30} 760 m/sec
- Figure 16. Sensitivity of 84th Percentile Deterministic Spectrum to Ground Motion Models Zone 0 and V_{S30} 760 m/sec
- Figure 17. 84th Percentile Deterministic Spectra for **M** 8.0 San Andreas Earthquake for Zones 0, 1, 2 and 3 V_{S30} 760 m/sec
- Figure 18. Comparison of Site-Specific 84th Percentile Deterministic Spectra and Uniform Hazard Response Spectra at a 2,475-Year Return Period for Zones 0, 1, 2 and 3
- Figure 19. Proposed Basecase V_S Profiles for Northcentral/East (Zones 1, 2 and 3)
- Figure 20. Basecase V_S Profiles for West (Zone 0)
- Figure 21. Randomized V_S Profiles for Northcentral/East Basecase P1
- Figure 22. Sample of Site-Specific Amplification Factors for Northcentral/East (Zones 1, 2, and 3), Preferred V_S Basecases P1, P4 and P7
- Figure 23. Sample of Site-Specific Amplification Factors for West (Zone 0), Preferred V_S Basecases P1, P4 and P7
- Figure 24. Site-Specific 5%-Damped, Horizontal Uniform Hazard Spectra at 2,475-Year Return Period for all Zones
- Figure 25. Site-Specific 5%-Damped, Horizontal 84th Percentile Deterministic Spectra for all Zones
- Figure 26. Calculation of Site-Specific Deterministic Horizontal MCE Spectrum as per ASCE 7-16, Chapter 21 for Zone 0
- Figure 27. Calculation of Site-Specific Probabilistic Horizontal MCE_R Spectrum as per ASCE 7-16, Chapter 21 for Zone 0
- Figure 28. Site-Specific Horizontal MCE_R Spectrum as per ASCE 7-16, Chapter 21 for Zone 0
- Figure 29. Site-Specific Horizontal DE Spectrum as per ASCE 7-16, Chapter 21 for Zone 0
- Figure 30. Calculation of Site-Specific Deterministic Horizontal MCE Spectrum as per ASCE 7-16, Chapter 21 for Zone 1
- Figure 31. Calculation of Site-Specific Probabilistic Horizontal MCE_R Spectrum as per ASCE 7-16, Chapter 21 for Zone 1
- Figure 32. Site-Specific Horizontal MCE_R Spectrum as per ASCE 7-16, Chapter 21 for Zone 1
- Figure 33. Site-Specific Horizontal DE Spectrum as per ASCE 7-16, Chapter 21 for Zone 1
- Figure 34. Calculation of Site-Specific Vertical MCE_R for Zone 0

- Figure 35. Site-Specific Horizontal and Vertical MCE_R Response Spectra for Zones 0, 1, 2 and 3
- Figure 36. Site-Specific Horizontal and Vertical DE Response Spectra for Zones 0, 1, 2 and 3
- Figure 37. Comparison of Site-Specific Horizontal MCE_R for Zone 0 with ASCE 7-16 MCE_R for Site Classes C and D
- Figure 38. Comparison of Site-Specific DE Spectrum for Zone 0 with ASCE 7-16 DE for Site Classes C and D
- Figure 39. Comparison of Site-Specific Horizontal MCE_R for Zone 1 with ASCE 7-16 MCE_R for Site Classes C and D
- Figure 40. Comparison of Site-Specific DE Spectrum for Zone 1 with ASCE 7-16 DE for Site Classes C and D
- Figure 41. Comparison of Site-Specific MCE_R Spectrum for Zone 2 with ASCE 7-16 MCE_R for Site Classes C and D
- Figure 42. Comparison of Site-Specific DE Spectrum for Zone 2 with ASCE 7-16 DE for Site Classes C and D
- Figure 43. Comparison of Site-Specific MCE_R Spectrum for Zone 3 with ASCE 7-16 MCE_R for Site Class D
- Figure 44. Comparison of Site-Specific DE Spectrum for Zone 3 with ASCE 7-16 DE for Site Class D
- Figure 45. Comparison of Site-Specific Horizontal MCE_R and DE Spectra for Zone 0 with 2013 Site-Specific MCE_R and DE Spectra
- Figure 46. Comparison of Site-Specific Horizontal MCE_R and DE Spectra for Zone 1 with 2013 Site-Specific MCE_R and DE Spectra
- Figure 47. Comparison of Site-Specific Horizontal MCE_R and DE Spectra for Zone 2 with 2013 Site-Specific MCE_R and DE Spectra
- Figure 48. Comparison of Site-Specific Horizontal MCE_R and DE Spectra for Zone 3 with 2013 Site-Specific MCE_R and DE Spectra
- Figure 49. Comparison of MCE_R Spectra for Site Classes C and D for Zone 1 using ASCE 7-10 and ASCE 7-16

EXECUTIVE SUMMARY

Stanford University is located about 6 km of the San Andreas fault within in the seismically active San Francisco Bay region. The campus spans approximately 8,200 acres and contains with numerous buildings, facilities, and structures. Stanford University's *Engineering and Architectural Seismic Design Guidelines* (EASDG) were developed in collaboration with the Seismic Advisory Committee (SAC) which serves to help ensure consistency in the application of engineering guidelines on Stanford projects (Stanford Land, Buildings and Real Estate, October 2019). The EASDG outlines performance objectives, earthquake loading levels and criteria, as well as seismic evaluation procedures for both seismic retrofit of existing buildings and design of new facilities. The EASDG contains site-specific design ground motions for the campus, which are periodically updated to account for revised design standards and or advances in earthquake engineering.

The objective of this study was to update the 2013 seismic hazard evaluation of the Stanford campus performed by URS Corporation (Thomas *et al.*, 2013) and to revise the campus-wide seismic design response spectra contained in the EASDG. In the 2013 study, site-specific probabilistic seismic hazard analysis (PSHA) and deterministic seismic hazard analysis (DSHA) were performed. Site response analyses were also performed to account for the effects of the near-surface geology beneath the Stanford campus. Based on the results of these analyses seismic design response spectra were developed following the standards of ASCE 7-10 *Minimum Design Loads for Buildings and Other Structures* and ASCE 41-13 *Seismic Rehabilitation of Existing Buildings*. Seismic design response spectra were developed for four zones (Zones 0, 1, 2 and 3), where zone boundaries were based on the near-surface geology and the variation of deterministic ground motions across campus.

Since the 2013 study, an update to ASCE 7 (ASCE 7-16) has been released and adopted by the 2019 California Building Code (CBC). As a result, the existing seismic design spectra for Stanford University require revision to meet the criteria of ASCE 7-16. In addition, new depth to bedrock information is available from the recent Escondido Village Graduate Housing Project, which improved the characterization of the depth to bedrock across campus.

As part of this study, updated site-specific PSHA, DSHA and site response analysis were performed to develop site-specific ground motions for each of the four zones. Based on a review of available shear-wave velocity (V_s) measurements and geotechnical information, including data from the Escondido Village Graduate Housing Project, the inputs to the site response analyses have been revised since the 2013 study. Based on the revised site-specific ground motions, seismic design spectra were developed in accordance with ASCE 7-16. Site-specific risk-adjusted Maximum Considered Earthquake (MCE_R) and Design Earthquake (DE) response spectra along with acceleration response parameters S_{DS} , S_{D1} , S_{MS} , and S_{M1} were developed following ASCE 7-16, Chapter 21. MCE_R and DE response spectra are equivalent to ASCE 41-17 Basic Safety Earthquake (BSE)-2N and BSE-1N. Stanford Seismic Design Guidelines do not permit the use of the lower ground motions BSE-2E and BSE-1E for existing



buildings as allowed by ASCE 41-17; instead, all buildings use MCE_R /BSE-2N and DE/BSE-1N spectra with reduced acceptable building performance levels for existing buildings relative to new buildings. Hence, BSE-2E and BSE-1E spectra are not presented in this report. Corresponding vertical seismic design spectra were developed using the site-specific V/H factors of Gulerce and Abrahamson (2011) and the criteria of ASCE 7-16.

Figures ES-1 and ES-2 show the updated horizontal and vertical MCE_R and DE response spectra for the four zones. For Zones 1, 2 and 3, ground motions decrease with increasing distance from the San Andreas fault as expected. The site-specific horizontal MCE_R spectra are similar for Zones 1 and 2, which have similar near-surface geology and only slight differences in firm rock ground motions due to differences in distance from the San Andreas fault. Zone 3, the farthest from the San Andreas fault, also has lower short-period (less than 0.5 sec) ground motions due in part to the lack of site class C minimum requirements for this zone where bedrock is deeper. For Zone 0, the site-specific horizontal MCE_R spectrum far exceeds the spectra for other zones in the 0.2 to 0.9 sec period range due to the stiffer soil and shallower bedrock in this western portion of campus, which is also the closest to the San Andreas fault. The site-specific horizontal and vertical MCE_R and DE response spectra are provided in Tables ES-1 to ES-4 for all four zones. Site-specific spectral acceleration design parameters S_{D5} and S_{D1} , calculated in accordance with ASCE 7-16, Section 21.4, are provided in Table ES-5.



Table ES-1. Site-Specific Horizontal and Vertical $MCE_R/BSE-2N$ and $DE/BSE-1N$ Spectra for Zone 0

Zone 0				
Period	Horizontal $MCE_R/BSE-2N$	Vertical $MCE_R/BSE-2N$	Horizontal $DE/BSE-1N$	Vertical $DE/BSE-1N$
(sec)	(g)	(g)	(g)	(g)
0.01	0.96	0.81	0.64	0.54
0.02	1.10	0.95	0.74	0.63
0.03	1.25	1.35	0.83	0.90
0.05	1.54	2.35	1.03	1.57
0.065	1.76	2.92	1.17	1.95
0.075	1.90	2.98	1.27	1.99
0.084	2.03	2.95	1.35	1.97
0.10	2.03	2.61	1.35	1.74
0.15	2.03	2.11	1.35	1.41
0.20	2.03	1.70	1.35	1.13
0.30	2.36	1.26	1.57	0.84
0.40	2.66	1.33	1.77	0.89
0.50	2.33	1.17	1.56	0.78
0.75	1.85	0.93	1.24	0.62
0.90	1.69	0.85	1.13	0.57
1.00	1.63	0.82	1.09	0.55
1.50	1.14	0.57	0.76	0.38
2.00	0.88	0.44	0.59	0.29
3.00	0.51	0.25	0.34	0.17
4.00	0.38	0.19	0.25	0.130
5.00	0.31	0.15	0.20	0.100
7.50	0.20	0.100	0.14	0.067
10.00	0.15	0.076	0.10	0.051



Table ES-2. Site-Specific Horizontal and Vertical $MCE_R/BSE-2N$ and $DE/BSE-1N$ Spectra for Zone 1

Zone 1				
Period	Horizontal $MCE_R/BSE-2N$	Vertical $MCE_R/BSE-2N$	Horizontal $DE/BSE-1N$	Vertical $DE/BSE-1N$
(sec)	(g)	(g)	(g)	(g)
0.01	0.94	0.86	0.63	0.57
0.02	1.09	1.01	0.72	0.67
0.03	1.23	1.46	0.82	0.97
0.05	1.52	2.62	1.01	1.75
0.065	1.73	3.29	1.16	2.19
0.075	1.88	3.38	1.25	2.25
0.083	2.00	3.36	1.33	2.24
0.10	2.00	2.96	1.33	1.97
0.15	2.00	2.12	1.33	1.41
0.20	2.00	1.68	1.33	1.12
0.30	2.00	1.24	1.33	0.83
0.40	2.00	1.00	1.33	0.67
0.417	2.00	1.00	1.33	0.67
0.50	1.75	0.87	1.17	0.58
0.75	1.68	0.84	1.12	0.56
1.00	1.68	0.84	1.12	0.56
1.50	1.30	0.65	0.87	0.43
2.00	1.06	0.53	0.70	0.35
3.00	0.81	0.41	0.54	0.27
4.00	0.65	0.32	0.43	0.21
5.00	0.42	0.21	0.28	0.140
7.50	0.20	0.100	0.13	0.067
10.00	0.15	0.075	0.10	0.050



Table ES-3. Site-Specific Horizontal and Vertical $MCE_R/BSE-2N$ and $DE/BSE-1N$ Spectra for Zone 2

Zone 2				
Period	Horizontal $MCE_R/BSE-2N$	Vertical $MCE_R/BSE-2N$	Horizontal $DE/BSE-1N$	Vertical $DE/BSE-1N$
(sec)	(g)	(g)	(g)	(g)
0.01	0.92	0.83	0.61	0.55
0.02	1.06	0.97	0.70	0.65
0.03	1.19	1.39	0.80	0.93
0.05	1.47	2.48	0.98	1.65
0.065	1.68	3.12	1.12	2.08
0.075	1.82	3.21	1.22	2.14
0.083	1.94	3.18	1.29	2.12
0.10	1.94	2.81	1.29	1.87
0.15	1.94	2.02	1.29	1.35
0.20	1.94	1.63	1.29	1.09
0.30	1.94	1.20	1.29	0.80
0.40	1.94	0.97	1.29	0.65
0.416	1.94	0.97	1.29	0.65
0.50	1.75	0.87	1.16	0.58
0.75	1.66	0.83	1.11	0.55
1.00	1.67	0.83	1.11	0.55
1.50	1.26	0.63	0.84	0.42
2.00	1.02	0.51	0.68	0.34
3.00	0.77	0.39	0.52	0.26
4.00	0.63	0.31	0.42	0.21
5.00	0.40	0.20	0.27	0.13
7.50	0.19	0.10	0.13	0.064
10.00	0.14	0.072	0.10	0.048

Table ES-4. Site-Specific Horizontal and Vertical $MCE_R/BSE-2N$ and $DE/BSE-1N$ Spectra for Zone 3

Zone 3				
Period	Horizontal $MCE_R/BSE-2N$	Vertical $MCE_R/BSE-2N$	Horizontal $DE/BSE-1N$	Vertical $DE/BSE-1N$
(sec)	(g)	(g)	(g)	(g)
0.01	0.66	0.68	0.44	0.45
0.02	0.72	0.68	0.48	0.45
0.03	0.77	0.91	0.51	0.61
0.05	0.87	1.82	0.58	1.210
0.065	0.95	1.82	0.63	1.21
0.075	1.00	1.82	0.67	1.21
0.10	1.13	1.82	0.75	1.21
0.15	1.39	1.82	0.92	1.21
0.18	1.53	1.60	1.02	1.07
0.20	1.53	1.46	1.02	0.98
0.30	1.57	1.08	1.05	0.72
0.40	1.71	0.87	1.14	0.58
0.50	1.65	0.83	1.10	0.55
0.75	1.56	0.78	1.04	0.52
1.00	1.56	0.78	1.04	0.52
1.50	1.19	0.60	0.80	0.40
2.00	0.97	0.49	0.65	0.32
3.00	0.74	0.37	0.49	0.25
4.00	0.60	0.30	0.40	0.20
5.00	0.38	0.19	0.25	0.130
7.50	0.18	0.091	0.12	0.060
10.00	0.14	0.070	0.090	0.050

Table ES-5. Site-Specific Spectral Acceleration Parameters for All Zones

	Zone 0	Zone 1	Zone 2	Zone 3
S_s	2.12	2.08	2.02	1.92
S_1	0.76	0.75	0.72	0.68
S_{DS}, Site-Specific	1.60	1.20	1.16	1.03
S_{D1}, Site-Specific	1.17	1.72	1.68	1.59
S_{MS}, Site-Specific	2.39	1.80	1.75	1.54
S_{M1}, Site-Specific	1.76	2.59	2.51	2.38
PGA_M	0.84	0.82	0.80	0.76

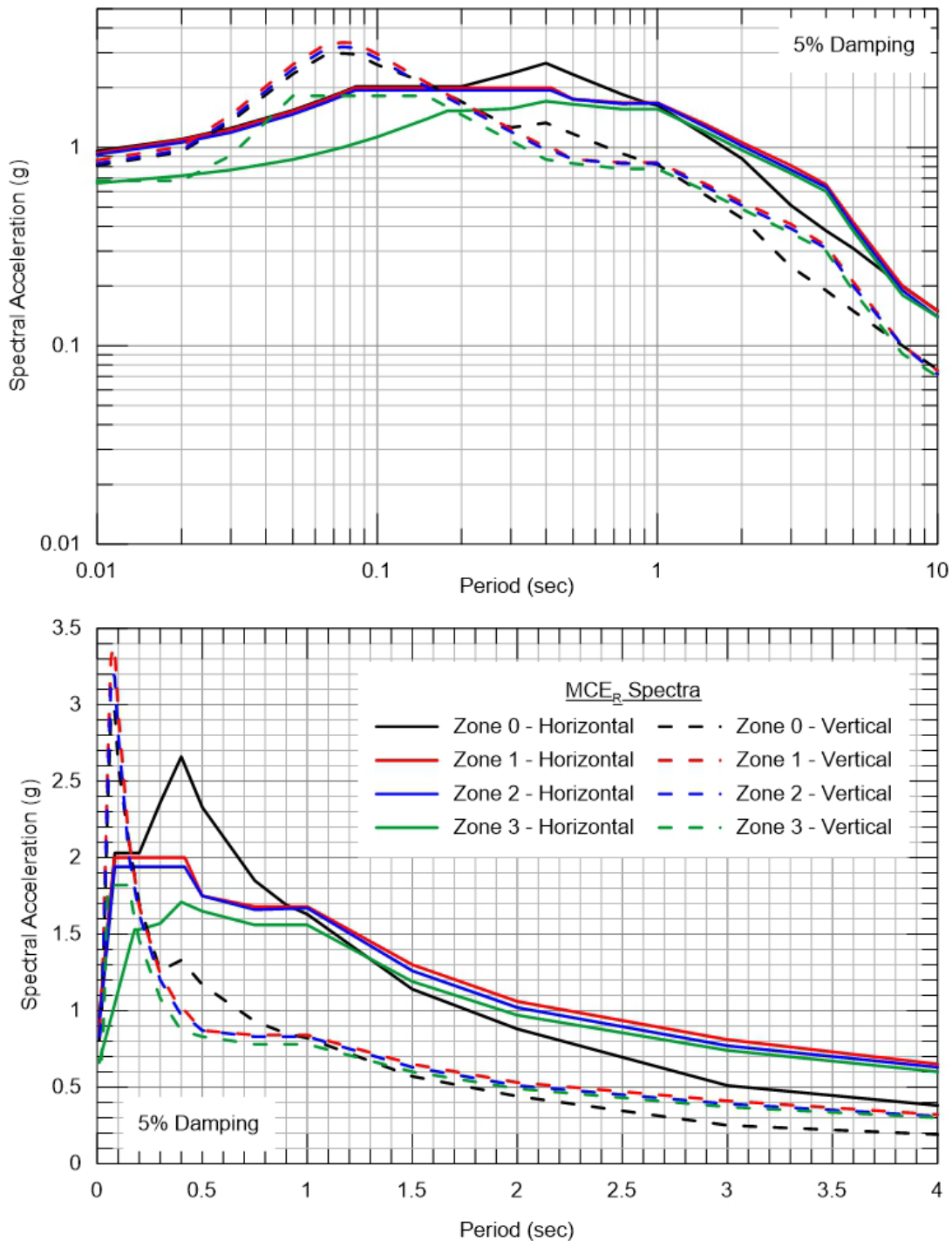


Figure ES-1. Site-Specific Horizontal and Vertical MCE_R/BSE-2N Response Spectra for Zones 0, 1, 2, and 3

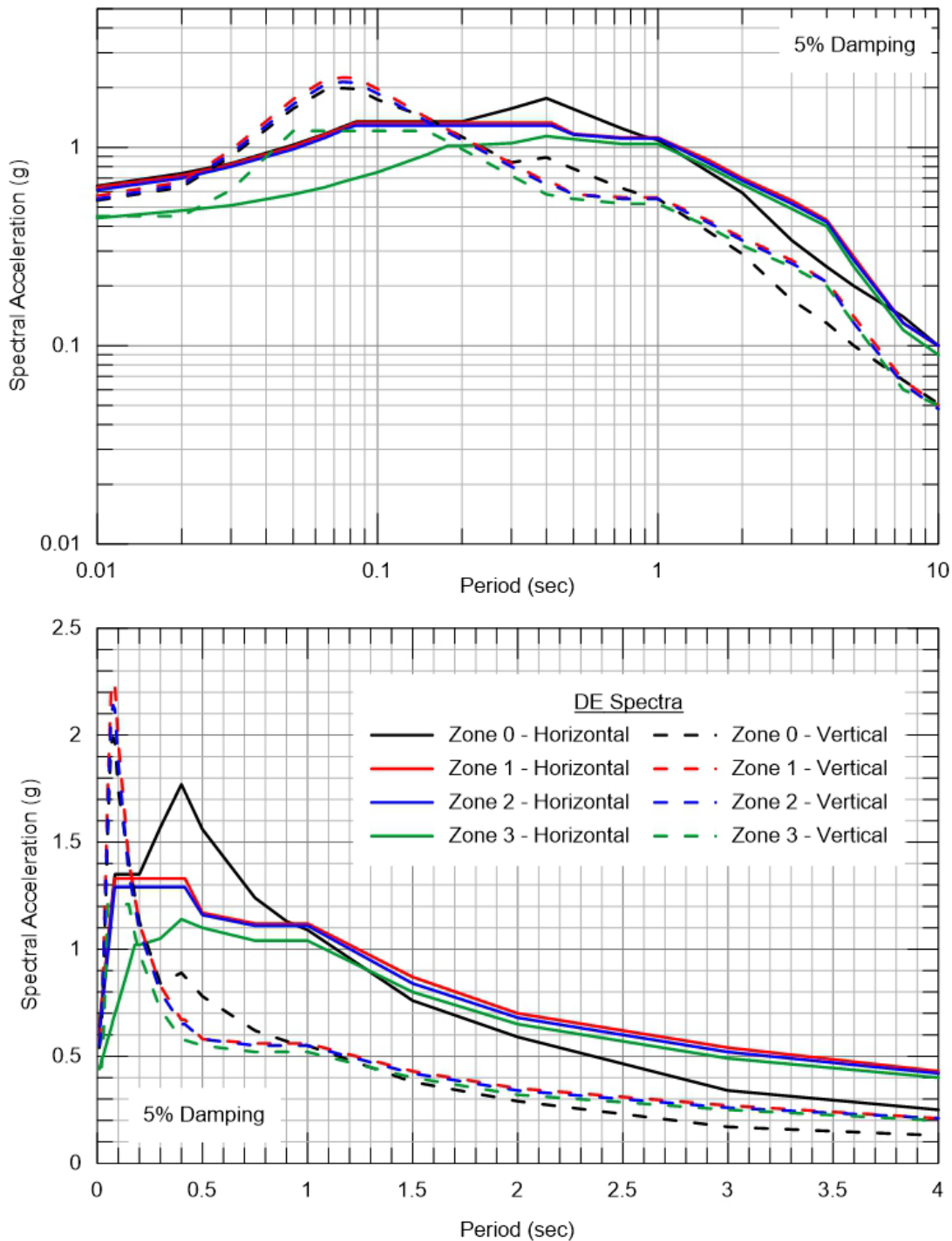


Figure ES-2. Site-Specific Horizontal and Vertical DE/BSE-1N Response Spectra for Zones 0, 1, 2, and 3

1.0 INTRODUCTION

At the request of Stanford University and its Seismic Advisory Committee (SAC), LCI has updated the 2013 seismic hazard evaluation of the campus performed by URS Corporation (Thomas *et al.*, 2013) and updated the campus-wide design ground motions. Stanford University is located within 6 km of the San Andreas fault within the seismically active San Francisco Bay region (Figure 1).

1.1 BACKGROUND AND PURPOSE

In the 2013 study, site-specific probabilistic seismic hazard analysis (PSHA) and deterministic seismic hazard analysis (DSHA) were performed. Site response analyses were also performed to account for the effects of the near-surface geology across Stanford campus. Based on the results of these analyses, seismic design response spectra were developed following the standards of ASCE 7-10 *Minimum Design Loads for Buildings and Other Structures* and ASCE 41-13 *Seismic Rehabilitation of Existing Buildings*. Seismic design response spectra were developed for four Zones (Zones 0, 1, 2 and 3), where Zone boundaries were based on the near-surface geology and the variation of deterministic ground motions across campus (Figure 2).

Since the 2013 study, an update to ASCE 7 (ASCE 7-16) has been released and adopted by the 2019 California Building Code (CBC). As a result, the existing seismic design spectra for Stanford University require revision to meet the criteria of ASCE 7-16. In addition, new depth to bedrock information is available from the recent Escondido Village Graduate Student Housing project, which improved characterization of the depth to bedrock beneath campus.

This report presents the results of an updated site-specific PSHA, DSHA, site response analysis, and the development of seismic design ground motions accordance with ASCE 7-16 for the Stanford campus. Site-specific risk-adjusted Maximum Considered Earthquake (MCE_R) and Design Earthquake (DE) response spectra along with acceleration response parameters S_{DS} , S_{D1} , S_{MS} , and S_{M1} were developed following ASCE 7-16, Chapter 21. MCE_R and DE response spectra are equivalent to ASCE 41-17 Basic Safety Earthquake (BSE)-2N and BSE-1N. The Stanford Seismic Design Guidelines do not permit the use of the lower ground motions BSE-2E and BSE-1E for existing buildings as allowed by ASCE 41-17; instead, all buildings use MCE_R /BSE-2N and DE/BSE-1N spectra with reduced acceptable building performance levels for existing buildings relative to new buildings. Hence, BSE-2E and BSE-1E spectra are not presented in this report. The development of time histories consistent with the seismic design spectra were beyond the scope of this project. However, recommendations for time history development are included in Section 7.

1.2 ACKNOWLEDGEMENTS

This work was performed under a contract with Stanford University. Our sincere thanks to Harry Jones and Michele DeWan for their support and assistance. Our appreciation to Claire Unruh and Whitney Newcomb for their assistance in the preparation of this report.

2.0 INPUTS TO HAZARD ANALYSES

The following section discusses the characterization of the seismic sources and the ground motion models (GMMs) selected and used in the PSHA and DSHA. The PSHA and DSHA were performed for reference rock conditions and the results used as input into the site response analysis (Section 4).

2.1 SEISMIC SOURCES

Seismic source characterization is concerned with three fundamental elements: (1) the identification, location and geometry of significant sources of earthquakes; (2) the maximum size of the earthquakes associated with these sources; and (3) the rate at which the earthquakes occur. The seismic source model includes crustal faults capable of generating large surface-faulting earthquakes (Section 3.1.1), and an areal source Zone, which accounts for background crustal seismicity that cannot be attributed to identified faults explicitly included in the seismic source model (Section 3.1.2).

2.1.1 Fault Sources

The fault model used in this study is adopted from a model originally developed as part of the California Department of Water Resources' Delta Risk Management Strategy Project (Wong *et al.*, 2008). The model is continually updated using the latest available geologic, seismologic, and paleoseismic data and the currently accepted models of fault behavior. Characterizations of the major faults in the San Francisco Bay region, including the San Andreas, Hayward/Rodgers Creek, Concord/Green Valley, San Gregorio, Greenville, and Mt. Diablo thrust faults, are adopted from the 1999 and 2002 Working Groups on California Earthquake Probabilities (WGCEP, 2003). These characterizations were updated based on a review of the recent Uniform California Earthquake Rupture Forecasts, UCERF2 and UCERF3.

Figure 1 shows the locations of the faults relative to the site. The faults included in the PSHA are judged to be at least potentially active and may contribute to the probabilistic hazard because of their maximum earthquakes and/or proximity to the site. The most significant fault to the site is the San Andreas fault.

San Andreas Fault

The dominant active fault in California is the San Andreas fault. The fault extends from the Gulf of California, Mexico, to Point Delgada on the Mendocino Coast in northern California, a total distance of 1,200 km. The San Andreas fault accommodates the majority of the motion between the Pacific and North American plates. This fault is the largest active fault in California and is responsible for the largest known earthquake in northern California, the 1906 **M** 7.9 San Francisco earthquake (Wallace, 1990). Movement on the San Andreas fault is right-lateral strike-slip, with a total offset of some 560 km (Irwin, 1990). Over most of its southern extent, the San Andreas fault is a relatively simple, linear fault trace. Immediately south of the San

Francisco Bay area, however, the fault splits into a number of branch faults or splays, including the Calaveras and Hayward faults. In the San Francisco Bay area, the main trace of the San Andreas fault forms a linear depression along the San Francisco Peninsula, occupied by the Crystal Springs and San Andreas Lake Reservoirs. Geomorphic evidence for Holocene faulting includes fault scarps in Holocene deposits, right-laterally offset streams, shutter ridges, and closed linear depressions (Hall, 1984; Wallace, 1990). The 1906 earthquake resulted from rupture of the fault from San Juan Bautista north along the San Francisco Peninsula, the northern California coast all the way to Point Delgada, a distance of approximately 475 km. The average slip on the fault was 5.1 m in the area north of the Golden Gate and 2.5 m in the Santa Cruz Mountains (WGNCEP, 1996).

Based on differences in geomorphic expression, fault geometry, paleoseismic chronology, slip rate, seismicity, and historical fault ruptures, the San Andreas fault is divided into a number of fault segments. Each of these segments may be capable of rupturing independently or in conjunction with adjacent segments. In the San Francisco Bay area, these segments include the Santa Cruz Mountains, Peninsula, and North Coast segments. Based on the lengths of the fault segments, they are capable of producing estimated mean maximum earthquakes of **M** 7.0, 7.15, and 7.45, respectively (WGCEP, 2003). The 1906 earthquake was the result of rupture of the Offshore (northernmost segment north of Point Arena), North Coast, Peninsula, and Santa Cruz Mountains segments. Two- or three-segment ruptures also may be possible (WGCEP, 2003). We estimate that the maximum earthquakes associated with these potential multi-segment ruptures may range from **M** 7.4 to **M** 7.7.

WGCEP (2003) assigns a mean recurrence interval of 378 years to a **M** 7.9 1906-type event on the San Andreas fault with a large uncertainty. WGCEP (2014) estimate a 72% probability of occurrence of one or more **M** 6.7 or larger earthquakes the San Francisco Bay region in the time period between 2014 and 2043 with a probability of 22% for the San Andreas fault.

2.1.2 Crustal Background Earthquakes

To account for the hazard from background (floating or random) earthquakes that are not associated with known or mapped faults, regional seismic source Zones are used in the PSHA. In most of the western U.S., the maximum magnitude of earthquakes not associated with known faults usually ranges from **M** 6 to 6½ (e.g., dePolo, 1994). Repeated events larger than these magnitudes generally produce recognizable fault-or-fold related features at the earth's surface. Examples of background earthquakes are the 1989 **M** 6.9 Loma Prieta, the 1986 **M** 5.7 Mt. Lewis, and the 31 October 2007 **M** 5.6 Alum Rock earthquakes, with the latter two having occurred east of San Jose and resulted in no discernable surface rupture.

Earthquake recurrence estimates of the background seismicity within each seismic source Zone are required. The site region is divided into two regional seismic source Zones: the Coast Ranges and Central Valley. The recurrence parameters for the Coast Ranges source Zone are adopted from Youngs *et al.* (1992). They calculated values for background earthquakes based on the historical seismicity record after removing earthquakes within 10-km-wide

corridors along each of the major faults. The recurrence values for the Central Valley Zone are adopted from URS Corporation/Jack Benjamin & Associates (2007). Maximum earthquakes for both Zones of $M 6.5 \pm 0.3$ are used in the PSHA.

2.2 GROUND MOTION MODELS

To estimate the ground motions for crustal earthquakes in the PSHA and DSHA, we have used GMMs appropriate for tectonically active crustal regions. The models, developed as part of the NGA-West2 Project sponsored by PEER Center Lifelines Program, were published in 2014. The NGA-West2 GMMs by Chiou and Youngs (2014), Campbell and Bozorgnia (2014), Abrahamson *et al.* (2014), and Boore *et al.* (2014) were used in the PSHA and DSHA. The models were weighted equally in the hazard analyses.

The NGA-West2 GMMs use the parameter V_{s30} (time-averaged shear-wave velocity in the top 30 m) as a proxy for site effects. The V_{s30} model or soils within the NGA-West2 GMMs are generally based on deep soil profiles that are not representative of the shallow soil over rock beneath campus (see Section 4.2). As a result, a site response analysis (Section 4) was performed to model near-surface ground motion effects including soil nonlinearity expected at the site. The PSHA and DSHA were performed for a firm rock V_{s30} value of 760 m/sec. As part of the site response analysis (Section 5), amplification functions were developed for the ground surface relative to the V_{s30} of 760 m/sec.

Other input parameters for the NGA-West2 GMMs include $Z_{2.5}$, the depth to the V_s of 2.5 km/sec (a proxy for basin effects), which is only used in one model, Campbell and Bozorgnia (2014). In addition, Abrahamson *et al.* (2014), Boore *et al.* (2014) and Chiou and Youngs (2014) use $Z_{1.0}$, the depth to the V_s of 1.0 km/sec. Consistent with the reference 760 m/sec profile used in the site response analysis, the default $Z_{1.0}$ and $Z_{2.5}$ based on the equations provided by the NGA-West2 developers were used in the PSHA and DSHA. Other parameters such as depth to the top of rupture (zero for all faults with surface expression unless specified otherwise), dip angle, rupture width, and aspect ratio were specified for each fault or calculated within the PSHA code.

Rupture directivity was incorporated using the model of Bayless and Somerville (Spudich *et al.*, 2013) in the development of the seismic design ground motions. As described in Section 6, the predicted fault-normal ground motions were compared to the maximum direction factors applied in development of the seismic design spectra. In accordance with ASCE 7-16 for near-field sites, time histories should be rotated to fault-normal and fault-parallel and a proportion of the time histories should include velocity pulses (Section 6).

As noted by Al Atik and Youngs (2014), the development of the NGA-West2 models was a collaborative effort with many interactions and exchanges of ideas among the developers. The developers indicated that additional epistemic uncertainty needs to be incorporated into the median ground motions in order to more fully represent an appropriate level of epistemic uncertainty. Hence, for each of the four NGA-West2 models, additional epistemic uncertainty on the median ground motion was included. The three-point distribution and model of Al Atik and

Youngs (2014) was applied. The model is a function of magnitude, style of faulting, and spectral period.

3.0 REFERENCE ROCK SEISMIC HAZARD RESULTS

The hazard results for the V_{s30} of 760 m/sec are described below and shown in Figures 3 to 17. These ground motions are input to the site response analysis to develop site-specific ground motions for each Zone (Section 4).

3.1 PSHA RESULTS

The PSHA was performed for a single site in each of the four Zones, with each of the sites selected to capture the largest ground motions within each Zone (Thomas *et al.*, 2013). The results of the PSHA are presented in terms of ground motion as a function of annual exceedance frequency (AEF). AEF is the reciprocal of the average return period. Figure 3 shows the mean, median (50th percentile), 5th, 15th, 85th, and 95th percentile hazard curves for peak horizontal ground acceleration (PGA) for Zone 0. Results for Zones 1 to 3 are similar. The range of uncertainty between the 5th and 95th percentile (fractiles) is about a factor of 1.9 at a return period of 2,475 years. These fractiles indicate the range of epistemic uncertainty about the mean hazard. The 0.2 and 1.0 sec horizontal spectral acceleration (SA) hazard curves are shown on Figures 4 and 5.

The contributions of the various seismic sources to the mean PGA, 0.2 and 1.0 sec SA hazard for Zone 0 are shown on Figures 6 to 11. Figure 6 shows the hazard curves for the most significant seismic sources as well as the total hazard, and Figure 7 shows a fractional contribution plot by source. As expected the hazard for all three spectral periods is dominated by the nearby San Andreas fault.

The hazard can also be deaggregated in terms of the joint magnitude-distance-epsilon probability conditional on the ground motion parameter (PGA or SA exceeding a specific value). Epsilon is the difference between the logarithm of the ground motion amplitude and the mean logarithm of ground motion (for that M and R) measured in units of standard deviation (ϵ). Thus positive epsilons indicate larger than average ground motions. By deaggregating the PGA and 1.0 sec SA hazard by magnitude, distance and epsilon bins, we can illustrate the contributions by events at various periods. Figures 12 to 14 illustrate the contributions by events for the 2,475-year return period. At PGA, events of M 6.6 to M 8.2 within 10 km of campus (San Andreas fault) dominate the hazard (Figure 12). The results are similar for 0.2 and 1.0 sec SA, with an increase in the contribution of M 7.6 to M 8.2 events to the 1.0 sec SA hazard (Figures 13 and 14).

Based on the magnitude and distance bins (Figures 12 to 14), the controlling earthquakes as defined by the mean magnitude ($M\text{-bar}$) and modal magnitude (M^*) and mean distance ($D\text{-bar}$) and modal distance (D^*) can be calculated. Figures 12 to 14 and Table 1 provide the $M\text{-bar}$, M^* , $D\text{-bar}$, and D^* at the 2,475-year return period for PGA, 0.2 and 1.0 sec horizontal SA. The mean magnitude and distance contributing to the PGA and 0.2 sec SA hazard is M 7.2 at 7.6 km (Figures 12 and 13). At 1.0 sec, the magnitude increases to a M 7.4 (Figure 14).

In Figure 15, the UHS at a 2,475-year return period are shown for the four Zones. A UHS depicts the ground motions at all spectral periods with the same annual exceedance frequency or return period. These UHS reflect the geometric mean of expected horizontal ground motions for each Zone for a V_{s30} 760 m/sec, as predicted by the NGA-West2 models. As expected, the ground motions are similar and decrease slightly with increasing distance from the San Andreas fault.

3.2 DSHA RESULTS

The controlling seismic source for the Stanford campus is the San Andreas fault (Figure 1). Figure 16 shows the 84th percentile, 5%-damped horizontal acceleration response spectra from each of the GMMs and the geometric mean horizontal spectrum for Zone 0. The range in these spectra represent the epistemic uncertainty in the ground motion from the **M** 8.0 scenario event. The geometric mean 84th percentile, 5%-damped horizontal acceleration response spectra for all Zones are shown on Figure 17. Table 2 provides the DSHA inputs for reference rock (V_{s30} 760 m/sec), respectively.

Figure 18 shows comparisons of the horizontal geometric mean deterministic spectra with the 2,475-year return period UHS. As expected for a region with numerous high slip rate faults, the 2,475-year return period UHS exceeds the 84th percentile spectra for periods less than 7.5 sec (Figure 18).

4.0 SITE RESPONSE ANALYSIS

A site response analysis was performed to model site effects of the near-surface materials on the ground motions. This section describes the site response methodology, inputs and resulting probabilistic and deterministic ground motions.

4.1 SITE RESPONSE METHODOLOGY

To compute the ground motions at the ground surface, the results of the PSHA and DSHA are modified using a site-response model. The conventional site response approach in quantifying the effects of soil and other unconsolidated sediments on strong ground motions involves the use of time histories compatible with the specified outcrop response spectra to serve as control (input) motions. The control motions are then used to drive a nonlinear computational formulation to transmit the motions through the profile.

The computational formulation that has been most widely employed to evaluate 1D site response assumes vertically-propagating plane S-waves. Departures of soil response from a linear constitutive relation are treated in an approximate manner through the use of the equivalent-linear formulation. The equivalent-linear formulation, in its present form, was introduced by Idriss and Seed (1968). A stepwise analysis approach was formalized into a 1D, vertically propagating S-wave code called SHAKE (Schnabel *et al.*, 1972). Subsequently, this code has become the most widely used and validated analysis package for 1D site response calculations.

The computational scheme employed to compute the amplification factors in this study uses an alternative approach employing random vibration theory (RVT) (Silva and Lee, 1987; Silva *et al.*, 1997; Appendix D in McGuire *et al.*, 2001). In this approach, as embodied in the computer program RASCALS, the control motion power spectrum is propagated through the 1D soil profile using the plane-wave propagators of Silva (1976). The power spectrum uses the magnitude of the controlling earthquake determined from the deaggregation of the UHS or from the DSHA. A range of distances (corresponding to 11 g level from 0.01 to 1.50 g) are also used in the calculation of the amplification functions. In this formulation only SH waves are considered.

The site response analysis was performed using both the 84th percentile deterministic spectrum and the probabilistic hazard curves for each of the Zones. Accordingly, Approaches 1 and 3 (McGuire *et al.*, 2001; Bazzurro and Cornell, 2004) were implemented, respectively. In Approach 1, the weighted mean transfer functions based on randomized soil profiles are applied to each of the reference site 84th percentile deterministic NGA-West2 spectra. In the implementation of Approach 3, the hazard at the soil surface is computed by integrating the site-specific hazard curves at a generic rock or soil level with the probability distribution of the amplification function. Both Approaches 1 and 3 employ the use of frequency-dependent amplification (mean transfer) functions that can account for nonlinearity in soil response.

The use of the full distribution of site amplification factors accommodates site aleatory variability. If the reference rock hazard curves are developed using empirical GMMs with their fully ergodic sigmas, there is some double-counting of variability, as the ergodic sigmas include variability from different input motions in addition to differences in average site factors. For this project, the firm rock hazard was developed using a fully ergodic sigma. Hence, only the mean amplification factors were used in Approach 3 for this project so as to not double count site variability.

4.2 SITE RESPONSE INPUTS

A major input for the site response analysis are shear-wave (V_S) profiles characterizing the near-surface materials across campus. As part of the 2010 URS seismic hazard study for Stanford, V_S data were collected. Specifically, Spectral-Analysis-of-Surface-Waves (SASW) surveys were performed at 15 locations on campus by the University of Texas at Austin under the direction of Dr. Kenneth Stokoe. As described in the 2013 URS study, the resulting V_S profiles were grouped together geographically based on similarities in the profiles and near-surface geology. Three groupings were developed: west campus, north-central campus, and east campus (Figure 3-1 in Thomas *et al.*, 2013). The seismic design Zone 0 corresponds to the west campus region, while Zones 1, 2 and 3 span the north-central and east regions (Figure 2). The lognormal average V_S profiles for the north-central and east campus regions were quite similar and as a result, these regions were combined into a single north-central/east campus region. The SASW surveys provided V_S profiles to depths of approximately 200 to 300 ft. In order to extend these profiles, estimates of depth to bedrock across campus were required. Based on the limited available data, depth to Franciscan rock was assumed to range from 100 to 500 ft for the west campus region. For the north-central/east region, depth to rock was assumed to range from 300 to 500 ft.

In 2016, as part of the Escondido Village Graduate Housing Project, a deep boring was drilled and downhole V_S measurements performed. For this site, bedrock was encountered at 890 ft, much deeper than anticipated in the 2013 URS study. As a result, for this study, basecase V_S profiles for site response analysis used in the 2013 study were revised based on a re-analysis of the available V_S profiles, available geotechnical reports and the new data from the Escondido Village Graduate Housing Project.

Figure 19 provides the updated basecase V_S profiles for the north-central/east region. Three V_S profiles (P1, P4 and P7) represent best-estimate near-surface V_S profile with depths of bedrock of 300, 750, 1,200 ft. For each of these best-estimate V_S profiles, upper and lower-range profiles were developed to account for the epistemic uncertainty in the V_S measurements. Best-estimate, upper and lower-range profiles are weighted 0.4, 0.3, and 0.3 respectively. To account for lateral variability in the depth to bedrock across the north-central/east campus region, the resulting hazard curves from the three depths to bedrock are enveloped. Similarly, Figure 20 provides the revised basecase V_S profiles for west region, where bedrock is assumed to range from 100 to 300 ft.

In the methodology used in this study, the V_s profiles must extend to the depth (8 km) at which the control motion power spectrum is input into the site 1D profiles. The basecase profiles were extended using the deeper portions of the reference mean V_s profile for a V_{s30} of 760 m/sec based on PE&A's V_s profile database (Kamai *et al.*, 2014).

For each of the nine basecase V_s profiles for both regions, 30 randomized V_s profiles were generated using the soil correlation model (Toro, 1996). As an example, Figure 21 shows the 30 randomized profiles for best-estimate V_s profile P1 for the north-central/east region. Associated with each randomized profile is a set of randomized dynamic material property curves. For the dynamic material properties, the EPRI (1993) sand curves (Revision 1) (M1) and Peninsular Range curves (Silva *et al.*, 1997) (M2) were used to cover the possible range of nonlinear soil behavior at the site. The two dynamic material models were weighted equally when combining the site response analyses results obtained from the basecase V_s models.

RASCALS was used to generate control motions and acceleration power response spectra for two earthquakes, **M** 5.0 and **M** 7.0 in order to fully cover the range of events contributing to the hazard. The results from each magnitude are weighted based on the deaggregation results of the firm rock hazard. The events were placed at a suite of distances to produce expected median rock peak accelerations of 0.01, 0.05, 0.10, 0.20, 0.30, 0.40, 0.50, 0.75, 1.00, 1.25 and 1.50 g. This standard suite of input ground motions covers the range of events contributing to the hazard.

4.3 SITE RESPONSE RESULTS

Based on the site response analyses for the 30 V_s profiles for each basecase profile and material properties, a probability distribution of amplification factors was calculated. For each input control motion, mean and standard deviation are computed from the 30 response spectra (from 30 randomized profiles). The mean response spectrum from the 30 convolutions is divided by the mean (log) spectrum for firm rock spectrum to produce the amplification factors. The amplification factors include the effects of the inherent aleatory variability (randomness) of the site properties about each basecase and any possible effects of magnitude of the control motions.

The amplification factors (the ratios of the response spectra at the top of the site profiles to the firm rock profiles) are a function of the firm rock peak acceleration (or SA), spectral frequency, and nonlinear soil response. The linear range of the soil response is from 0.01 to 0.1 g and amplification factors for 0.10 g are used for all lower ground motion levels. At high ground motions, the 1D equivalent-linear method can overestimate damping in soils, which can result in unconservative design surface ground motions. For this project, a minimum amplification factor of 0.5 was imposed.

Examples of these amplification factors are shown on Figures 22 and 23 for the north-central/east and west regions, respectively. For the north-central/east region and the best-estimate V_s profiles, the amplification factors all show amplification of ground motion at

moderate to long periods (Figure 22). As the intensity of ground motion increases, there is deamplification for short to moderate-period ground motions due to soil nonlinearity. The impact of the depth to bedrock can be seen in the shift of the peak of the amplification functions to longer periods with increasing depth to bedrock (Figure 22). For instance, for a firm rock PGA of 0.5 g (center plot on left side), the peak of the amplification factors shifts from approximately 1.2 to 2.3 to 3.2 sec for basecases with depth to bedrock of 300 ft (P1), 750 ft (P4), and 1,200 ft (P7), respectively. The amplification functions for the stiffer soils in the west region generally show less amplification of long-period ground motions and less deamplification at short periods (Figure 23). The shallower depths to bedrock in the west region also results in amplification functions that peak at shorter periods than in the north-central/east regions. Note that these figures show amplification functions less than 0.5, but a 0.5 minimum is imposed when applying these to the firm rock results.

The firm rock hazard curves derived from the PSHA and the amplification factors relative to firm rock were integrated to arrive at site-specific amplified hazard curves. Design surface hazard curves were computed for each combination of basecase velocity profile (P1 to P9), basecase material property curves (M1 and M2) and control motion magnitude (**M** 5.0 and **M** 7.0). The uncertainty or epistemic variability in seismic hazard is typically represented by a set of weighted hazard curves. Using these sets of curves as discrete probability distributions, they can be sorted by the frequency of exceedance at each ground-motion level and summed into a cumulative probability mass function. When the cumulative probability mass function for a particular exceedance frequency equals or exceeds fractile y , then the exceedance frequency represents the y^{th} fractile. The weighted-mean hazard curve is the weighted average of the exceedance frequency values. This approach is a standard practice in PSHA.

Figure 24 shows the ground surface UHS for the 2,475 year return period for all four Zones resulting from the site response analysis. Note that the amplification factors from the west region are used for Zone 0, while the amplification factors from the north-central/east region are used for Zones 1, 2, and 3. Also shown on Figure 24 are the input firm rock UHS for the four Zones. As expected, there is significant amplification of long-period motions at the 2,475-yr return period, with factors of ranging from 1.9 to 2.0 between the firm rock (V_{s30} 760 m/sec) and surface ground motions at 1.0 sec, respectively. For Zone 0, there is amplification for periods greater than 0.25 sec, with a peak in the site-specific spectrum at 0.4 sec (Figure 24). For Zones 1, 2 and 3, there is amplification for periods greater than 0.4 sec, and the site-specific spectra are generally broader due to both the larger range of depths to bedrock (extends to greater depths), and a softer near-surface V_s profile.

For the DSHA, amplification factors are applied to the 84th percentile firm rock (V_{s30} 760 m/sec) spectra for each Zone to arrive at site-specific 84th percentile spectra. The site-specific 84th percentile spectra along with the firm rock spectra are shown on Figure 25. Amplification patterns for each Zone are similar to those for the PSHA (Figures 24 and 25). These site-specific UHS and 84th percentile spectra are the basis of seismic design spectra developed in Section 5.

5.0 SITE-SPECIFIC DESIGN GROUND MOTIONS

This section describes the development of site-specific MCE_R and DE acceleration response spectra in accordance with ASCE 7-16. MCE_R and DE acceleration response spectra were developed for each of the four Zones. Based on the range of measured V_{S30} within each Zone (Thomas *et al.*, 2013) and the estimated range of depth to bedrock, ASCE 7-16 minimum criteria for both site classes C and D were used in developing site-specific design spectra for Zones 0, 1 and 2. For Zone 3, where bedrock is the deepest an, only site class D was used for ASCE 7-16 minimum criteria.

ASCE 7-16 recognizes potential shortcomings in structural analyses for buildings on softer sites (site classes D and E) when a code spectrum is developed from only two spectral periods (see Section C11.4.8 of ASCE 7-16 Commentary). For these sites, the code-shaped spectrum may be unconservative at long periods, as the shape of code-based spectrum along with site factors (from previous versions of ASCE 7) do not fully capture the large soil non-linearity for soft soils at high ground motions. While moving to a multi-period response spectrum would eliminate these potential issues, ASCE 7-16 provides a short-term solution by requiring a site-specific analyses or for some cases, general code spectra may be developed using conservative site coefficients (ASCE 7-16, Section 11.4.8). When site-specific analyses are performed for site class D sites, F_v for minimum spectra are based on the values for site amplification (Table 11.4-2) multiplied by a spectrum shape adjustment factor (see ASCE 7-16 Commentary, Section 21.3). For site class D with S_1 greater than 0.2 g, ASCE 7-16 requires $F_v = 2.5$ (ASCE 7-16, Section 21.3). This change from ASCE 7-10, which was used to develop the seismic design spectra in 2013, leads to larger minimum response spectra. As described below, the minimum response spectra control the final site-specific design spectra for the Stanford campus over wide period ranges. Note that the USGS is currently developing ground motions for a range of V_{S30} representing site classes from A to E for a range of spectral periods. These will be implemented in ASCE 7-22, eliminating both the need for site factors to adjust firm rock results to various site classes and the simplified code-shaped spectrum based solely on 0.2 and 1.0 sec SA. As a result, the minimum spectra for the Stanford campus based on ASCE 7-22 may differ significantly from ASCE 7-16.

5.1 SITE-SPECIFIC HORIZONTAL MCE_R AND DE SPECTRA

Figures 26 through 29 illustrate the development of the site-specific horizontal MCE_R and DE spectra as per ASCE 7-16. Spectra are shown on both log-linear and linear-linear plots. The horizontal MCE_R spectrum is defined as the lesser of the deterministic MCE and probabilistic MCE_R ground motions. The deterministic MCE response spectrum is the 84th percentile, maximum-direction response spectrum from the characteristic event on the controlling active fault. As per ASCE 7-16 (Supplement 1), the largest SA in the deterministic MCE must not be less than $1.5 \cdot F_a$, where F_a for site classes C and D is determined using Table 11.1.4 with the value of S_s taken as 1.5. For all Zones, F_a for site classes C and D are 1.2 and 1.0, respectively. Figure 26 shows the 84th percentile deterministic response spectrum for a **M** 8.0 scenario earthquake on the San Andreas fault at a rupture distance of 5.6 km and the

adjustment from RotD50 (geometric mean) ground motions predicted by the NGA-West2 GMMs to maximum direction ground motions using the factors from Shahi and Baker (2013). Note that the maximum direction adjustment factors of Shahi and Baker (2013) differ slightly from those in ASCE 7-16, Section 21.2, but are used in this study because they are recommended in the 2015 NEHRP provisions, the ATC 136-1 study, and are recommended for use in currently proposed changes for ASCE 7-22. For comparison, the 84th percentile fault-normal spectrum was also computed using the directivity model of Bayless and Somerville (Spudich *et al.*, 2013) for the deterministic scenario. Given the close distance to the **M** 8.0 rupture, the model predicts a strong increase in ground motions for periods greater than 0.6 sec. To account for directivity effects, the envelope of the fault-normal and the maximum direction spectra is used in developing the deterministic MCE spectrum.

Also shown on Figure 26 is the deterministic minimum value ($1.5*F_a$) for both site classes C and D for which the maximum SA in the deterministic MCE must meet or exceed (horizontal lines on Figure 26). For Zone 0, the enveloped maximum-direction/fault-normal 84th percentile spectrum far exceeds these limits. Hence, the site-specific deterministic MCE spectrum for Zone 0 is the 84th percentile maximum-direction/fault-normal spectrum (Figure 26).

The probabilistic MCE_R spectrum for Zone 0 was calculated using Method 1 in ASCE 7-16, Chapter 21 (Figure 27). The site-specific 2,475-year return-period UHS was adjusted to maximum-direction ground motions and also adjusted using a risk coefficient to obtain a spectrum that is expected to achieve a 1% probability of collapse within a 50-year period. The risk coefficient, C_R is equal to C_{RS} at periods less than or equal to 0.2 sec and equal to C_{R1} at periods greater or equal to 1.0 sec. The values of C_{RS} and C_{R1} for Zone 0, obtained through the USGS website (<https://seismicmaps.org/> accessed 12 July 2019) are 0.896 and 0.886, respectively.

Figure 28 compares the probabilistic MCE_R (risk-adjusted 2,475-year UHS) and the deterministic MCE spectrum for Zone 0. The site-specific MCE_R is the lesser of these spectra, but not less than 80% of the general code MCE_R spectrum for site classes C and D ($S_s = 2.117$ g, $S_1 = 0.763$ g). For Zone 0, the horizontal MCE_R is the deterministic MCE spectrum between 0.2 and 1.7 sec, while the probabilistic MCE_R controls between approximately 1.7 and 3 sec. At shorter and longer periods, the MCE_R is controlled by the 80% minimum for site classes C and D, respectively (Figure 28). Figure 29 provides the horizontal DE spectrum, which is defined as 2/3 the horizontal MCE_R response spectra, but not less than 80% of the general DE spectrum for site classes C and D. Note that these spectra have not been smoothed to avoid adding additional conservatism. However, for the development of time histories smoothing may be desirable, as discussed in Section 7.

Similarly, the development of site-specific, horizontal MCE_R and DE spectra for Zone 1 are shown in Figures 30 to 33. Similar to Zone 0, the deterministic MCE is the envelope of the maximum direction and fault-normal 84th percentile deterministic spectra (Figure 30). Very slight scaling was performed to meet the minimum deterministic spectrum requirement of $1.5*F_a$ for site class C (Figure 30). The site-specific, horizontal MCE_R for Zone 1 is shown on Figure

32, and is controlled by the deterministic MCE (Figure 30) for periods between approximately 0.5 and 1.5 sec, the probabilistic MCE_R (Figure 31) between periods between 1.5 and 7 sec, and the 80% minimum for site classes C and D for shorter and longer periods, respectively. For both Zone 0 and 1, the general MCE_R spectrum for site class C for these sites far exceeds that predicted by the site-response analysis, which predicts deamplification of short period ground motions relative to firm rock (Section 6). The site-specific, horizontal DE spectrum for Zone 1 is shown on Figure 33.

The development of site-specific, horizontal MCE_R and DE spectra for Zones 2 and 3 are similar to Zone 1. However, for Zone 3 only site class D minimum spectra are used, as site class C is not applicable based on the measured V_{S30} for this area of campus (Thomas *et al.*, 2013). All site-specific, horizontal MCE_R and DE spectra are provided in Tables ES-1 to ES-4.

Site-specific spectral acceleration design parameters S_{DS} and S_{D1} were calculated in accordance with ASCE 7-16, Section 21.4 (Table ES-5). S_{DS} is defined as the 90% of the maximum SA for periods between 0.2 and 5 sec. S_{D1} is defined as the maximum of T*SA for periods between 1.0 and 5.0 sec. S_{MS} and S_{M1} are defined as 1.5 times S_{DS} and S_{D1}.

5.2 SITE-SPECIFIC VERTICAL MCE_R AND DE SPECTRA

Unlike ASCE 7-10, ASCE 7-16 also provides requirements for vertical design spectra. Vertical spectra can be developed using site-specific procedures, such as V/H models applied to site-specific horizontal spectra, but must not be less than 80% of code-based vertical design spectra (ASCE 7-16 Section 11.9) nor 50% of the site-specific horizontal design spectra.

For all Zones, site-specific vertical MCE_R spectra were developed using the median V/H ratios of Gülerce and Abrahamson (2011), but then checked against the minimum requirements of ASCE 7-16. The median V/H ratios are a function of magnitude, distance, V_{S30} and level of shaking as defined by the corresponding PGA for a V_{S30} of 1,100 m/sec (PGA_{1,100}). Figure 34 illustrates development of the site-specific, vertical MCE_R for Zone 0. The vertical spectrum using site-specific V/H factors is compared to 80% of code vertical spectra for site classes C and D and also 0.5 times the site-specific horizontal, with the site-specific vertical MCE_R taken as the envelope of these spectra (Figure 34). For Zone 0, the 80% code minimum controls the spectrum between approximately 0.15 and 0.3 sec and the 50% horizontal spectrum minimum controls for longer periods. Site-Specific vertical MCE_R spectra for Zones 1, 2, and 3 were similarly developed. As per ASCE 7-16, the site-specific vertical DE spectra are taken as 2/3rds of the site-specific, vertical MCE_R spectra. All site-specific, vertical MCE_R and DE spectra are provided in Tables ES-1 to ES-4.

Figure 35 compares the site-specific horizontal and vertical MCE_R spectra for all Zones. For Zones 1, 2 and 3, ground motions decrease with increasing distance from the San Andreas fault as expected. The site-specific, horizontal MCE_R spectra are similar for Zones 1 and 2, which have similar near-surface geology and only slight differences in firm rock ground motions due to differences in distance from the San Andreas fault. Zone 3, the farthest from the San Andreas

fault, also has lower short-period (less than 0.5 sec) ground motions due to the lack of site class C minimum requirements for this Zone where bedrock is deeper. For Zone 0, the site-specific, horizontal MCE_R spectrum far exceeds the spectra for other Zones in the 0.2 to 0.9 sec period range due to the stiffer soil and shallower bedrock in this western portion of campus, which is also the closest to the San Andreas fault. Figure 36 shows a similar comparison of the site-specific horizontal and vertical DE spectra for all Zones.

5.3 COMPARISON WITH ASCE 7-16 MCE_R AND DE SPECTRA

Figures 37 to 44 compare the site-specific, horizontal MCE_R and DE spectra for each Zone with the ASCE 7-16 MCE_R spectra for site classes C and D. For periods of 1 sec and longer, the site-specific horizontal spectra are generally similar to the code spectra. For large ranges of periods less than 1.0 sec, the site-specific horizontal spectra are controlled by the 80% minimum spectra for the appropriate site class. As discussed in Section 5.0, there will likely be significant changes in these minimum spectra when ASCE 7-22 incorporates the use of multi-period spectra computed for each site class by the USGS. The multi-period spectra will have spectral shapes consistent with the site response embedded in the V_{S30} scaling of the NGA-West2 GMMs. The site-specific spectra computed for the Stanford campus, however, will still differ due to the use of site-specific V_S profiles versus the generic V_{S30} profiles implied by the V_{S30} models of the NGA-West2 models, which generally have bedrock at great depths.

5.4 COMPARISON WITH 2013 SITE-SPECIFIC SPECTRA

Figures 45 to 48 compare the site-specific horizontal MCE_R and DE spectra to those from the 2013 study. For Zone 0, the spectra are more peaked than the 2013 spectra, but also show the impact of the increased ASCE 7-16 general code spectrum for site class C relative to that from ASCE 7-10 used in the development of the 2013 site-specific spectra (Figure 45). For Zones 1 and 2, the site-specific MCE_R and DE spectra are similar to the 2013 spectra at periods less greater than 0.5 sec, but significantly higher at shorter periods where the ASCE 7-16 general code spectrum for site class C minimum controls the current spectra (Figures 46 and 47). For Zone 3, where only site class D is appropriate, the updated MCE_R and DE spectra are similar to those from the 2013 study, but lower at periods less than 0.2 sec (Figure 48).

To better understand the differences between the 2013 and updated Stanford design spectra, the differences in MCE_R and DE spectra from ASCE 7-10 and ASCE 7-16 are illustrated in Figure 49 for Zone 1. The 80% minimum criteria impact the short-period site-specific spectra, as the site response analysis results lower short-period ground motions than the 80% code spectra. The increase in long-period ground motions in site class D code spectra does not impact the site-specific spectra, as the site response analysis results in ground motions larger than the 80% minimums.

6.0 RECOMMENDATIONS FOR TIME HISTORIES

Development of time histories was beyond the scope of this project. Individual buildings, facilities, and structures have different ranges of periods of interest and as a result, developing time histories applicable for all structures would lead to conservatism for any one structure. This section contains general recommendations for the development of time histories based on the results of this seismic hazard study and the site-specific design ground motions.

The development of time histories consistent with the $MCE_R/BSE-2N$ and/or $DE/BSE-1N$ response spectra should follow the criteria of ASCE 7-16, Section 16. The Stanford campus is a near-field site, and so time histories should include near-fault and directionality effects such as velocity pulses. The design spectra are controlled by an 84th percentile ground motions from a **M** 8.0 event on the San Andreas fault at rupture distances ranging from 5.6 to 7.5 km. The proportion of ground motions containing near-fault velocity pulses predicted by the model of Hayden *et al.* (2014) is 51 to 60%. Hence, for 11 sets of time histories, we recommend that at least six contain velocity pulses.

The $MCE_R/BSE-2N$ and $DE/BSE-1N$ (Figures ES-1 and ES-2) are the result of combining site-specific response spectra with minimum spectra based on the criteria from ASCE 7-16 which led to spectra that are not smooth with spectral period. Smoothing was not done to avoid adding conservatism at any particular period. However, during the development of time histories it may be advantageous to smooth the target spectra, especially if spectral matching is used.

Other criteria related to time history development, such as amplitude scaling and spectral-matching approaches along with application of ground motions to the structural model are contained within ASCE 7-16, Section 16.

7.0 REFERENCES CITED

- Abrahamson, N.A. and Silva, W.J., and Kamai, R., 2014, Summary of the ASK14 ground-motion relation for active crustal regions: *Earthquake Spectra*, v. 30, p. 1025-1055.
- Al Atik, L. and Youngs, R., 2014, Epistemic uncertainty for NGA-West2 models: *Earthquake Spectra*: v. 30, p. 1301-1318.
- Bazzurro, P. and Cornell, C.A., 2004, Nonlinear soil-site effects in probabilistic seismic-hazard analysis: *Bulletin of the Seismological Society of America*, v. 94, p. 2110-2123.
- Boore, D.M., Stewart, J.P., Seyhan, E., Atkinson, G.M., 2014, NGA-West2 equations for predicting PGA, PGV, and 5%-damped PSA for shallow crustal earthquakes: *Earthquake Spectra*, v. 30, p. 1057-1085.
- Campbell, K.W. and Bozorgnia, Y., 2014, NGA-West2 ground motion model for the average horizontal components of PGA, PGV, and 5%-damped linear acceleration response spectra: *Earthquake Spectra*, v. 30, p. 1087-1115.
- Cao, T.C., Bryant, W.A., Rowshandel, B., Branum, D., and Wills, C.J., 2003, The revised 2002 California probabilistic seismic hazard maps, June 2003: California Geological Survey website.
- Chiou, B-S.J. and Youngs, R.R., 2014, Update of the Chiou and Youngs NGA ground motion model for average horizontal component of peak ground motion and response spectra: *Earthquake Spectra*, v. 30, p. 1117-1153.
- Electric Power Research Institute (EPRI), 1993, Guidelines for determining design basic ground motions, v. 1: Method and guidelines for estimating earthquakes ground motion in eastern North America: EPRI Report TR-102293.
- Gülerce, Z. and Abrahamson, N., 2011, Site-specific design spectra for vertical ground motion: *Earthquake Spectra*, v. 27, p. 1023-1047.
- Hale, C., Abrahamson, N. and Bozorgnia, Y., 2018, Probabilistic seismic hazard analysis code verification: Pacific Earthquake Engineering Research Center, PEER Report 2018/03, 105 p.
- Hayden, C. P., Bray, J. D., and Abrahamson, N. A., 2014, Selection of near-fault pulse motions: *Journal of Geotechnical and Geoenvironmental Engineering*, v. 140, Paper 04014030, [http://dx.doi.org/10.1061/\(ASCE\)GT.1943-5606.0001129](http://dx.doi.org/10.1061/(ASCE)GT.1943-5606.0001129).
- Idriss, I.M. and Seed, H.B., 1968, Seismic response of horizontal soil layers: *Journal of the Soil Mechanics and Foundations Division*, v. 94, p. 1003-1031.
- Kamai, R., Abrahamson, N. A., and Silva, W. J., 2014, Nonlinear horizontal site amplification for constraining the NGA-West2 GMPEs: *Earthquake Spectra*, v. 30, p. 1223 – 1240.
- McGuire, R.K., Silva, W.J., and Costantino, C.J., 2001, Technical basis for revision of regulatory guidance on design ground motions: Hazard- and risk-consistent ground motion spectra guidelines: U.S. Nuclear Regulatory Commission NUREG/CR-6728.
- Schnabel, P.B., Lysmer, J. and Seed, H.B., 1972, SHAKE - A computer program for earthquake analysis of horizontally layered sites: *Earthquake Engineering Research Center, University of California, Berkeley*, Report No. EERC 72-12.

-
- Shahi, S.K. and Baker, J.W., 2014, NGA-West2 models for ground-motion directionality: *Earthquake Spectra*, v. 30, no. 3, pp. 1285-1300.
- Silva, W.J., 1976, Body waves in a layered anelastic solid: *Bulletin of the Seismological Society of America*, v. 66, p. 1539-1554.
- Silva, W.J. and Lee, K., 1987, WES RASCAL code for synthesizing earthquake ground motions: State-of-the-art for Assessing Earthquake Hazards in the United States, Report 24: U.S. Army Engineer Waterways Experiment Station Miscellaneous Paper S-73-1, 120 p.
- Silva, W.J., Abrahamson, N.A., Toro, G., and Constantino, C., 1997, Description and validation of the stochastic ground motion model: unpublished report prepared for the Brookhaven National Laboratory. Spudich, P., Bayless, J.R., Baker, J.W., Chiou, B.S.I., Rowshandel, B., Shahi, S., and Somerville, P., 2013, Final report of the NGA-West2 Directivity Working Group: PEER Report 2013/09, 143 p.
- Stanford Land, Buildings and Real Estate, 2019, *Engineering and Architectural Seismic Design Guidelines*, October 2019, 47 p.
- Thomas, P, Wong, I....., 2013,
- Thomas, P.A., Wong, I.G., and Abrahamson, N., 2010, Verification of probabilistic seismic hazard analysis software programs: Pacific Earthquake Engineering Research Center, PEER Report 2010/106, 173 p.
- Toro, G.R., 1996, Probabilistic models of site velocity profiles for generic and site-specific ground motion amplification studies." Published as an appendix in Silva et al (1996).
- URS Corporation/Jack R. Benjamin & Associates, Inc., 2007, Technical memorandum topical area: seismic hazard, Delta Risk Management Study (DRMS) Phase 1, unpublished report submitted to California Department of Water Resources.
- WGCEP (Working Group for California Earthquake Probabilities), 2008, The uniform earthquake rupture forecast, version 2 (UCERF2): U.S. Geological Survey Open-File Report 2007-1437.
- WGCEP (Working Group on California Earthquake Probabilities), 2003, Earthquake probabilities in the San Francisco Bay region: 2002–2031: U.S. Geological Survey. Open-File Report 03-214.
- WGNCEP (Working Group On Northern California Earthquake Potential), 1996, Database of potential sources for earthquakes larger than magnitude 6 in Northern California: U.S. Geological Survey Open-File Report 96-705
- Wong, I.G., Thomas, P.A., Unruh, J., Hanson, K., and Youngs, R.R., 2008, characterizing the earthquake ground shaking hazard in the Sacramento-San Joaquin Delta, California: *Geotechnical Engineering and Soil Dynamics IV Conference Proceedings*, pp. 1-11.
- Youngs, R.R, Coppersmith, K.J., Taylor, C.L., Power, M.S., Di Silvestro, L.A., Angell, M.L., Hall, N.T., Wesling, J.R., and Mualchin, L., 1992, A comprehensive seismic hazard model for the San Francisco Bay Region, *in Proceedings of the Second Conference on Earthquake Hazards in the Eastern San Francisco Bay Area*, Borchartd, G., Hirschfeld, S.E., Lienkaemper, J.J., McClellan, P., Williams, P.L. and Wong, I.G. (eds.), California Division of Mines and Geology Special Publication 113, p. 431-441.

Tables

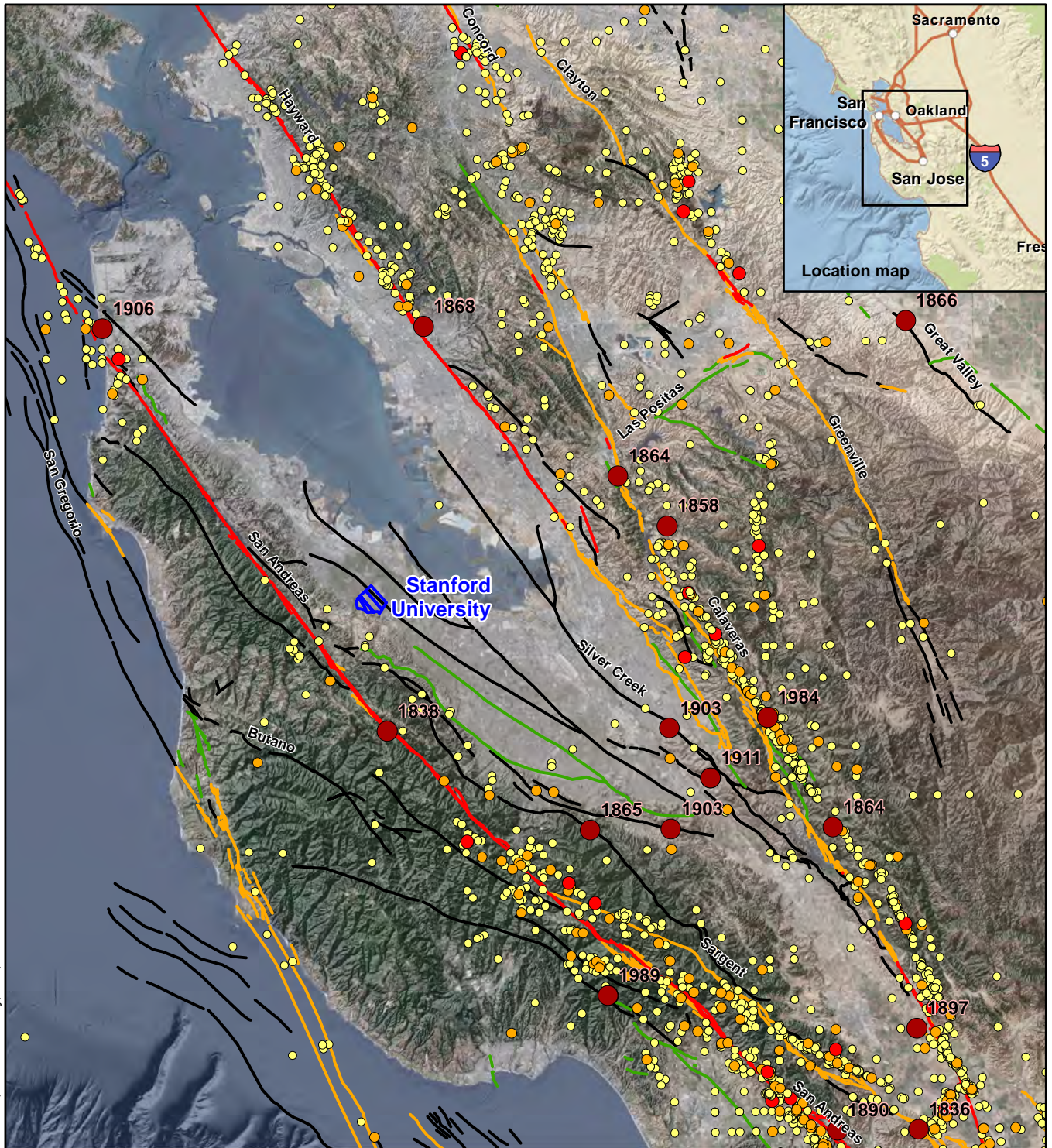
Table 1. Magnitude and Distance Deaggregation

ZONE	PGA				1.0 SEC SA			
	M*	D*	M-BAR	D-BAR	M*	D*	M-BAR	D-BAR
0	7.1	7.5	7.2	7.6	7.1	7.5	7.4	7.7
1	7.1	7.5	7.2	7.6	7.1	7.5	7.4	7.7
2	7.1	7.5	7.2	7.7	7.1	7.5	7.4	7.8
3	7.1	7.5	7.2	7.8	7.1	7.5	7.4	8.0

Table 2. Inputs for DSHA

INPUT PARAMETER	INPUT PARAMETER DEFINITION	ZONE 0	ZONE 1	ZONE 2	ZONE 3
<i>M</i>	Moment magnitude	8.0	8.0	8.0	8.0
<i>R_{RUP}</i>	Closest distance to coseismic rupture (km)	5.6	6.1	6.6	7.5
<i>R_{JB}</i>	Closest distance to surface projection of coseismic rupture (km)	5.6	6.1	6.6	7.5
<i>R_X</i>	Horizontal distance from top of rupture measured perpendicular to fault strike (km)	5.6	6.1	6.6	7.5
<i>R_{yo}</i>	The horizontal distance off the end of the rupture measured parallel to strike (km)	0.0	0.0	0.0	0.0
<i>U</i>	Unspecified-mechanism factor: 1 for unspecified; 0 otherwise	0	0	0	0
<i>F_{RV}</i>	Reverse-faulting factor: 0 for strike slip, normal, normal-oblique; 1 for reverse, reverse-oblique and thrust	0	0	0	0
<i>F_N</i>	Normal-faulting factor: 0 for strike slip, reverse, reverse-oblique, thrust and normal-oblique; 1 for normal	0	0	0	0
<i>F_{HW}</i>	Hanging-wall factor: 1 for site on down-dip side of top of rupture; 0 otherwise	0	0	0	0
<i>Z_{TOR}</i>	Depth to top of coseismic rupture (km)	0	0	0	0
<i>Dip</i>	Average dip of rupture plane (degrees)	90	90	90	90
<i>V_{S30}</i>	The average shear-wave velocity (m/s) over a subsurface depth of 30 m	760	760	760	760
<i>V_{S30} Flag</i>	1 for measured; 0 for inferred V _{s30}	1	1	1	1
<i>Z_{HYP}</i>	Hypocentral depth from the earthquake	Default	Default	Default	Default
<i>Z_{1.0}</i>	Depth to V _s =1 km/sec	Default	Default	Default	Default
<i>Z_{2.5}</i>	Depth to V _s =2.5 km/sec	Default	Default	Default	Default
<i>W</i>	Fault rupture width (km)	13	13	13	13
<i>Region</i>	Specific Regions considered in the models	CA	CA	CA	CA

Figures



File path: S:\1834\Figures\Figure_01.mxd; Date: 01/09/2020; User: Whitney, LCI; Rev.1

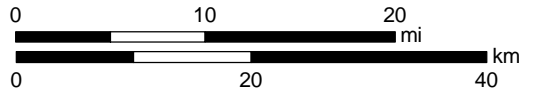
EXPLANATION

▬ Ground Motion Zones

Magnitude

- 3.0 - 4.0
- 4.1 - 5.0
- 5.1 - 6.0
- 6.1 - 7.0

- ▬ Historic faults
- ▬ Holocene faults
- ▬ Late Quaternary faults
- ▬ Quaternary faults



Map projection and scale: NAD 1983 UTM Zone 10N, 1:642,000

**Historical Seismicity (M > 3.0, 1800 - 2019)
and Quaternary Faults in the San Francisco
Bay Region**

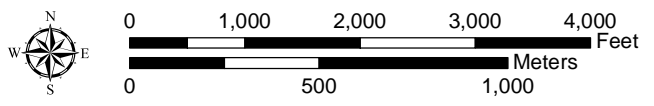
STANFORD UNIVERSITY

Lettis Consultants International, Inc.

Figure **1**



File path: S:\1834\Figures\Figure_02.mxd; Date: 10/28/2019; User: Whitney, LCI; Rev: 1

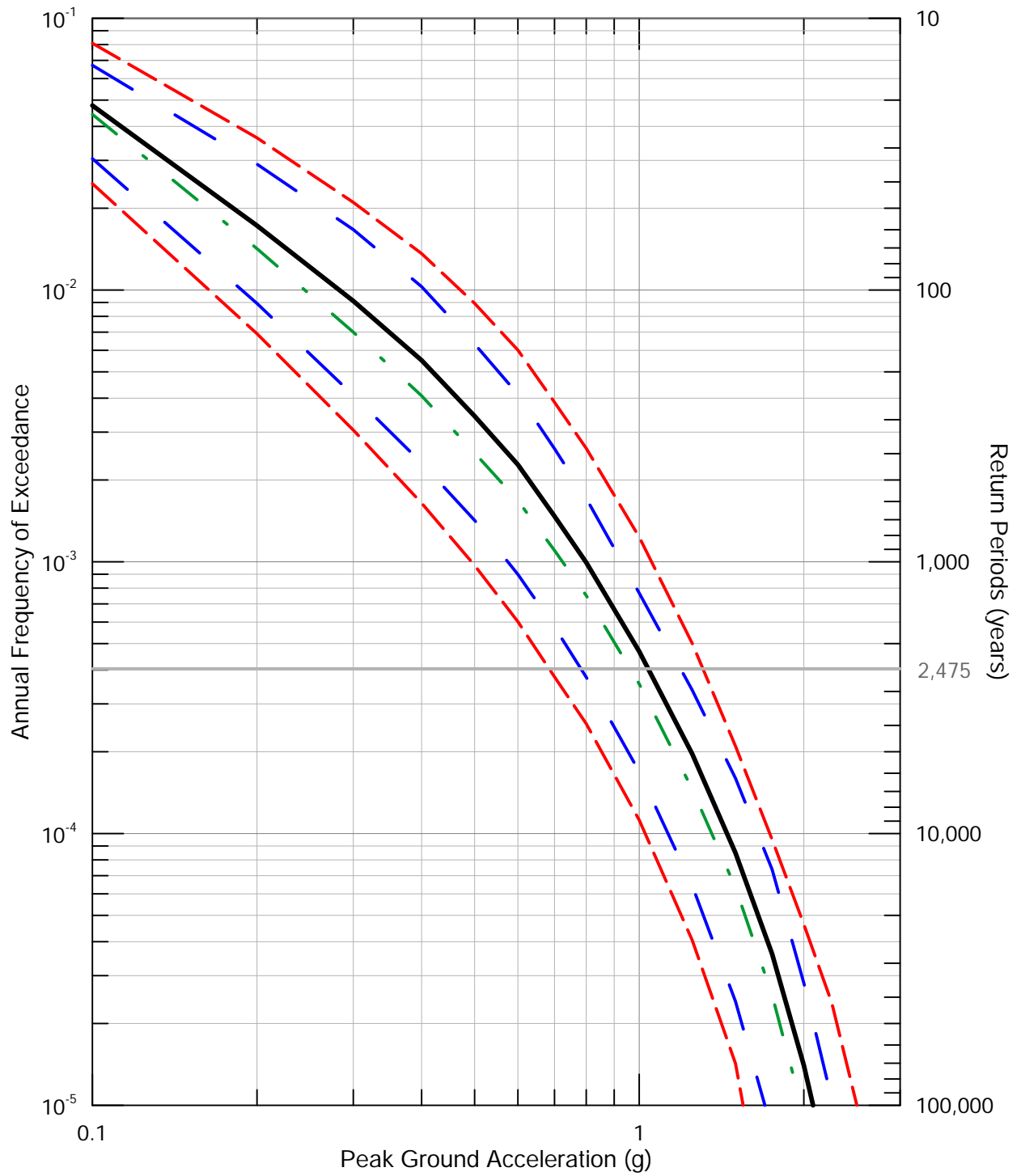


Map projection and scale: NAD 1983 UTM Zone 10N, 1:20,000

Design Ground Motion Zones

STANFORD UNIVERSITY

Note: Imagery basemap from ESRI.



- Mean Hazard
- - - 5th and 95th Percentiles
- - - 15th and 85th Percentiles
- - - 50th Percentile (Median)

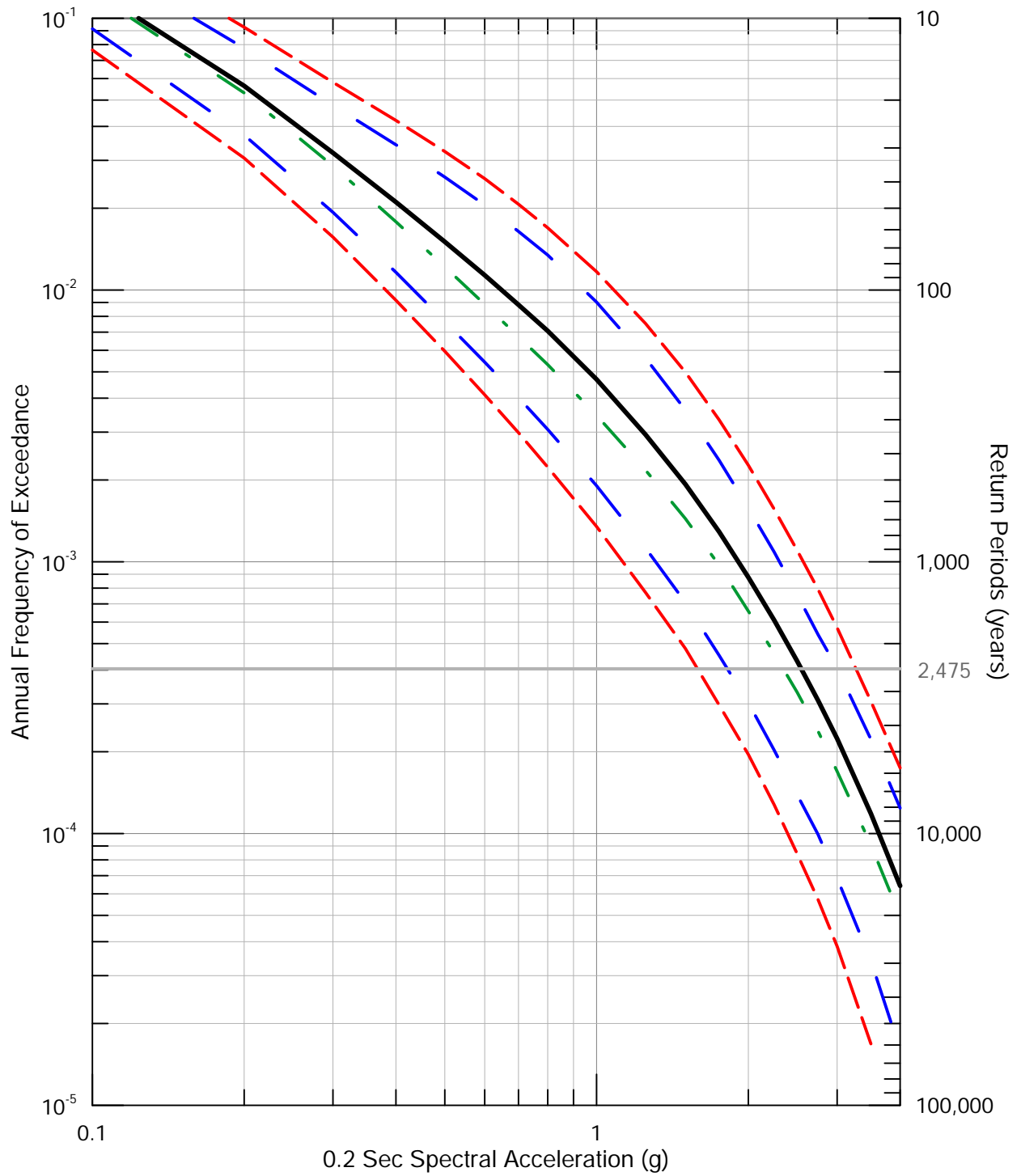
**Seismic Hazard Curves
for Peak Horizontal Acceleration
for Zone 0 and V_s 30 760 m/sec**

STANFORD UNIVERSITY



Lettis Consultants International, Inc.

Figure 3



- Mean Hazard
- 5th and 95th Percentiles
- 15th and 85th Percentiles
- 50th Percentile (Median)

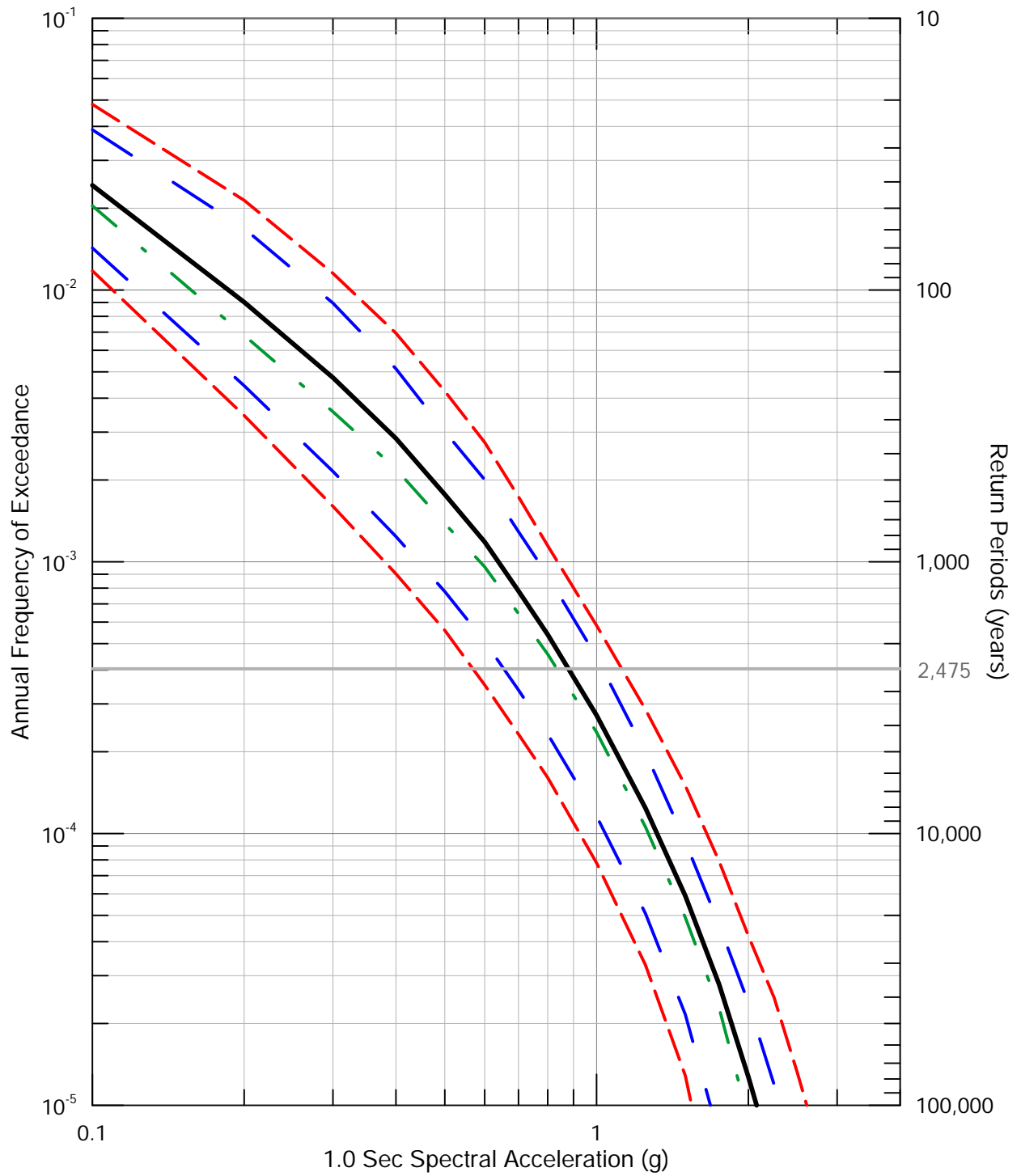
**Seismic Hazard Curves
for 0.2 Sec Horizontal Spectral Acceleration
for Zone 0 and V_s 30 760 m/sec**

STANFORD UNIVERSITY



Lettis Consultants International, Inc.

Figure 4



- Mean Hazard
- - - 5th and 95th Percentiles
- - - 15th and 85th Percentiles
- - - 50th Percentile (Median)

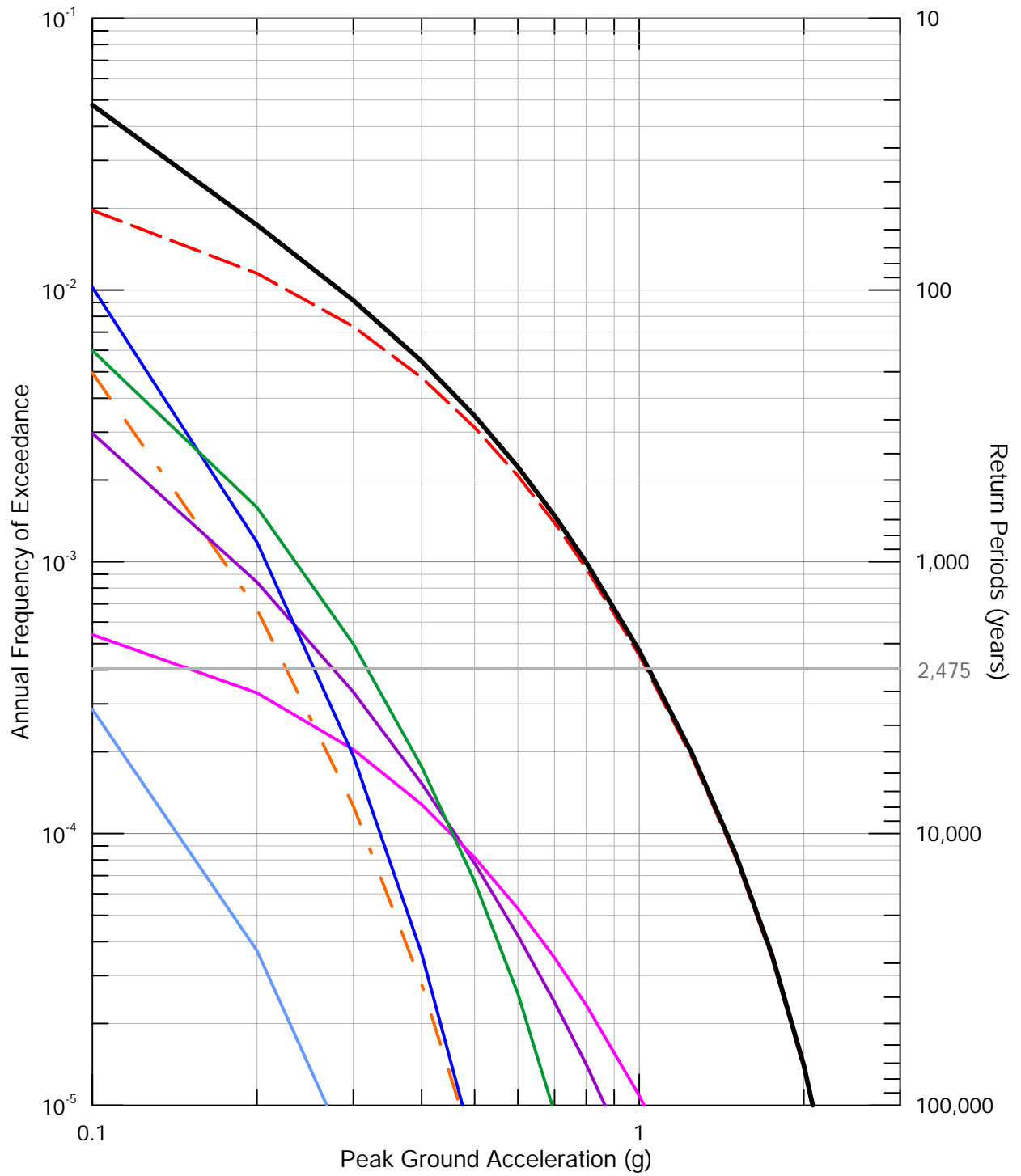
**Seismic Hazard Curves
for 1.0 Sec Horizontal Spectral Acceleration
for Zone 0 and V_s 30 760 m/sec**

STANFORD UNIVERSITY



Lettis Consultants International, Inc.

Figure 5



- Total Mean
- - - San Andreas
- Hayward-Rodgers Creek
- Calaveras
- Foothill Thrust Belt
- San Gregorio
- Coast Range Background Zone
- - - All other sources

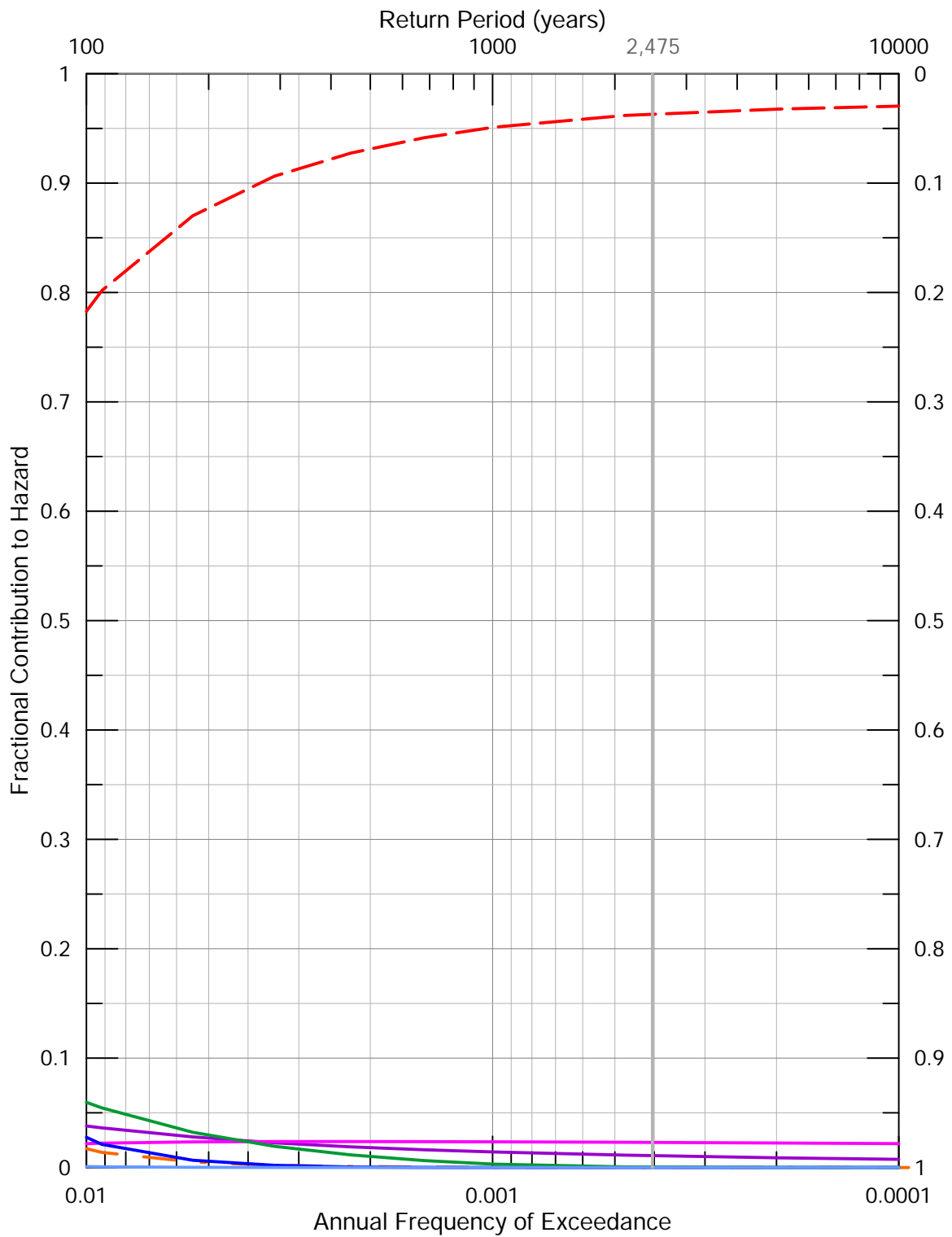
**Seismic Source Contributions
to Peak Horizontal Acceleration
for Zone 0 and V_s 30 760 m/sec**

STANFORD UNIVERSITY



Lettis Consultants International, Inc.


Figure 6

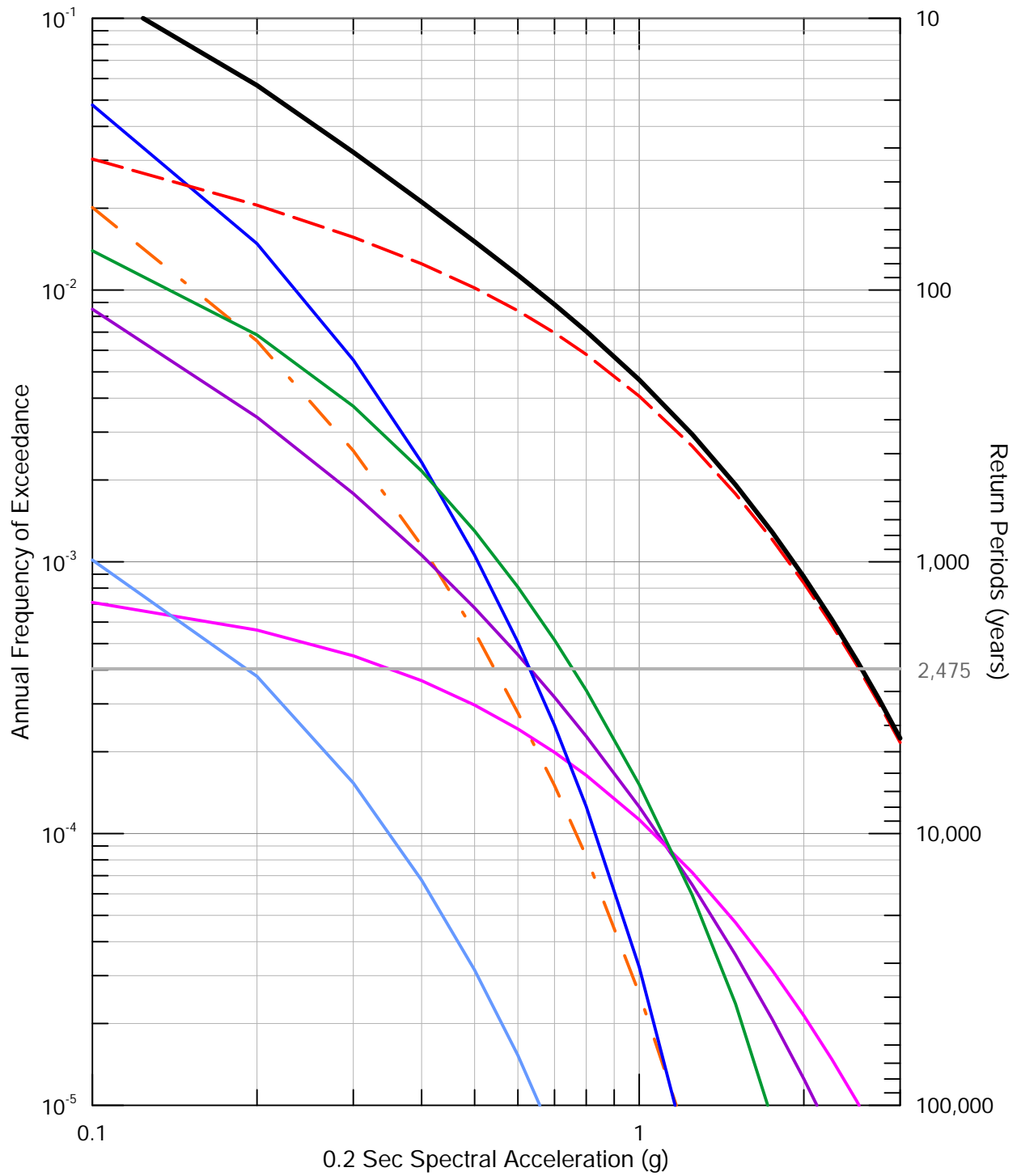


- San Andreas
- Hayward-Rodgers Creek
- Calaveras
- Foothill Thrust Belt
- San Gregorio
- Coast Range Background Zone
- All other sources

**Seismic Source Fractional Contributions
to Peak Horizontal Acceleration
for Zone 0 and V_s 30 760 m/sec**

STANFORD UNIVERSITY


Lettis Consultants International, Inc.
Figure 7



- Total Mean
- - - San Andreas
- Hayward-Rodgers Creek
- Calaveras
- Foothill Thrust Belt
- San Gregorio
- Coast Range Background Zone
- · - All other sources

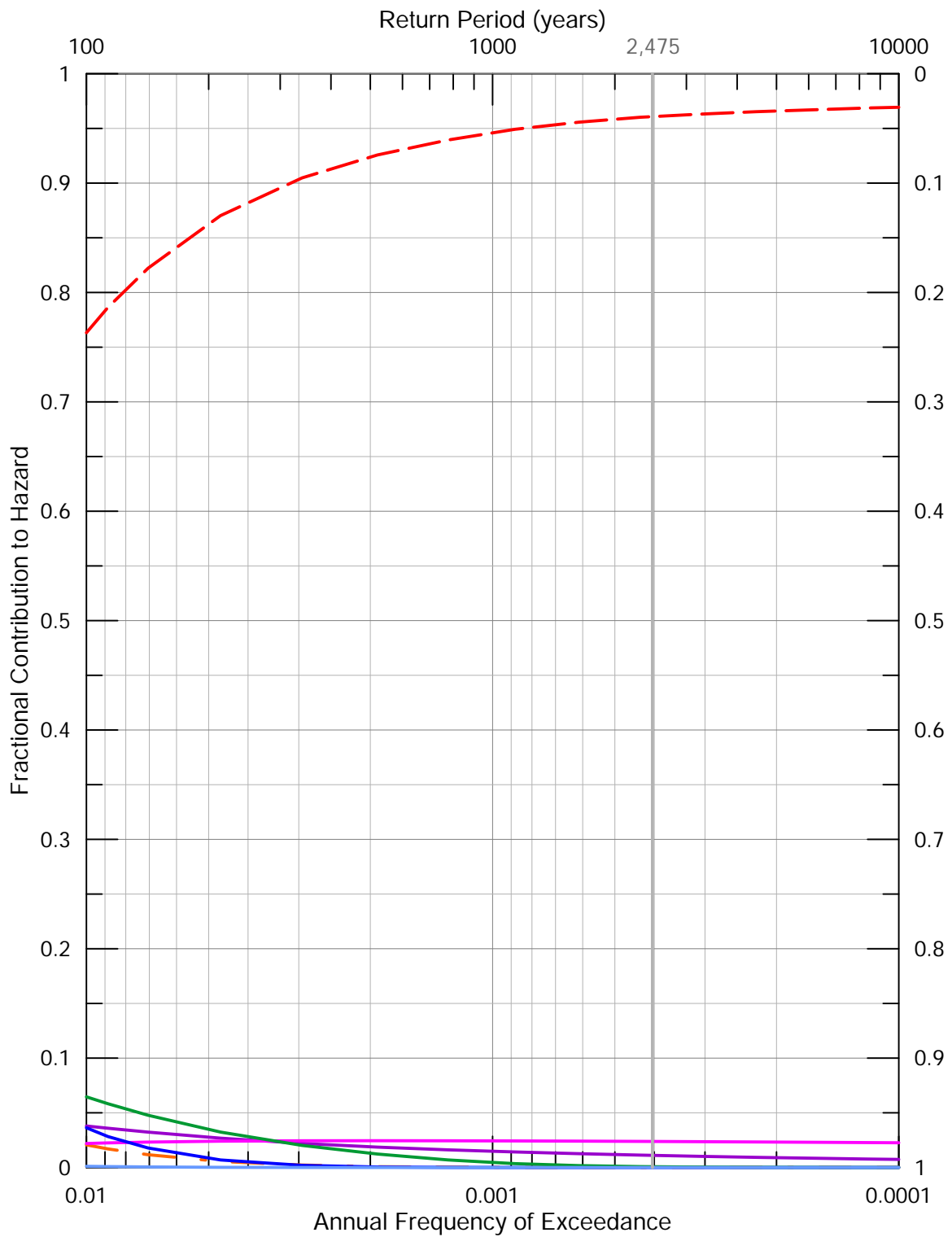
**Seismic Source Contributions
to 0.2 Sec Horizontal Spectral Acceleration
for Zone 0 and V_s 30 760 m/sec**

STANFORD UNIVERSITY



Lettis Consultants International, Inc.


Figure 8

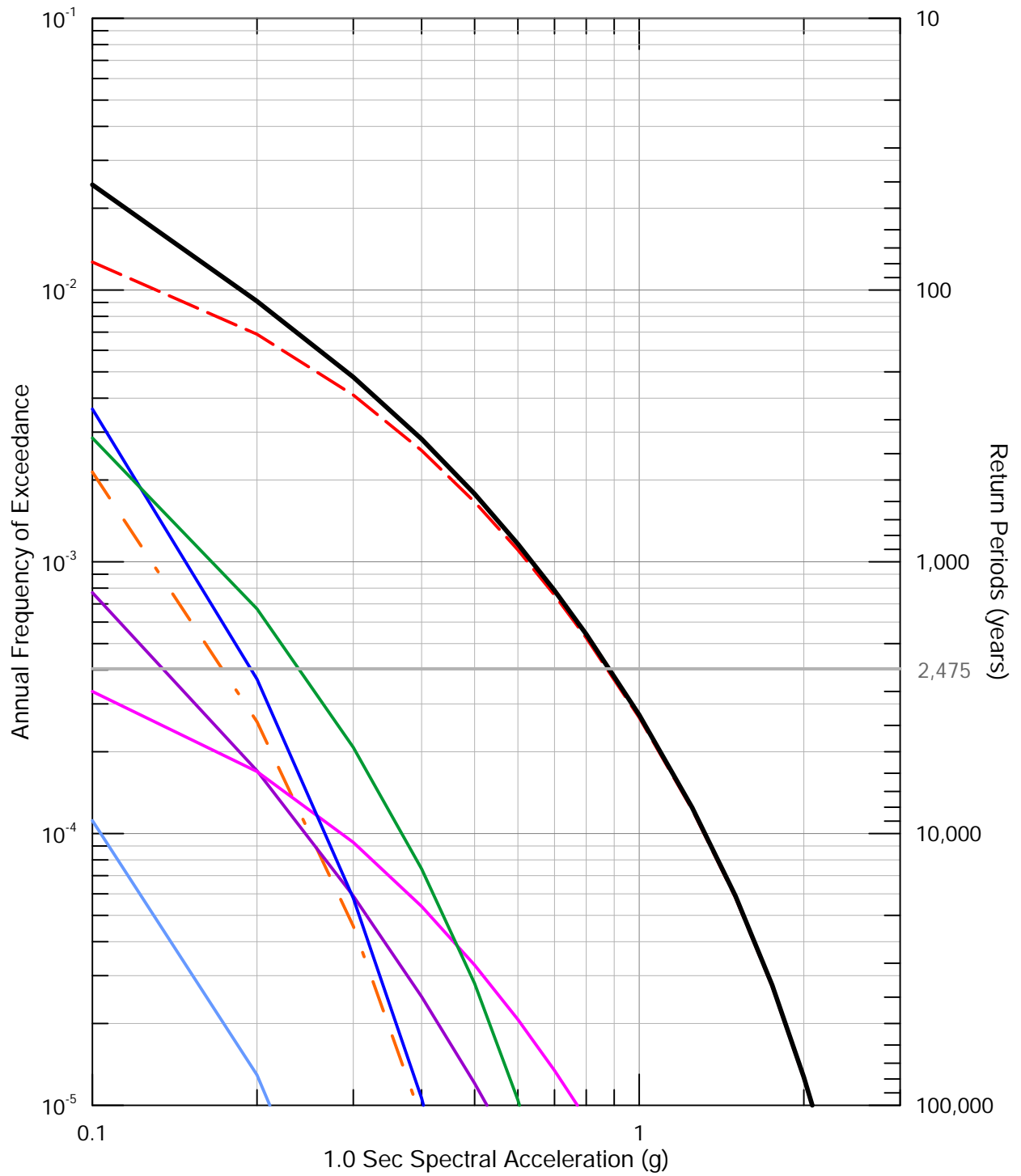


- San Andreas
- Hayward-Rodgers Creek
- Calaveras
- Foothill Thrust Belt
- San Gregorio
- Coast Range Background Zone
- All other sources

**Seismic Source Fractional Contributions
to 0.2 Sec Horizontal Spectral Acceleration
for Zone 0 and V_s 30 760 m/sec**

STANFORD UNIVERSITY


Lettis Consultants International, Inc.
Figure 9



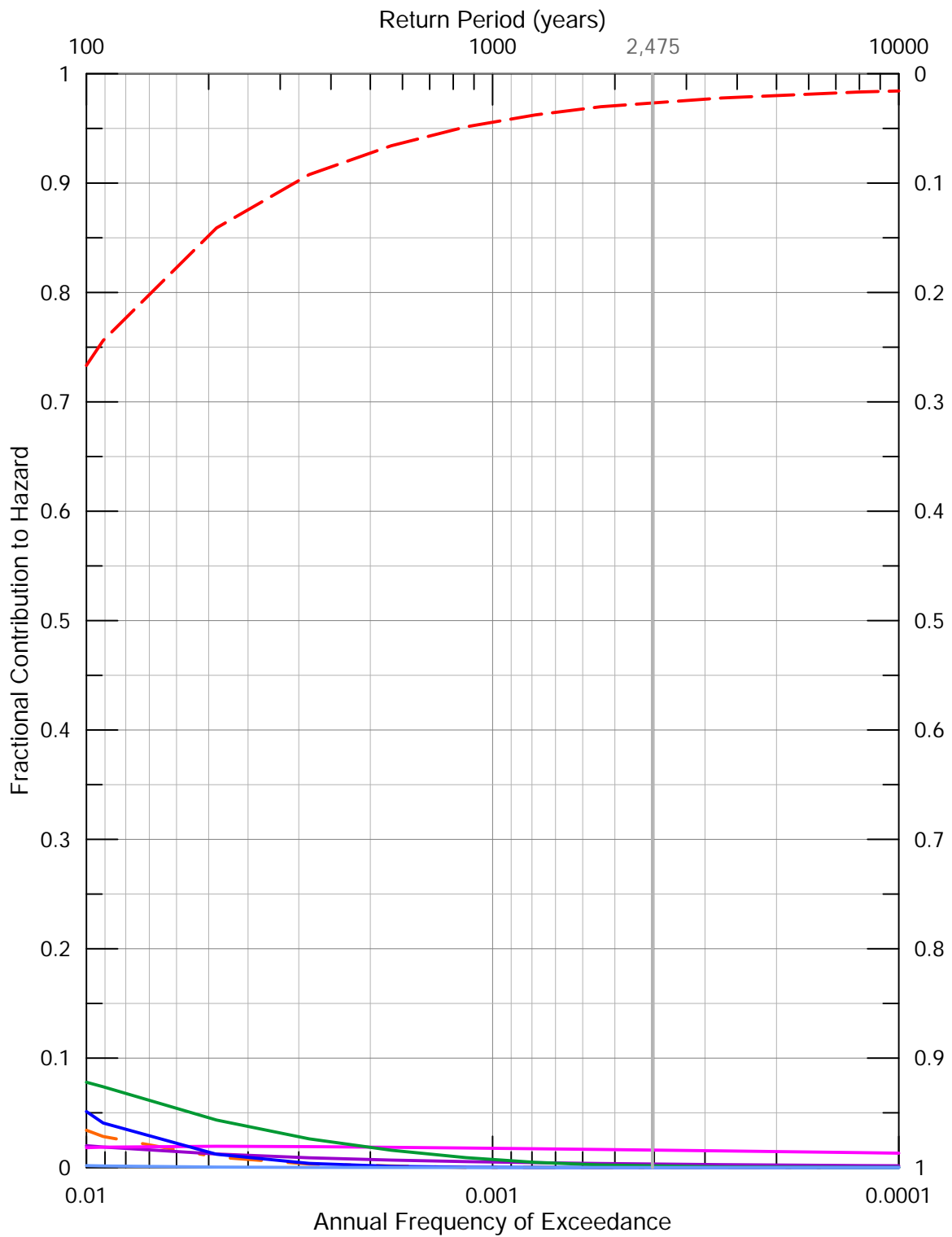
**Seismic Source Contributions
to 1.0 Sec Horizontal Spectral Acceleration
for Zone 0 and V_s 30 760 m/sec**

STANFORD UNIVERSITY



Lettis Consultants International, Inc.

Figure 10



- San Andreas
- Hayward-Rodgers Creek
- Calaveras
- Foothill Thrust Belt
- San Gregorio
- Coast Range Background Zone
- All other sources

**Seismic Source Fractional Contributions
to 1.0 Sec Horizontal Spectral Acceleration
for Zone 0 and V_s 30 760 m/sec**

STANFORD UNIVERSITY



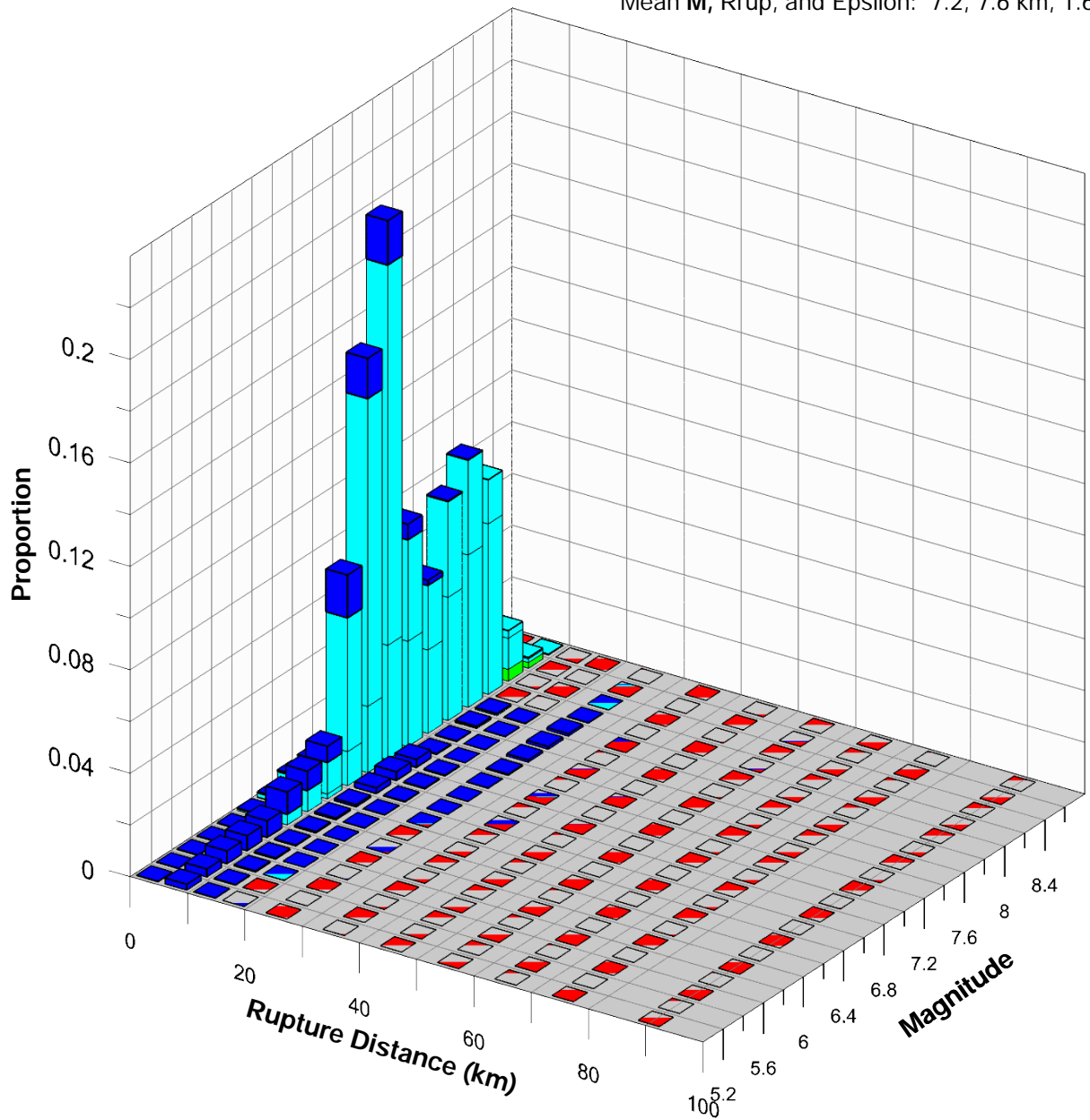
Lettis Consultants International, Inc.

Figure 11

2,475-Year Return Period

Modal **M**, **Rrup**, and **Epsilon***: 7.1, 7.5 km, 1.71

Mean **M**, **Rrup**, and **Epsilon**: 7.2, 7.6 km, 1.66



- Epsilon
- >2
 - 1 to 2
 - 0 to 1
 - -1 to 0
 - -2 to -1
 - <-2

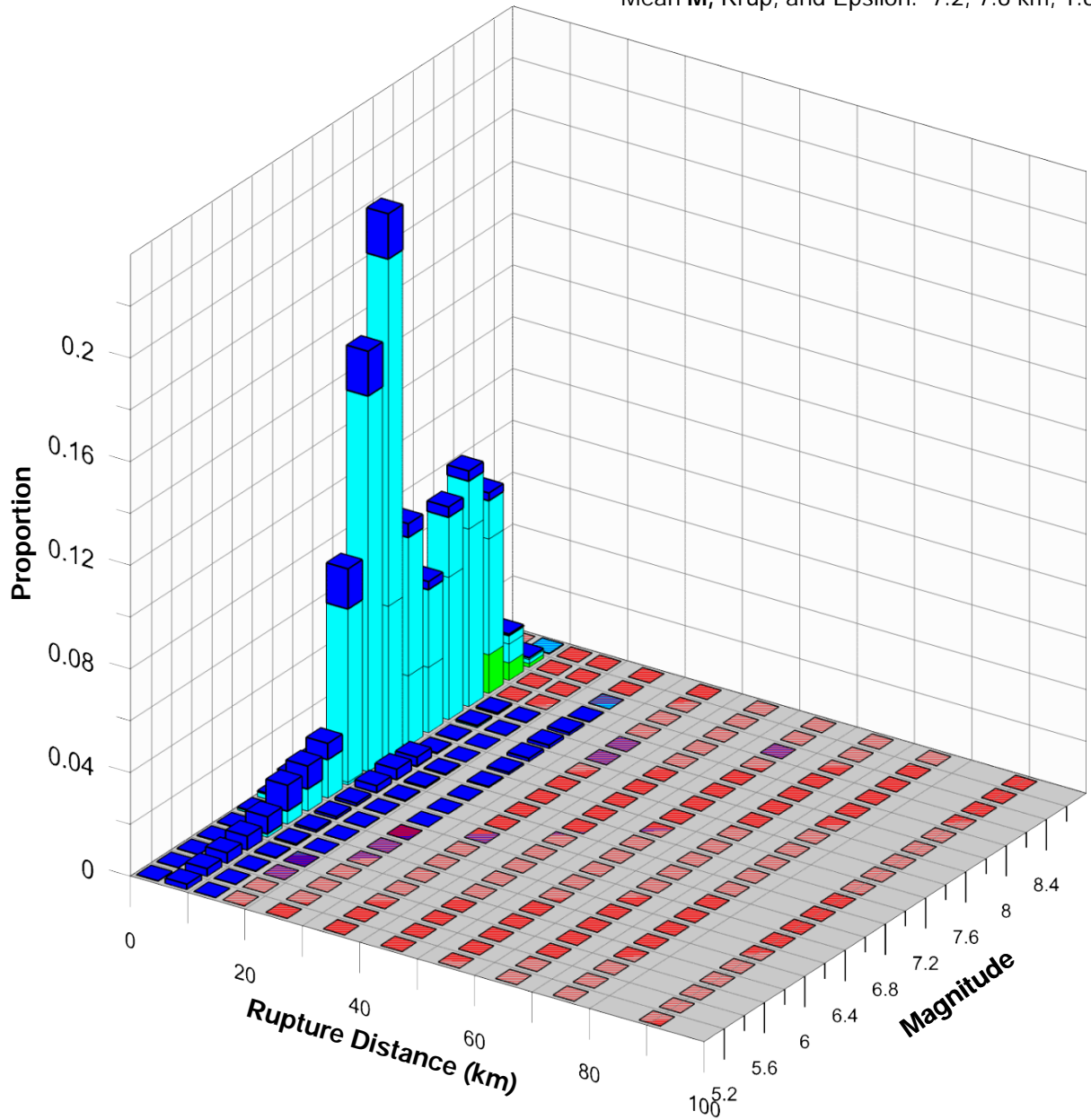
Magnitude, Distance, and Epsilon Contributions to the Mean Peak Horizontal Acceleration Hazard at 2,475-Year Return Period for Zone 0 and V_s 30 760 m/sec

STANFORD UNIVERSITY

2,475-Year Return Period

Modal **M**, **Rrup**, and **Epsilon***: 7.1, 7.5 km, 1.67

Mean **M**, **Rrup**, and **Epsilon**: 7.2, 7.6 km, 1.69



- Epsilon
- >2
 - 1 to 2
 - 0 to 1
 - -1 to 0
 - -2 to -1
 - <-2

Magnitude, Distance, and Epsilon Contributions to the Mean 0.2 Sec Horizontal Spectral Acceleration Hazard at 2,475-Year Return Period for Zone 0 and V_s 30 760 m/sec

STANFORD UNIVERSITY



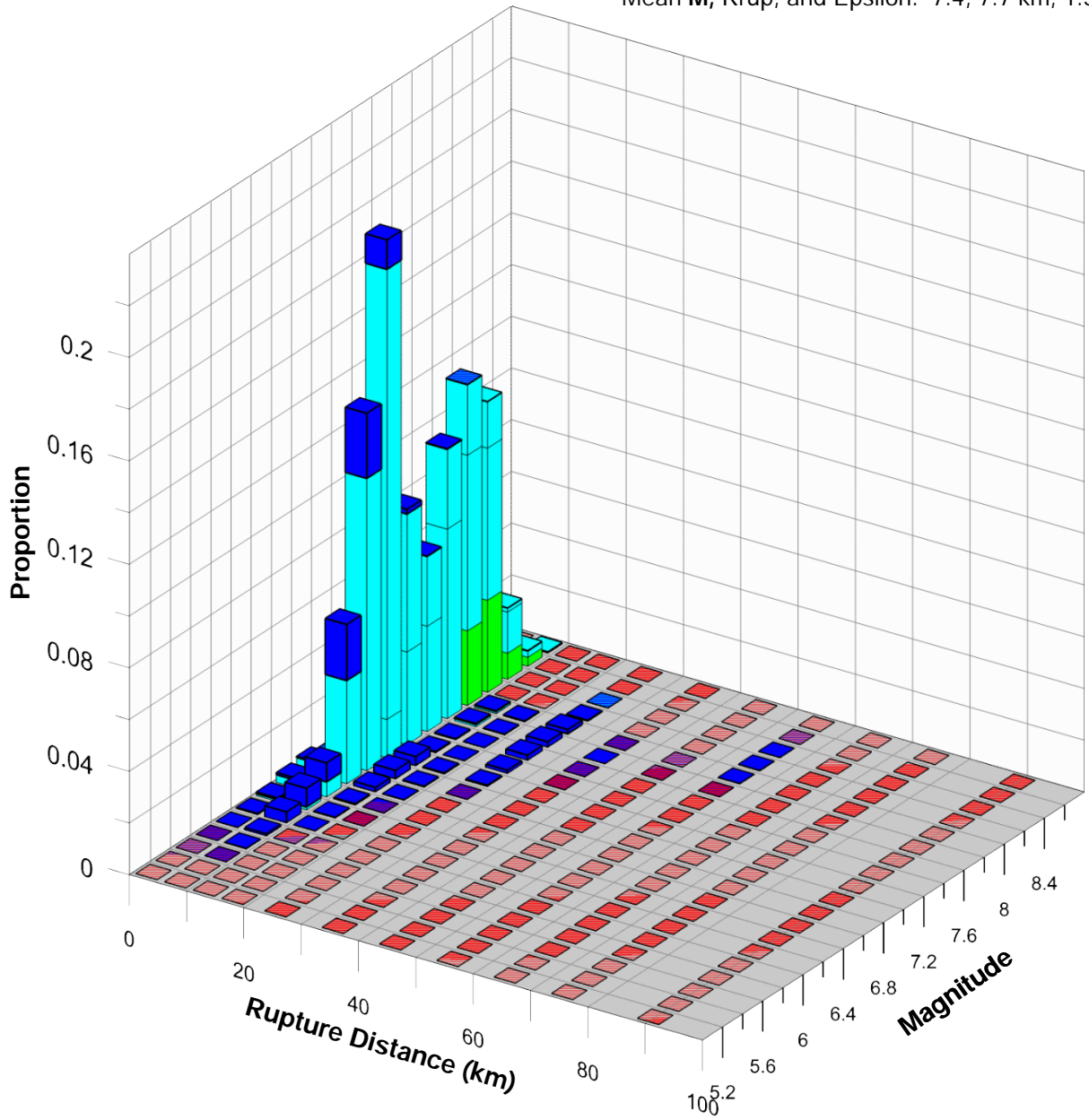
Lettis Consultants International, Inc.

Figure 13

2,475-Year Return Period

Modal **M**, **Rrup**, and **Epsilon***: 7.1, 7.5 km, 1.76

Mean **M**, **Rrup**, and **Epsilon**: 7.4, 7.7 km, 1.59



- Epsilon
- >2
 - 1 to 2
 - 0 to 1
 - -1 to 0
 - -2 to -1
 - <-2

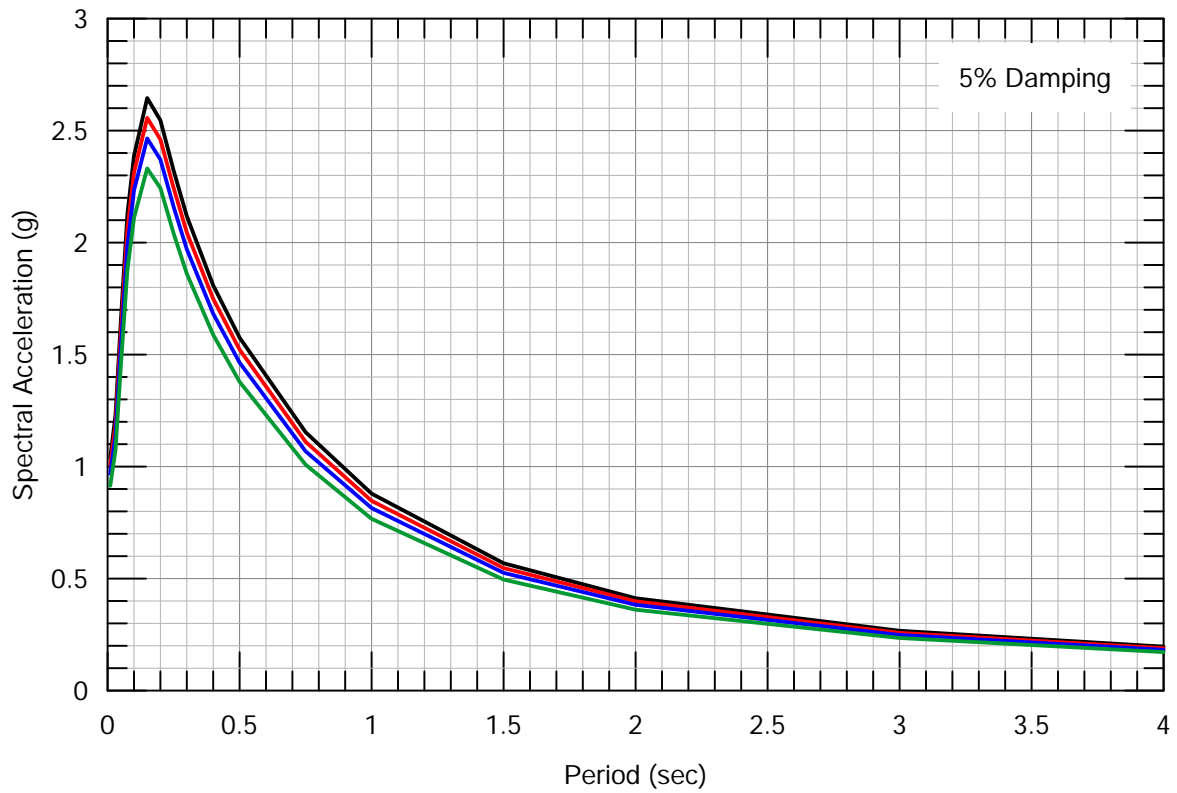
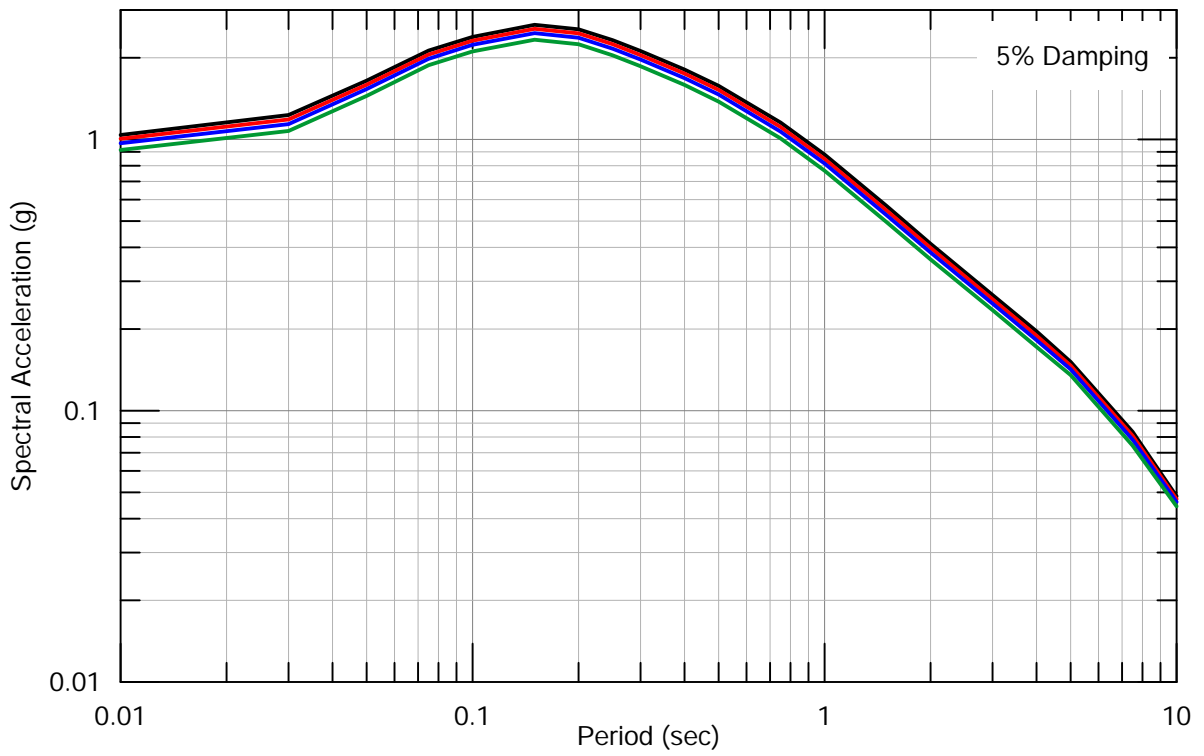
Magnitude, Distance, and Epsilon Contributions to the Mean 1.0 Sec Horizontal Spectral Acceleration Hazard at 2,475-Year Return Period for Zone 0 and V_s 30 760 m/sec

STANFORD UNIVERSITY



Lettis Consultants International, Inc.

Figure 14



- Zone 0
- Zone 1
- Zone 2
- Zone 3

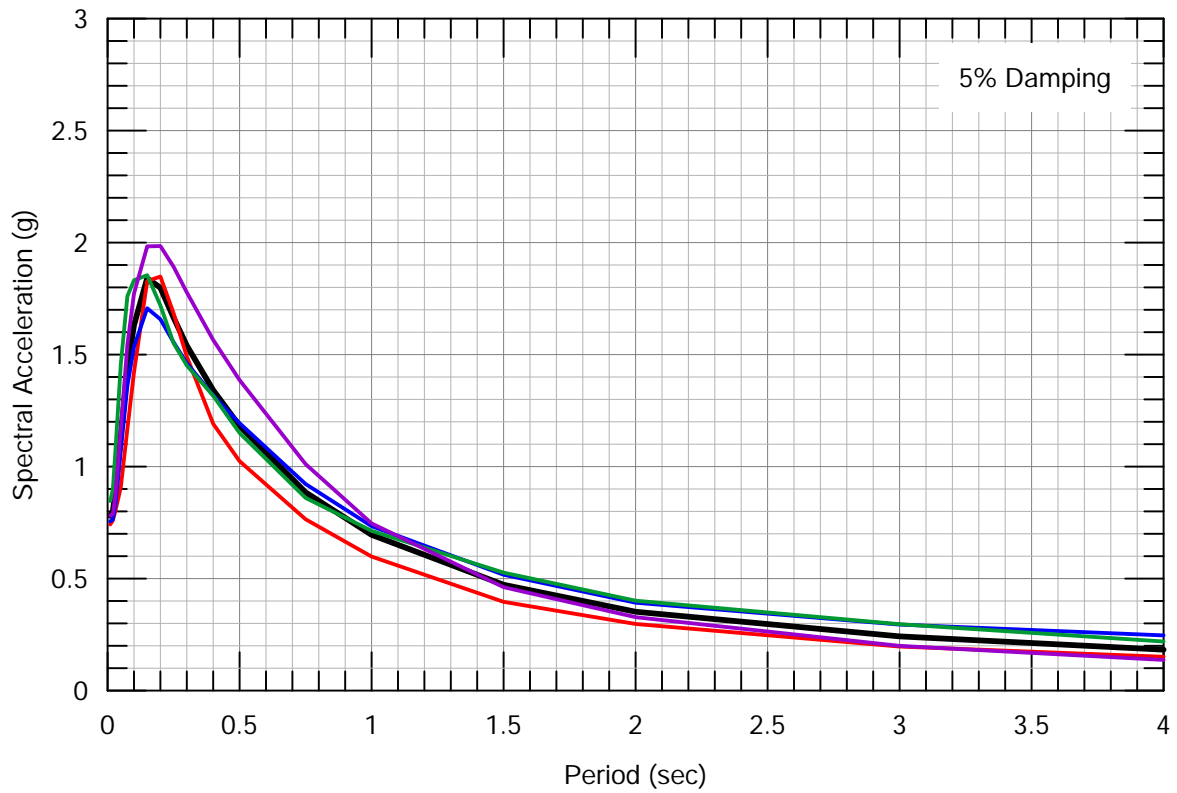
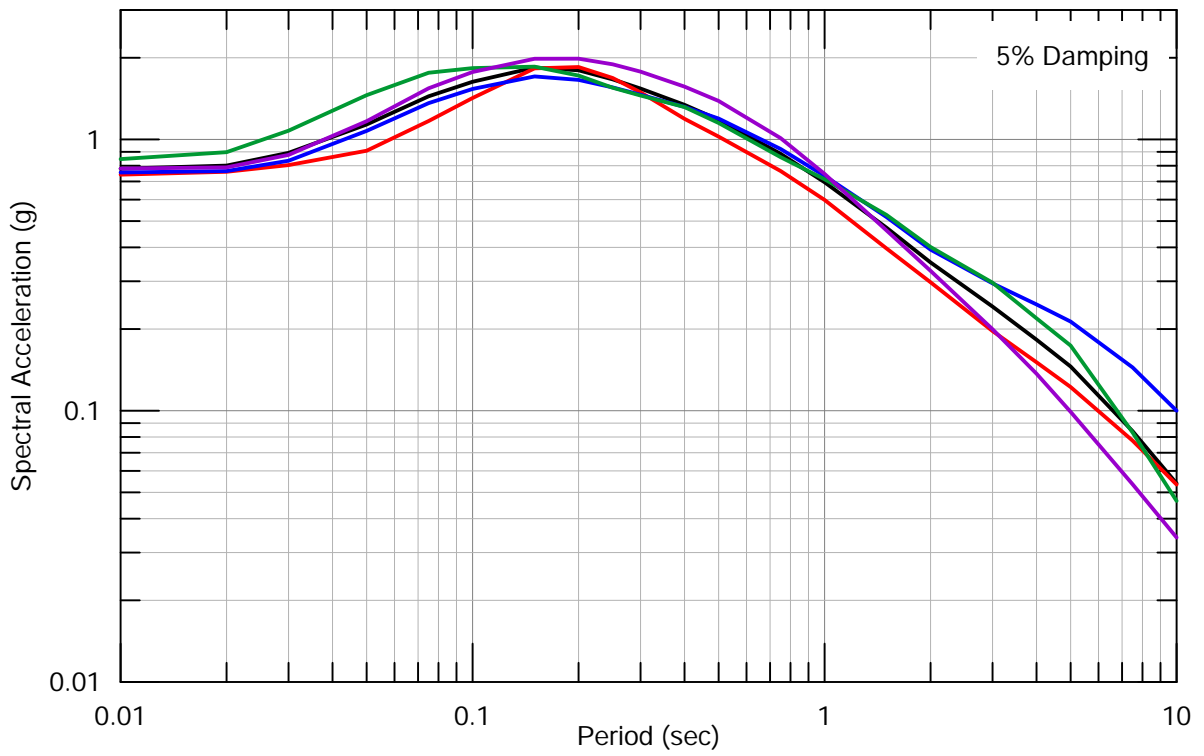
**Uniform Hazard Response Spectra
at a 2,475-Year Return Period for
Zones 0, 1, 2 and 3 and V_s 30 760 m/sec**

STANFORD UNIVERSITY



Lettis Consultants International, Inc.

Figure 15



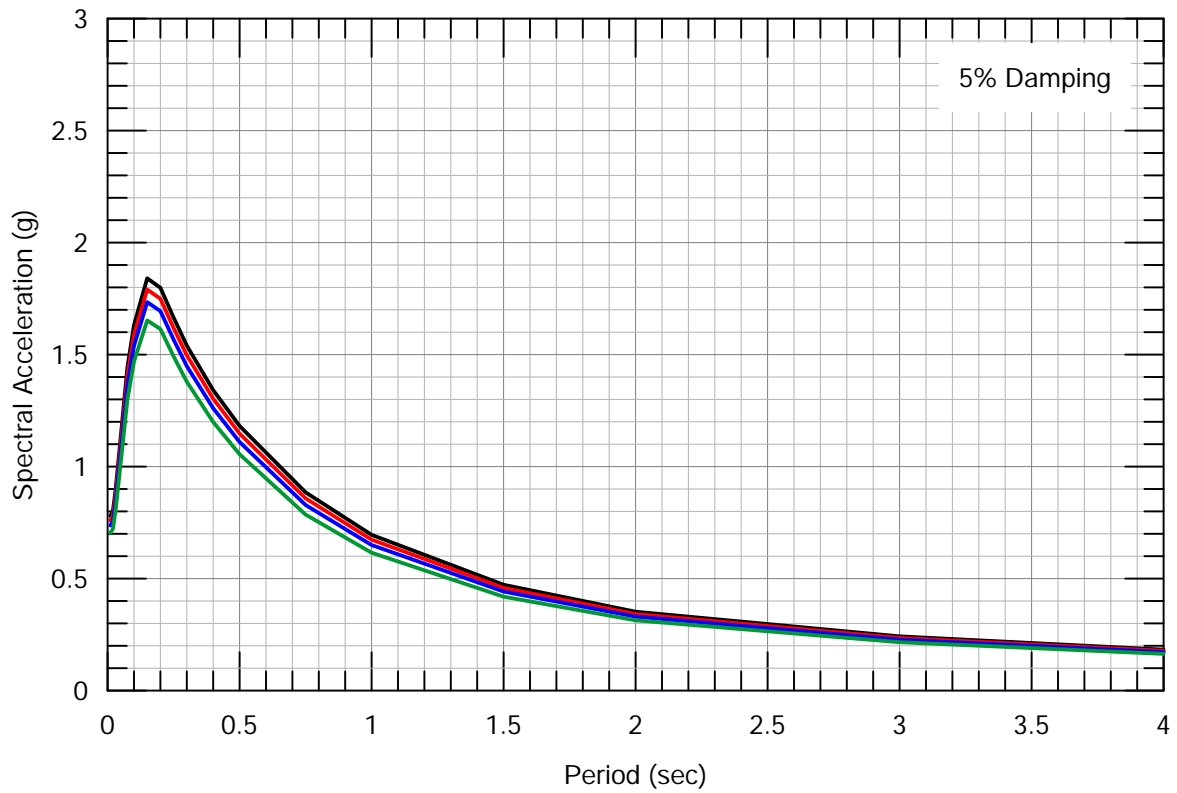
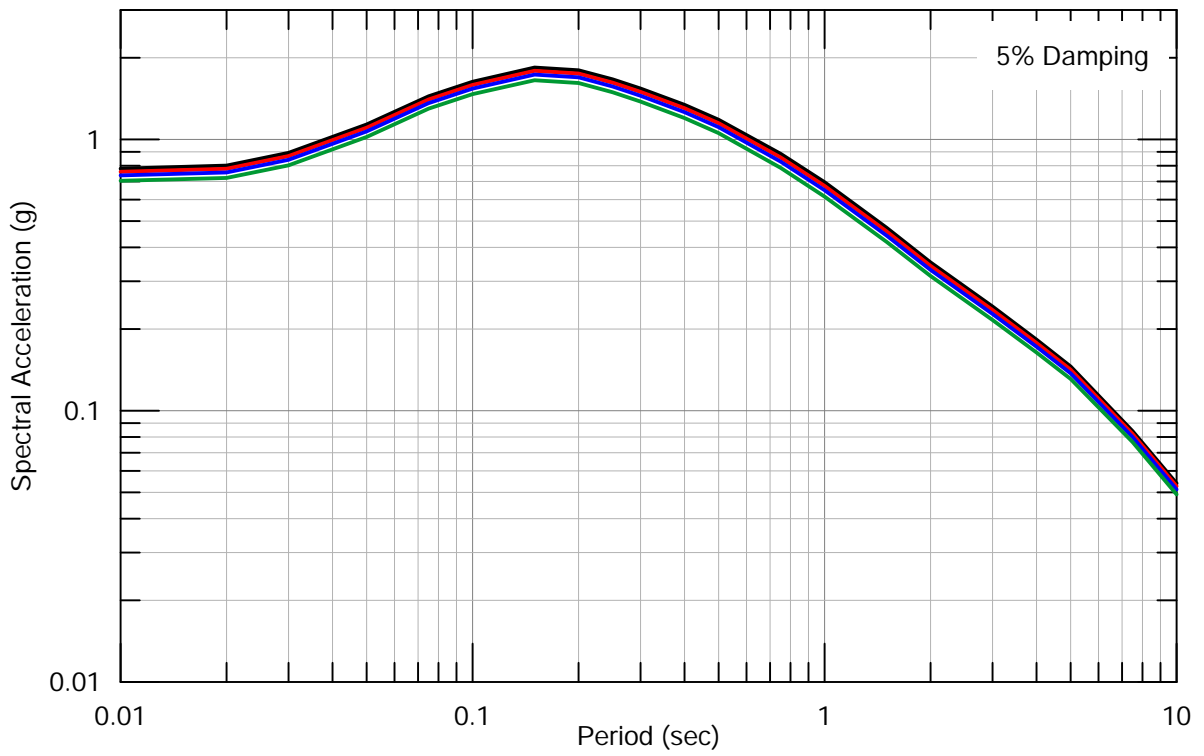
- Geometric Mean
- Abrahamson et al. (2014)
- Boore et al. (2014)
- Campbell and Bozorgnia (2014)
- Chiou and Youngs (2014)

**Sensitivity of 84th Percentile Deterministic Spectrum to Ground Motion Models
Zone 0 and V_s 30 760 m/sec**

STANFORD UNIVERSITY



Lettis Consultants International, Inc.



- Zone 0
- Zone 1
- Zone 2
- Zone 3

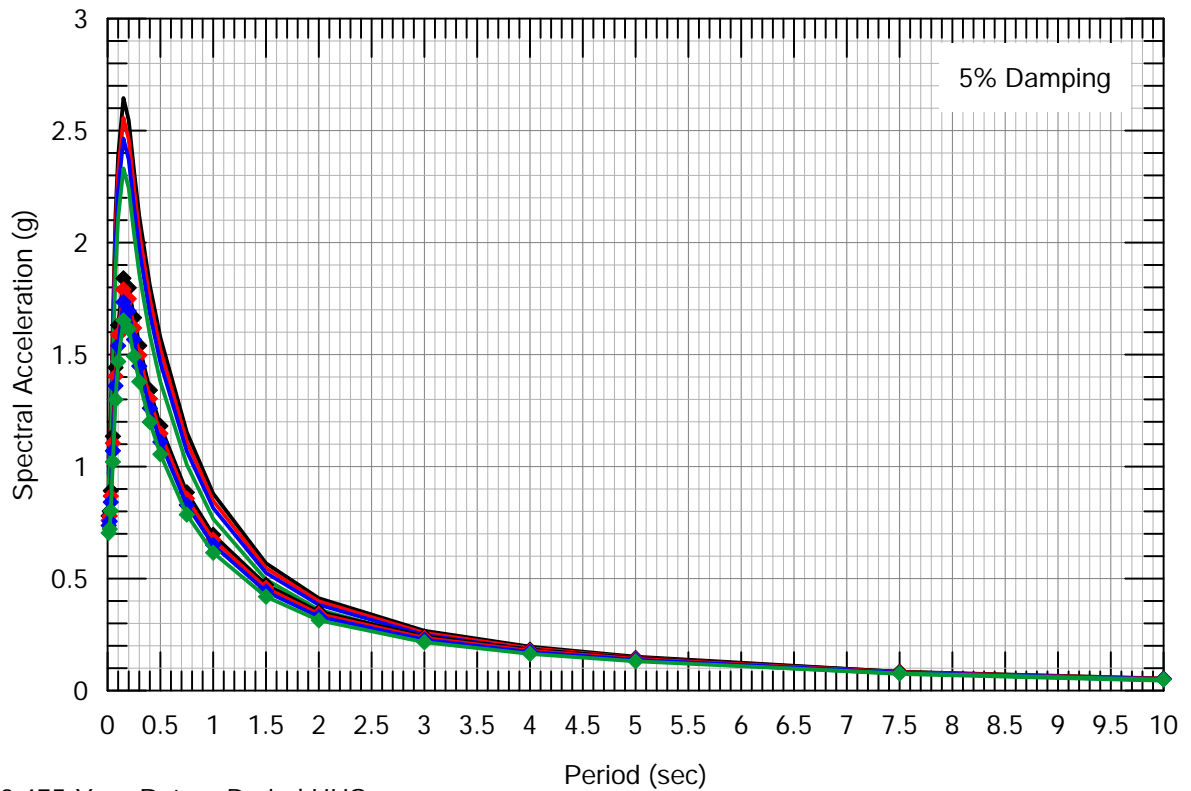
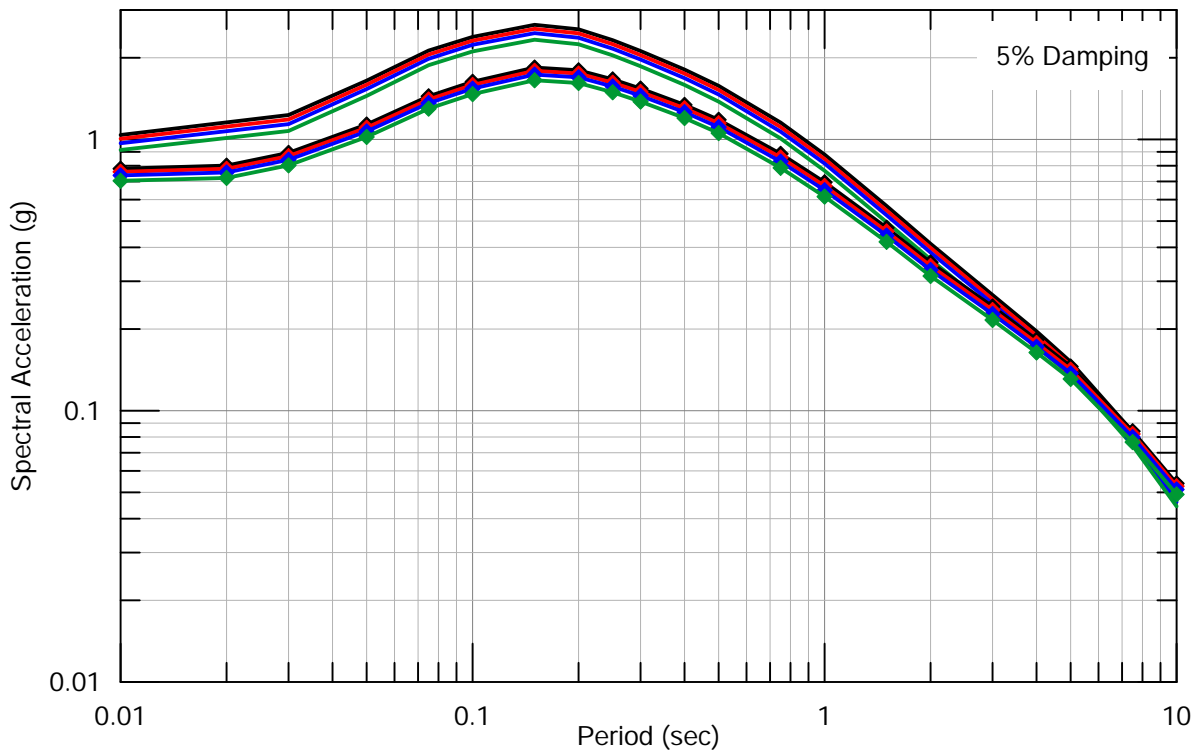
**84th Percentile Deterministic Spectra
for M 8.0 San Andreas Earthquake for
Zones 0, 1, 2 and 3 and V_s 30 760 m/sec**

STANFORD UNIVERSITY

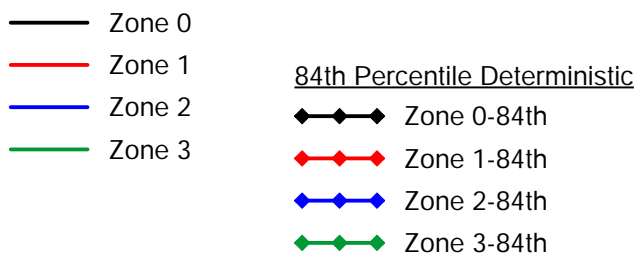


Lettis Consultants International, Inc.

Figure 17



2,475-Year Return Period UHS

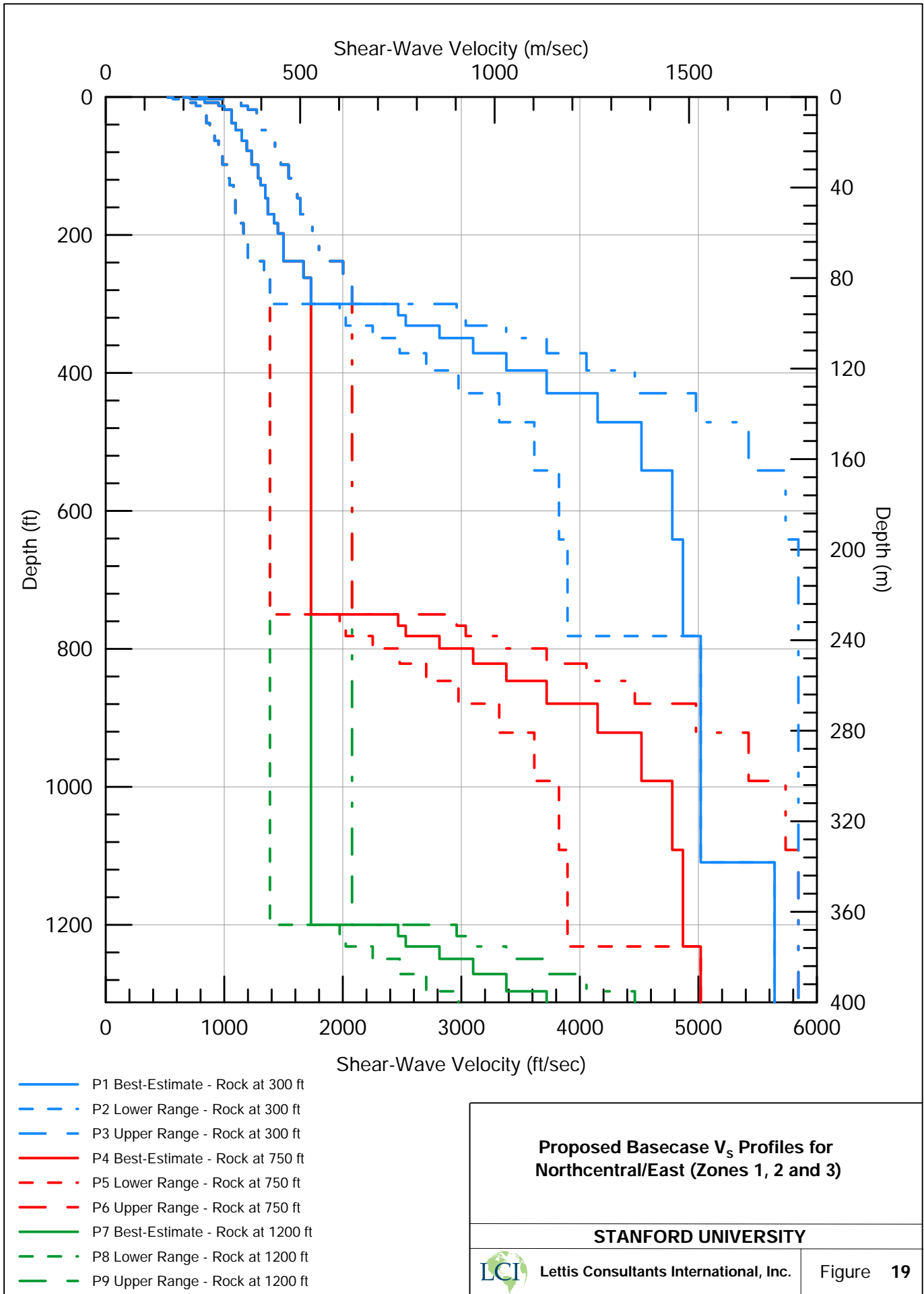


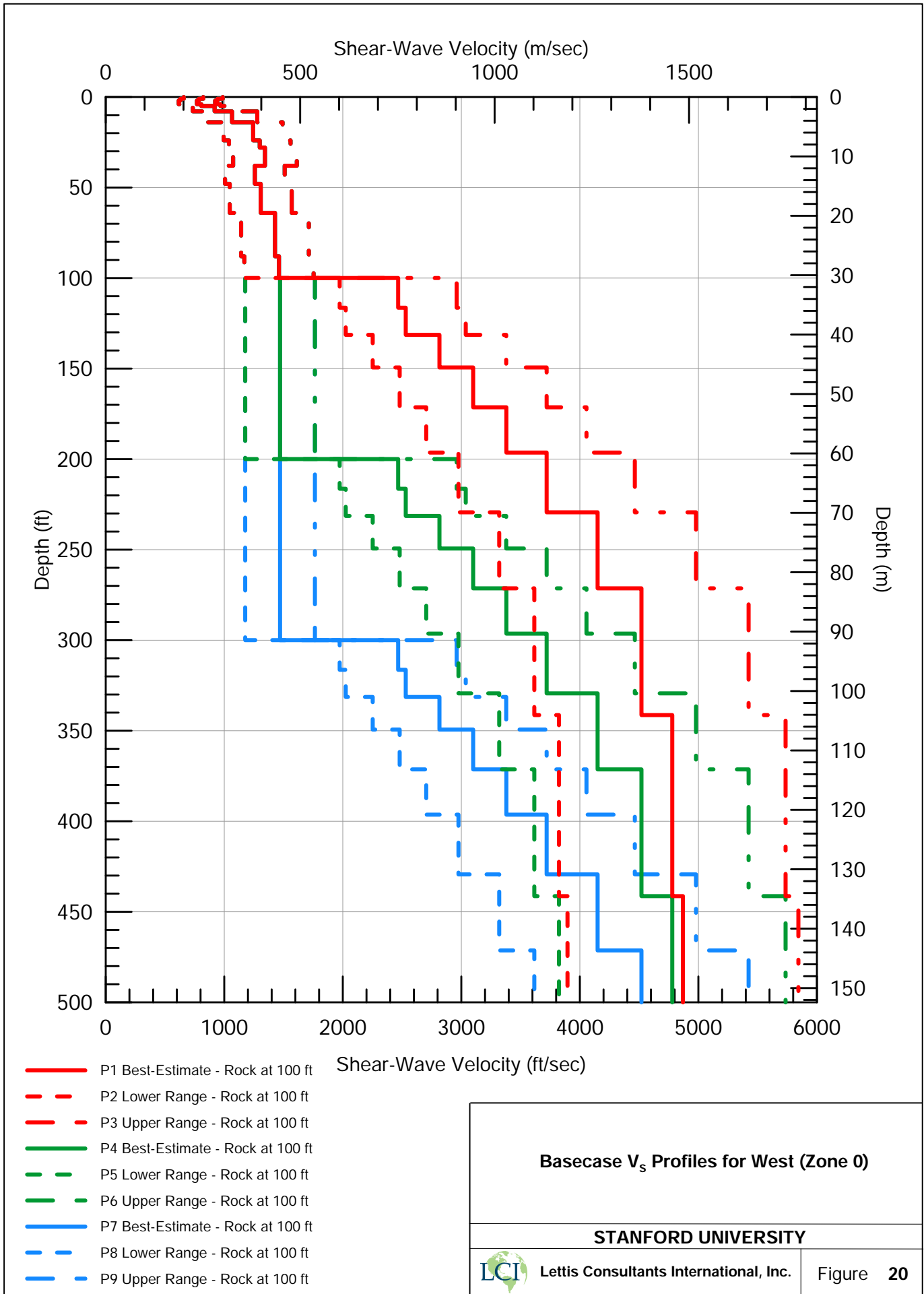
Comparison of Site-Specific 84th Percentile Deterministic Spectra and Uniform Hazard Response Spectra at a 2,475-Year Return Period for Zones 0, 1, 2 and 3

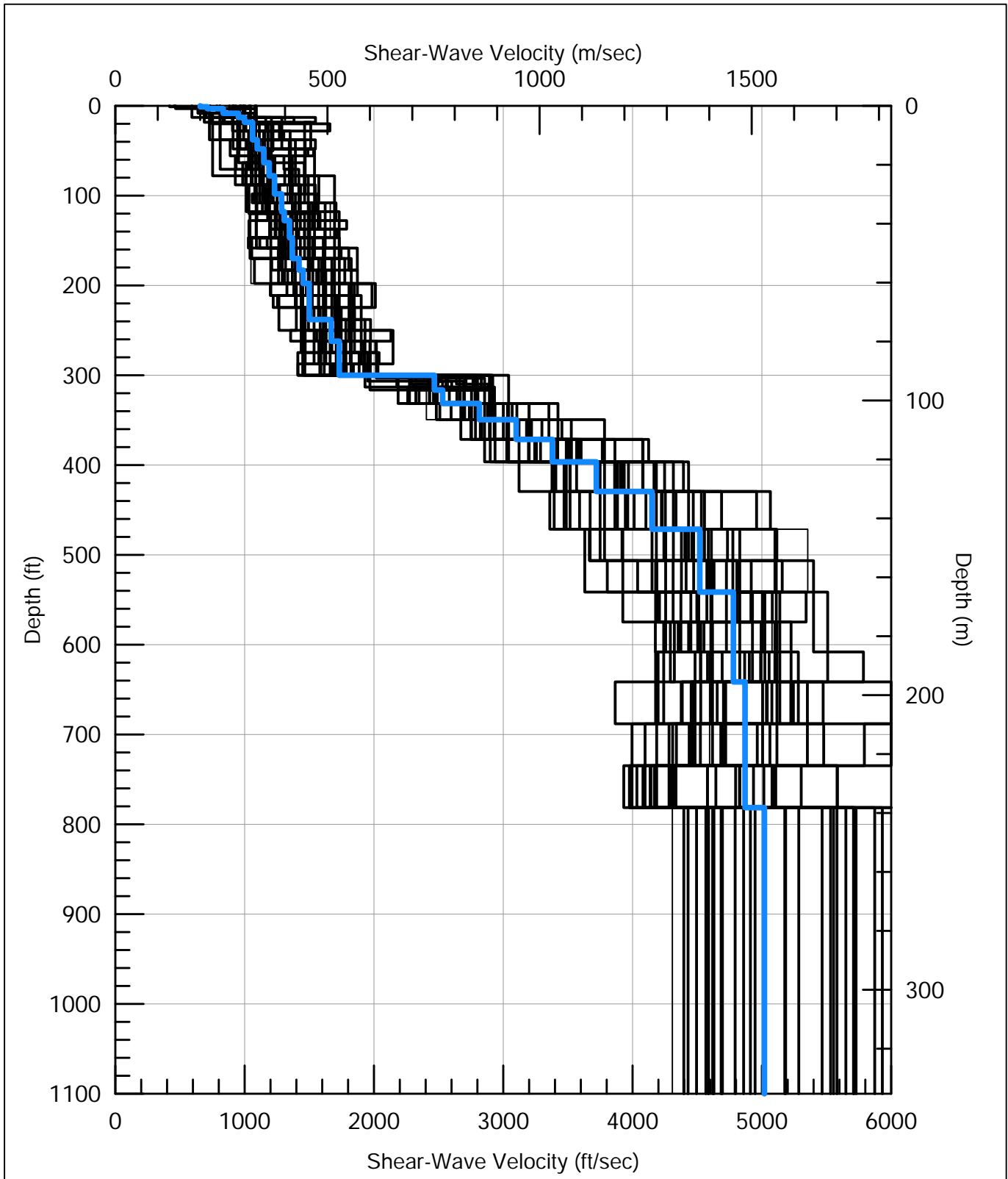
STANFORD UNIVERSITY



Lettis Consultants International, Inc.







Northcentral/East

- P1 Best-Estimate - Rock at 300 ft
- 30 Randomized Vs Profiles

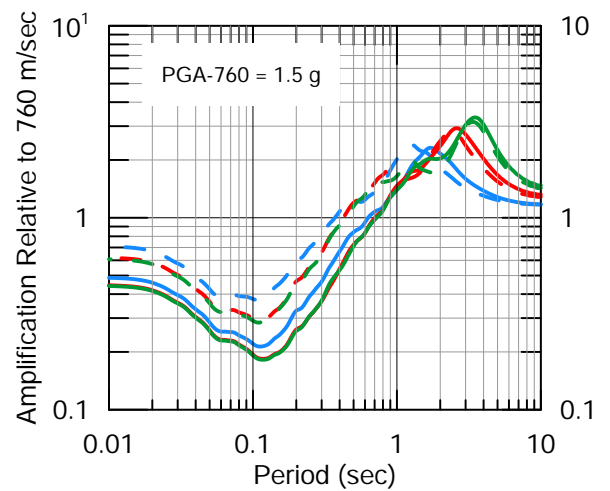
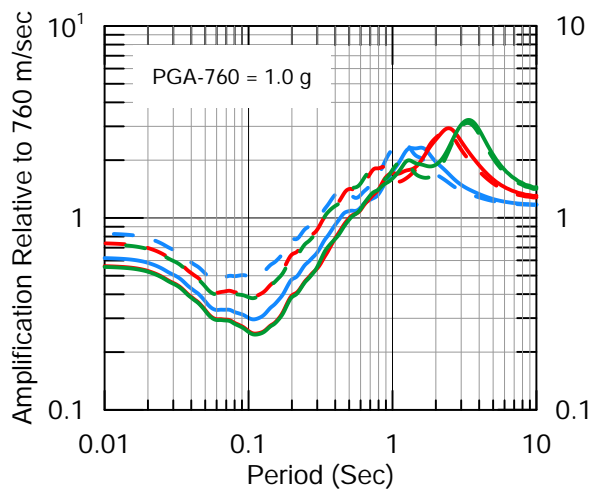
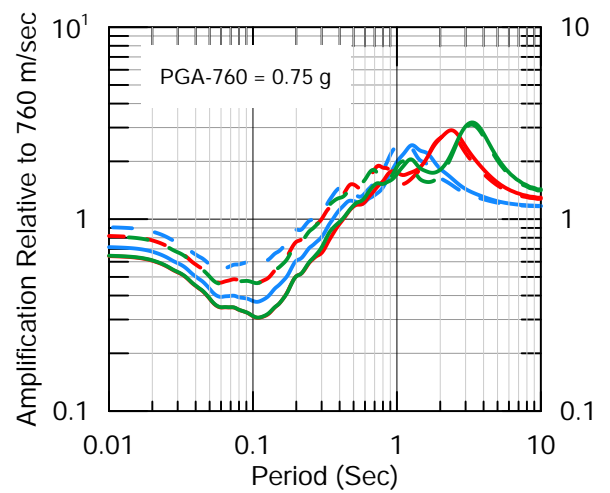
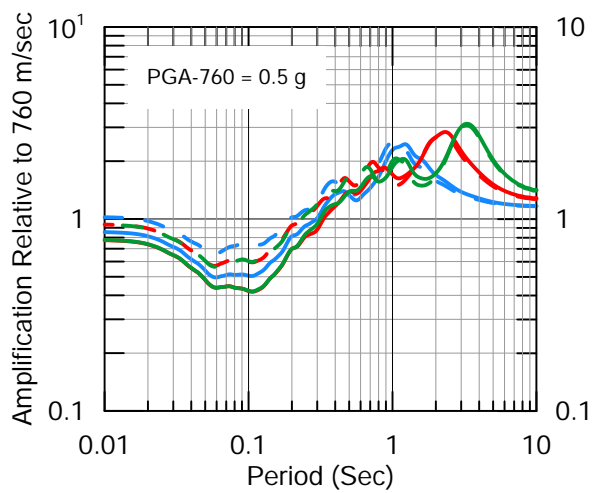
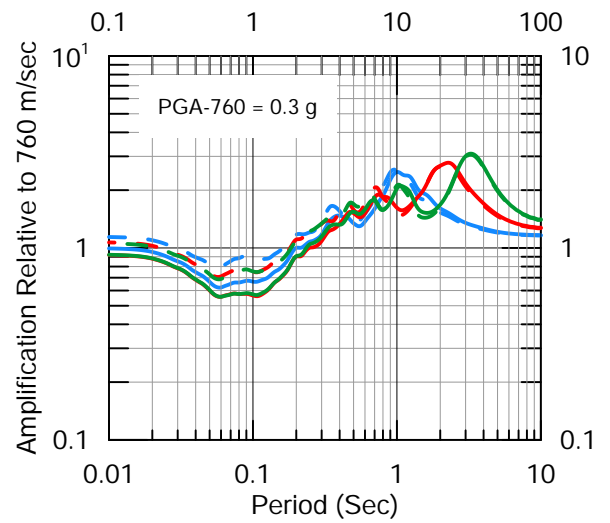
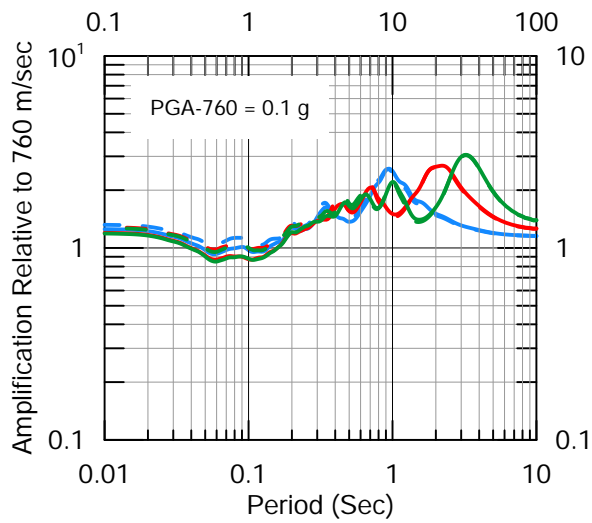
**Randomized Vs Profiles
for Northcentral/East Basecase P1**

STANFORD UNIVERSITY



Lettis Consultants International, Inc.

Figure 21



Site Amplification Factors for Preferred Basecases

- P1, M 7.0, M1
- - - P1, M 7.0, M2
- P4, M 7.0, M1
- - - P4, M 7.0, M2
- P7, M 7.0, M1
- - - P7, M 7.0, M2

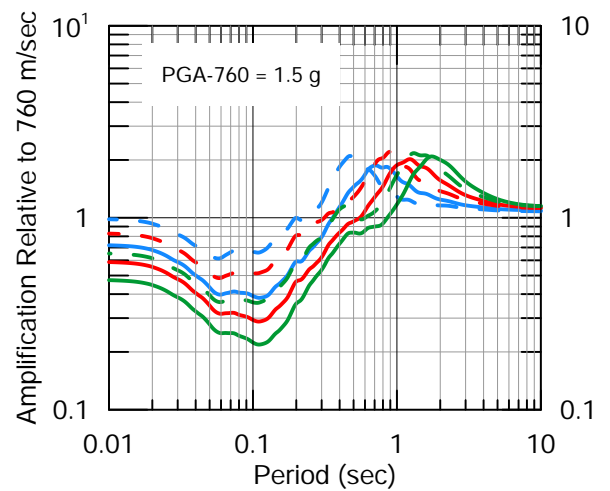
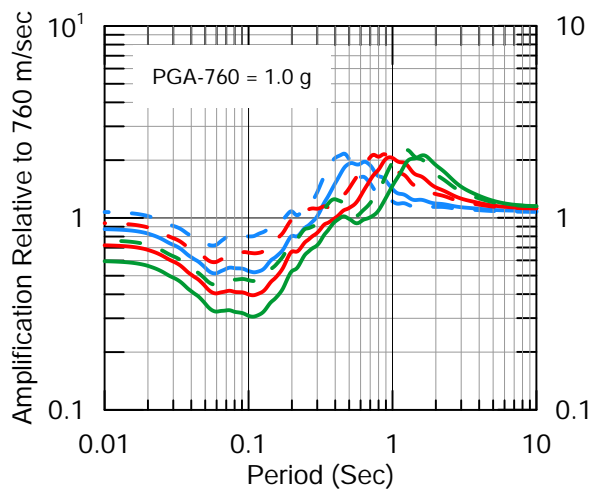
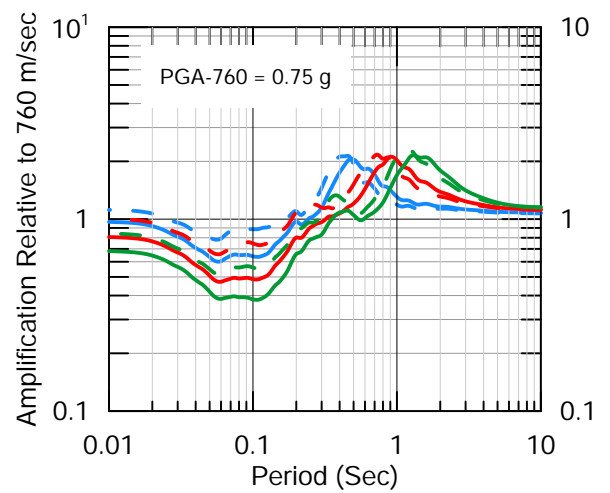
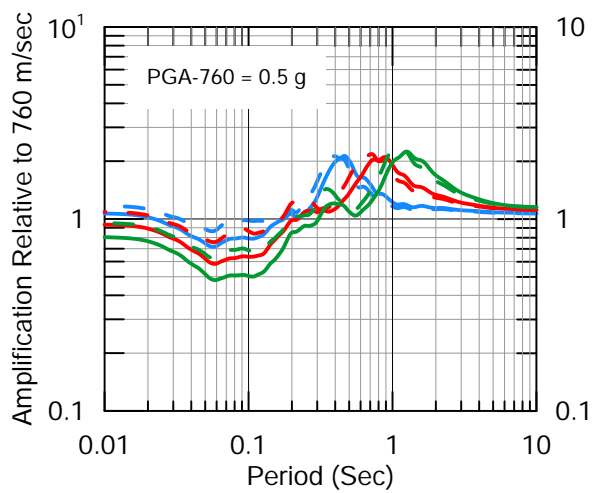
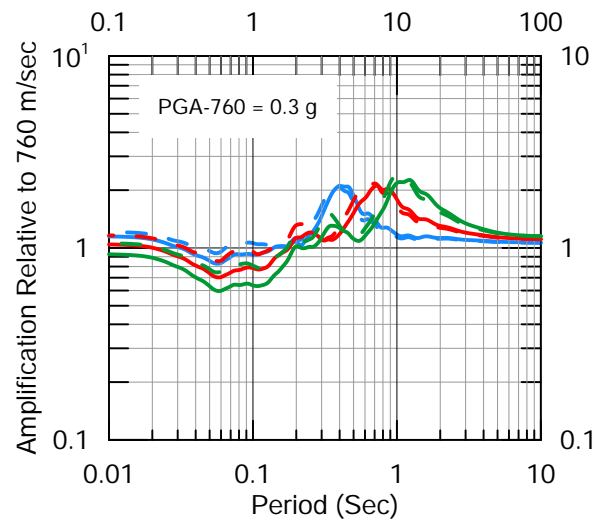
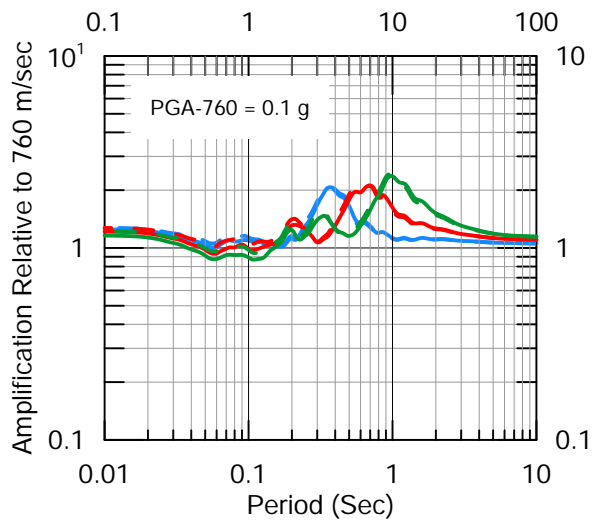
**Sample of Site-Specific Amplification Factors
for Northcentral/East (Zones 1, 2, and 3),
Preferred V_s Basecases P1, P4 and P7**

STANFORD UNIVERSITY



Lettis Consultants International, Inc.

Figure 22



Site Amplification Factors for Preferred Basecases

- P1, M 7.0, M1
- - - P1, M 7.0, M2
- P4, M 7.0, M1
- - - P4, M 7.0, M2
- P7, M 7.0, M1
- - - P7, M 7.0, M2

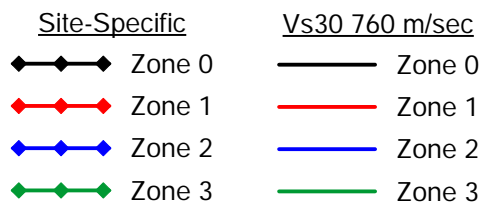
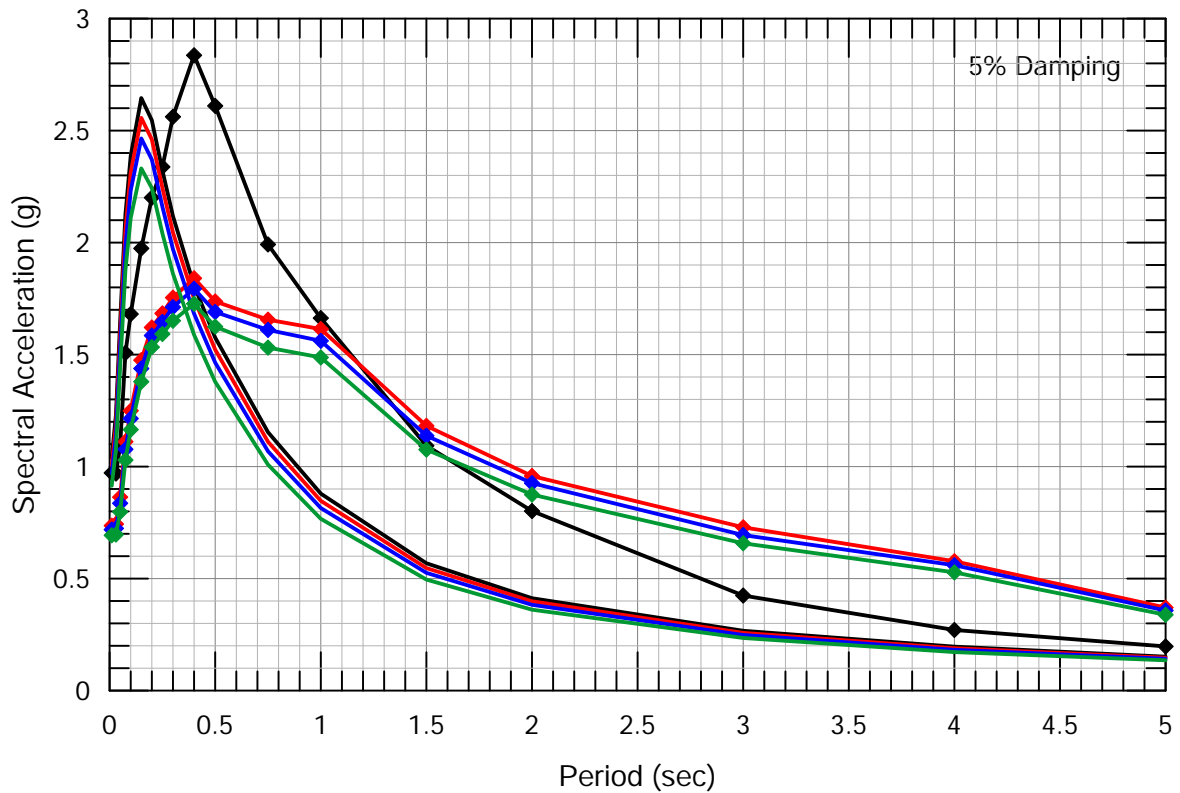
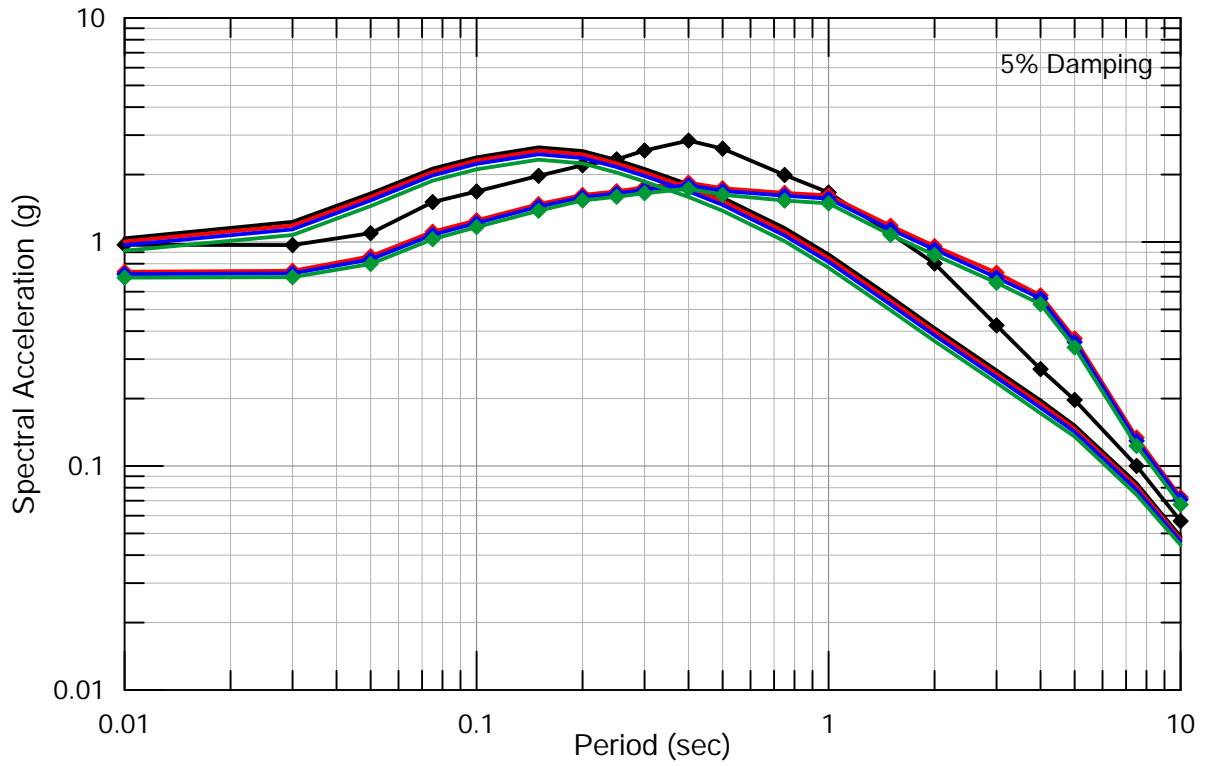
**Sample of Site-Specific Amplification Factors
for West (Zone 0),
Preferred V_s Basecases P1, P4 and P7**

STANFORD UNIVERSITY



Lettis Consultants International, Inc.

Figure 23



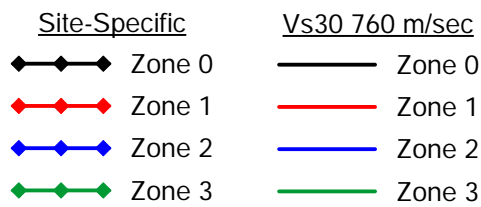
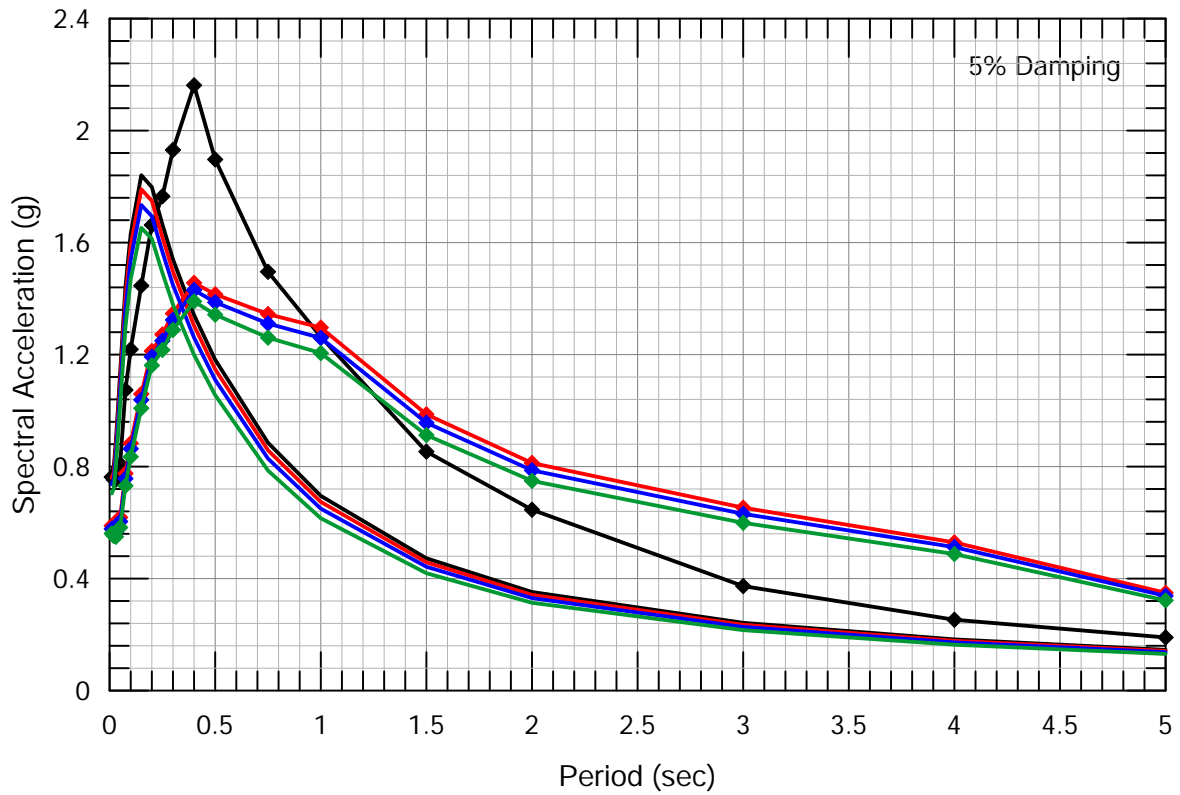
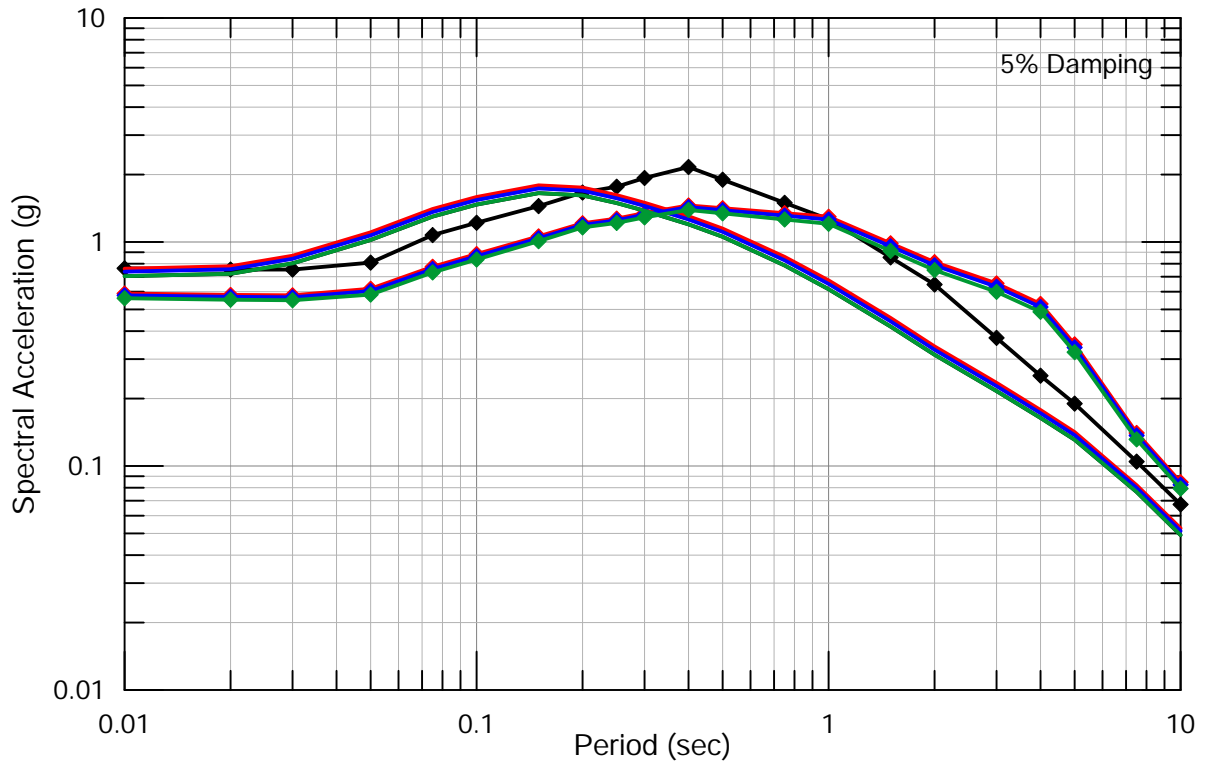
**Site-Specific 5%-Damped, Horizontal
Uniform Hazard Spectra
at 2,475-Year Return Period
for all Zones**

STANFORD UNIVERSITY



Lettis Consultants International, Inc.

Figure 24



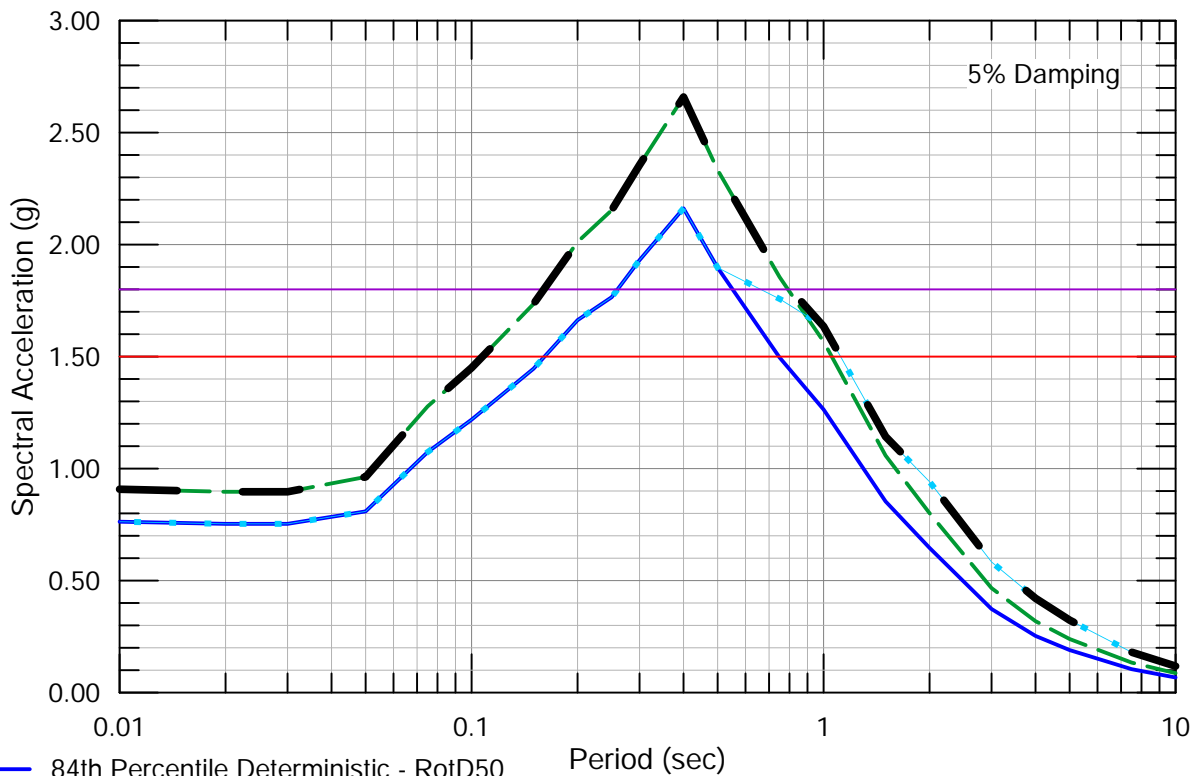
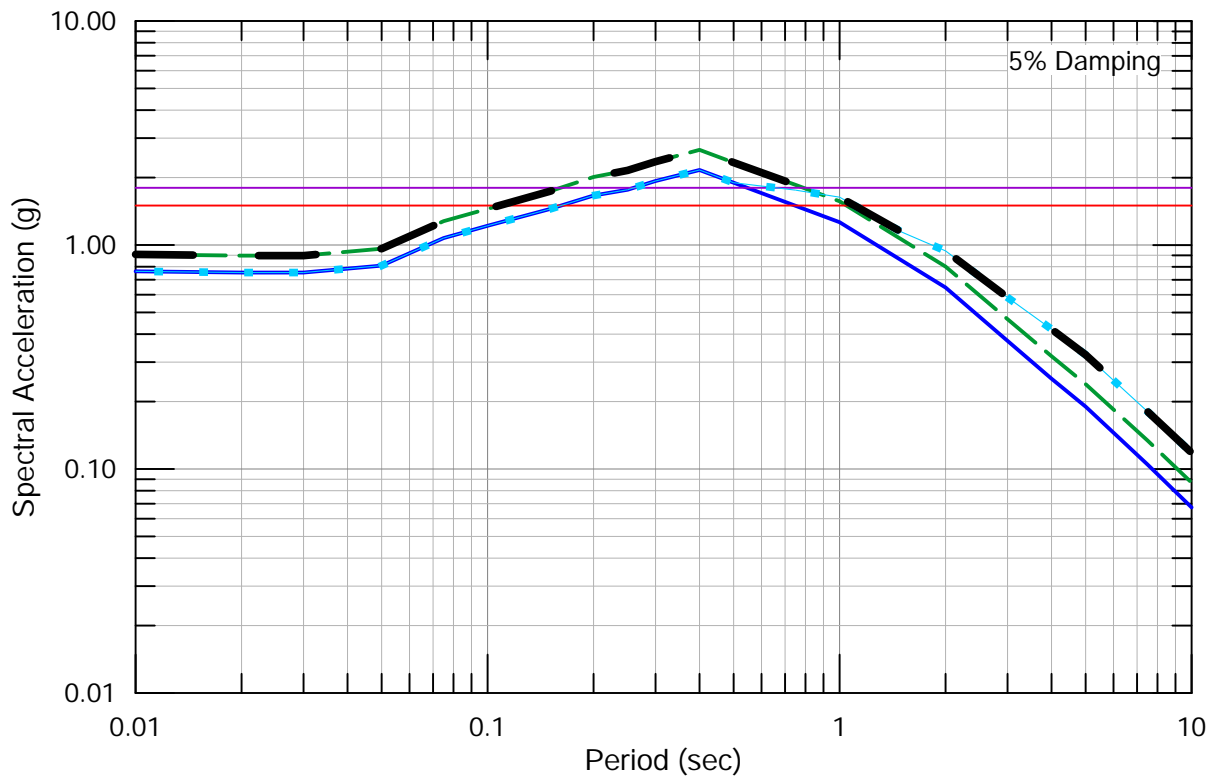
Site-Specific 5%-Damped, Horizontal
84th Percentile Deterministic Spectra
for all Zones

STANFORD UNIVERSITY



Lettis Consultants International, Inc.

Figure 25



- 84th Percentile Deterministic - RotD50
- - 84th Percentile Deterministic - Maximum Direction
- · - 84th Percentile - Fault Normal
- Minimum Deterministic, Site Class C¹
- Minimum Deterministic, Site Class D¹
- Site-Specific Deterministic MCE

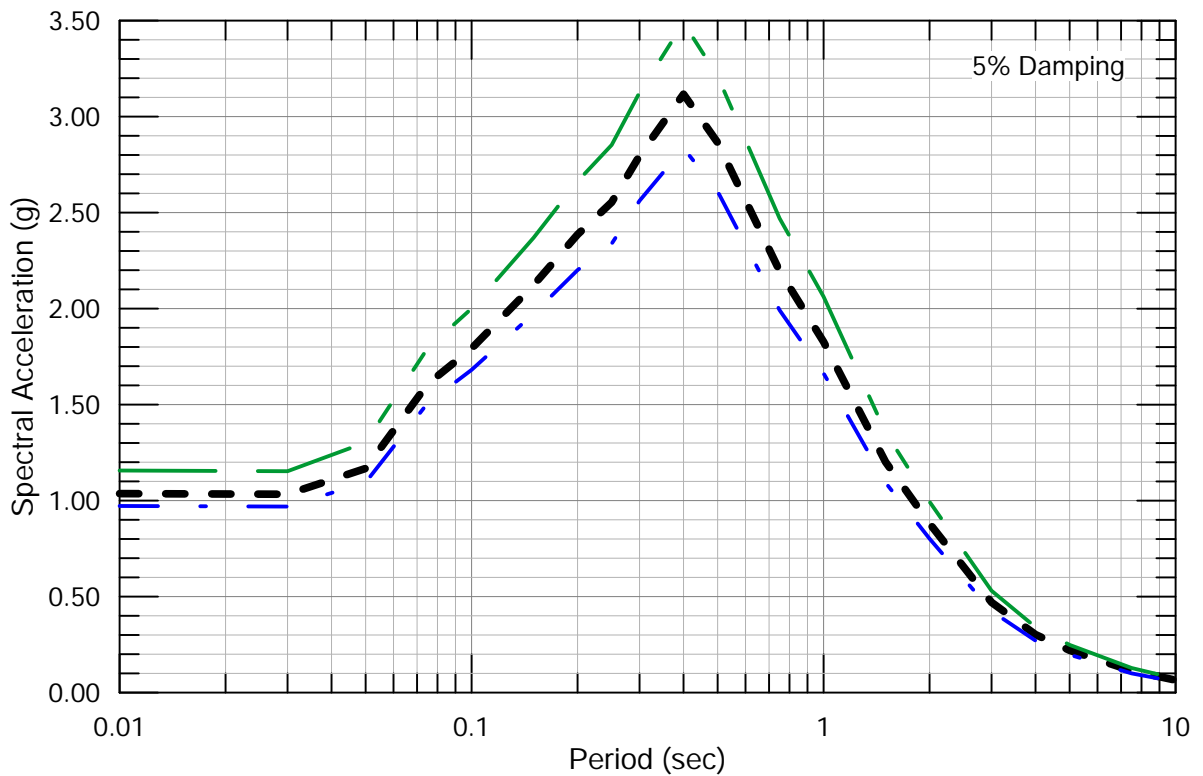
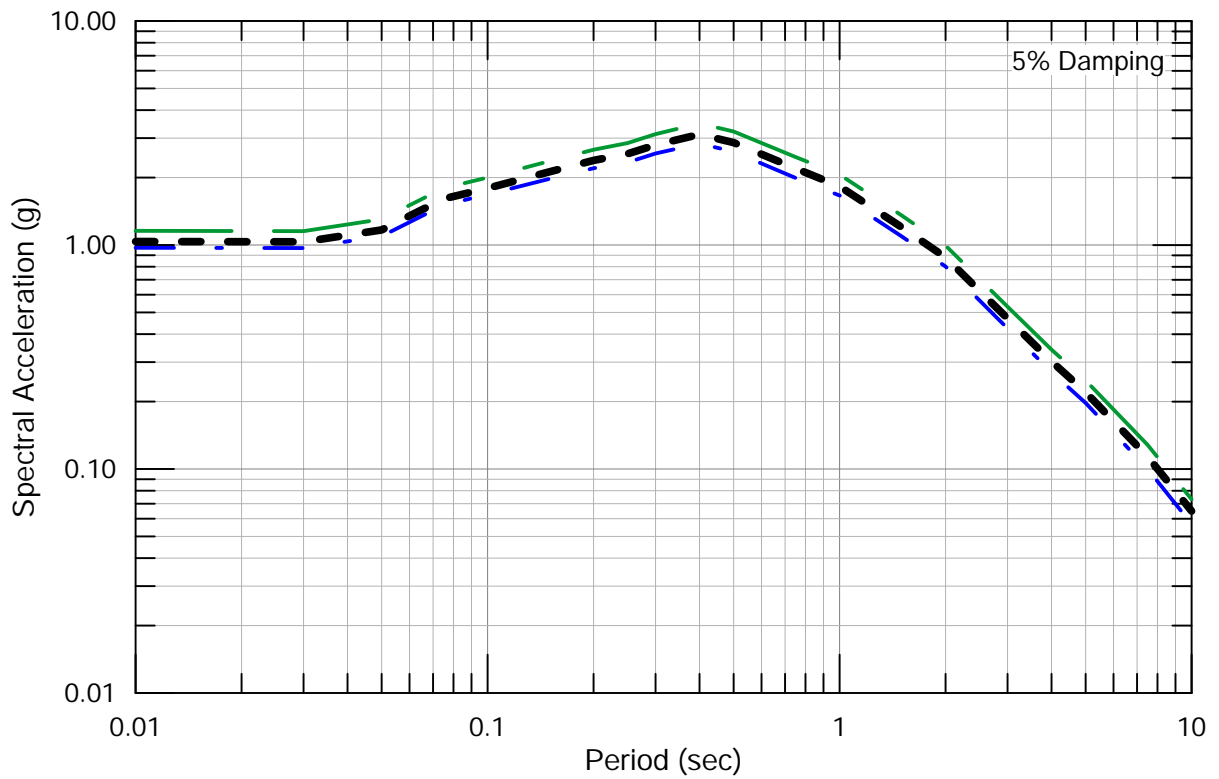
¹As per ASCE 7-16, Supplement 1, largest SA in 84th percentile deterministic spectra must be equal or greater to 1.5*F_a

**Calculation of Site-Specific Deterministic
Horizontal MCE Spectrum as per ASCE 7-16,
Chapter 21 for Zone 0**

STANFORD UNIVERSITY



Lettis Consultants International, Inc.



- · — 2,475-yr UHS - RotD50
- 2,475-yr UHS - Maximum Direction
- - · - - Site-Specific Probabilistic MCE_R -
= Maximum Direction, Risk-Targeted UHS

Note:
Risk coefficients $C_{RS} = 0.896$, $C_{R1} = 0.886$ from
USGS Website

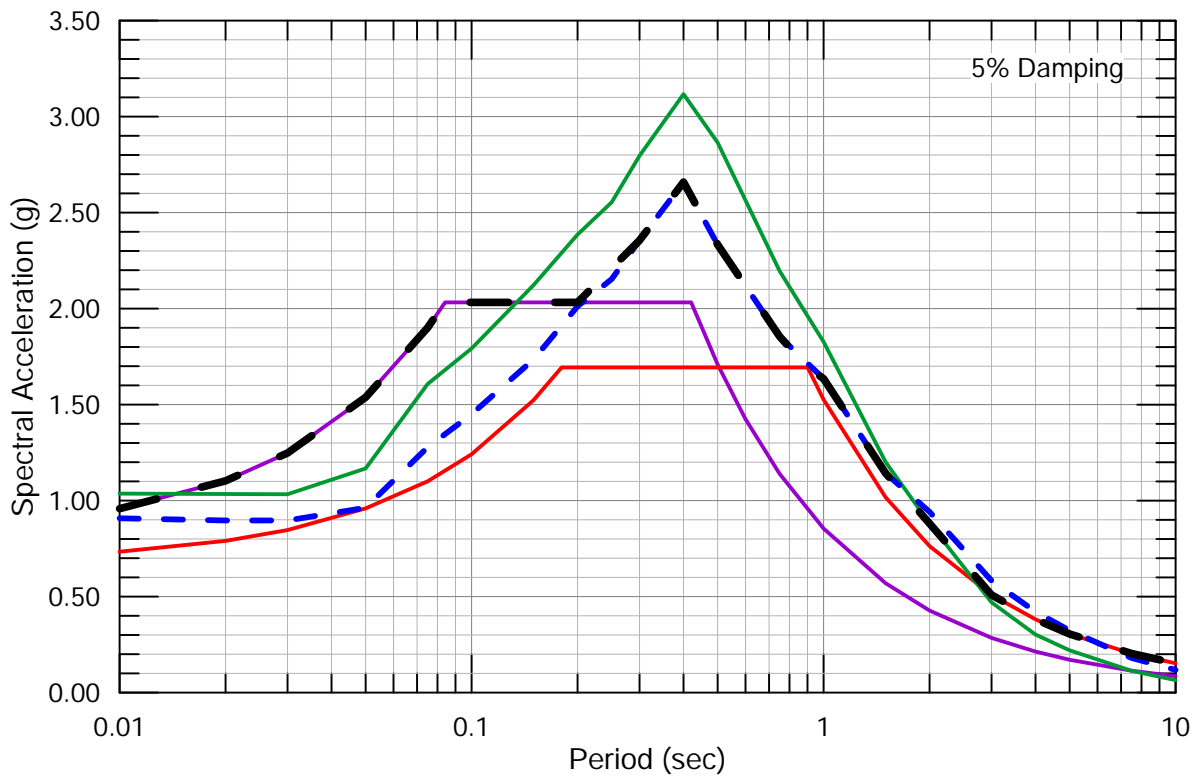
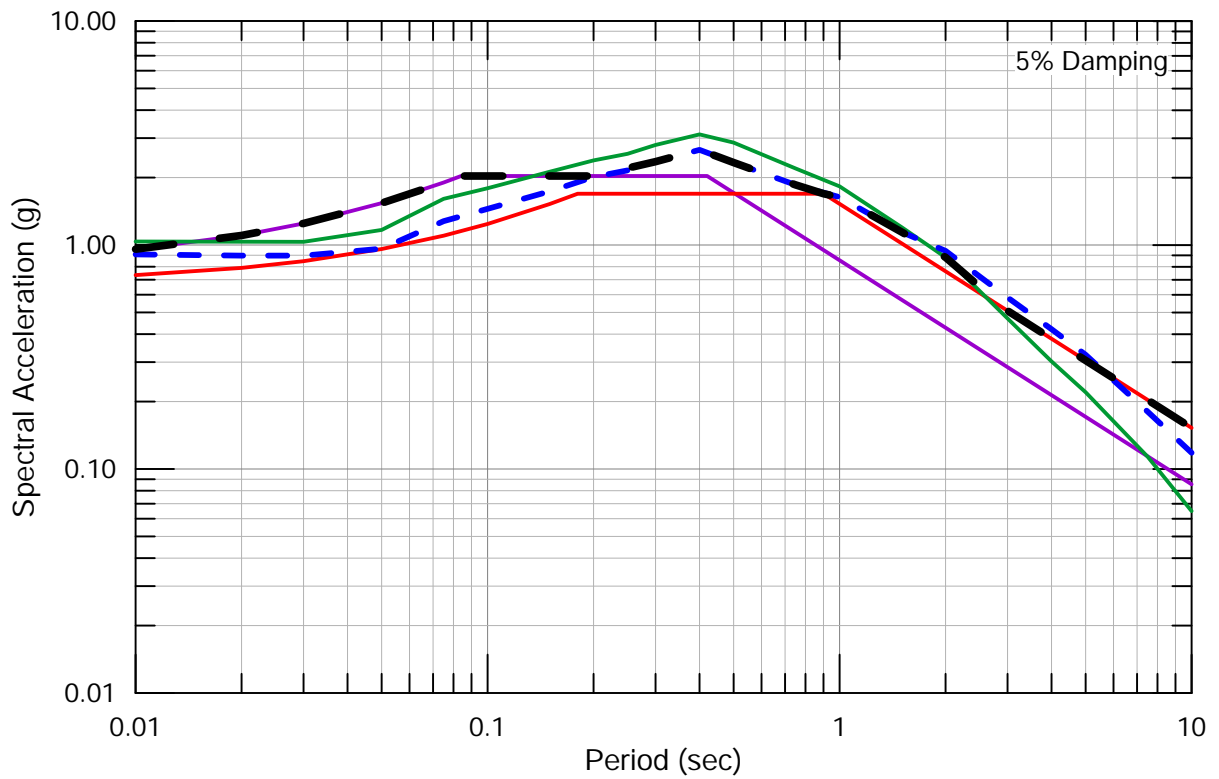
**Calculation of Site-Specific Probabilistic
Horizontal MCE_R Spectrum as per ASCE 7-16,
Chapter 21 for Zone 0**

STANFORD UNIVERSITY



Lettis Consultants International, Inc.

Figure 27



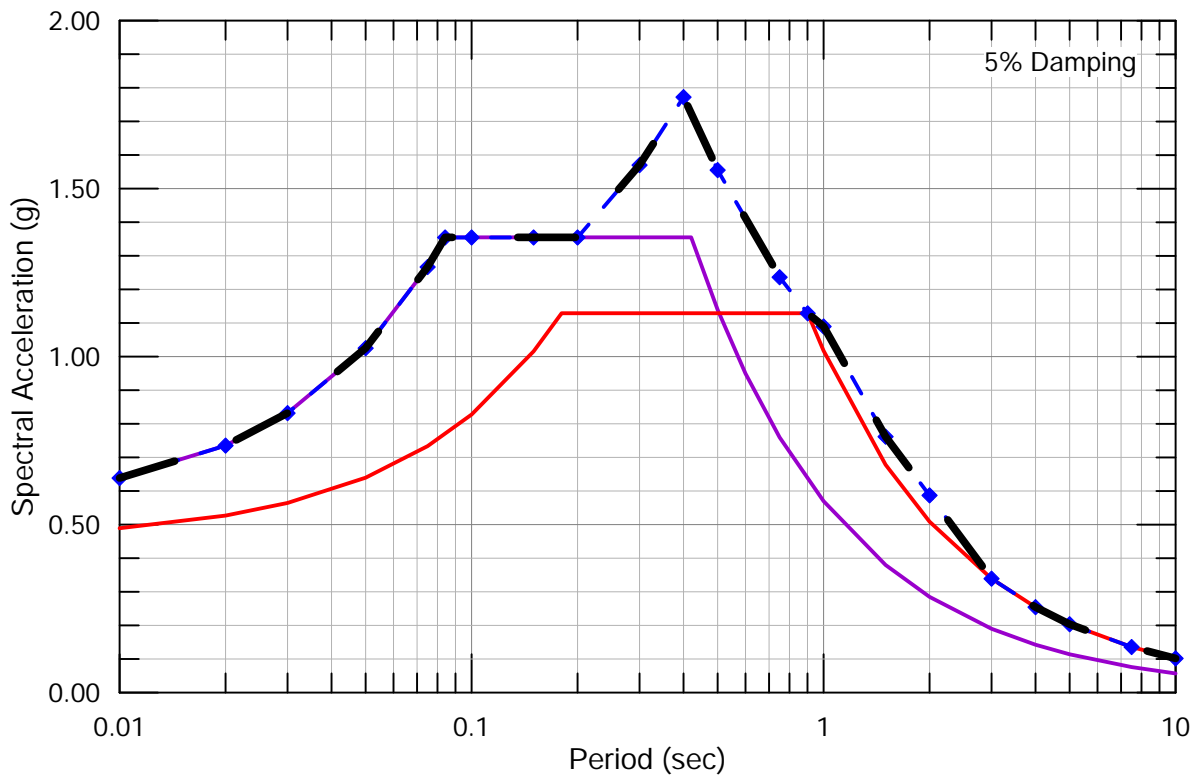
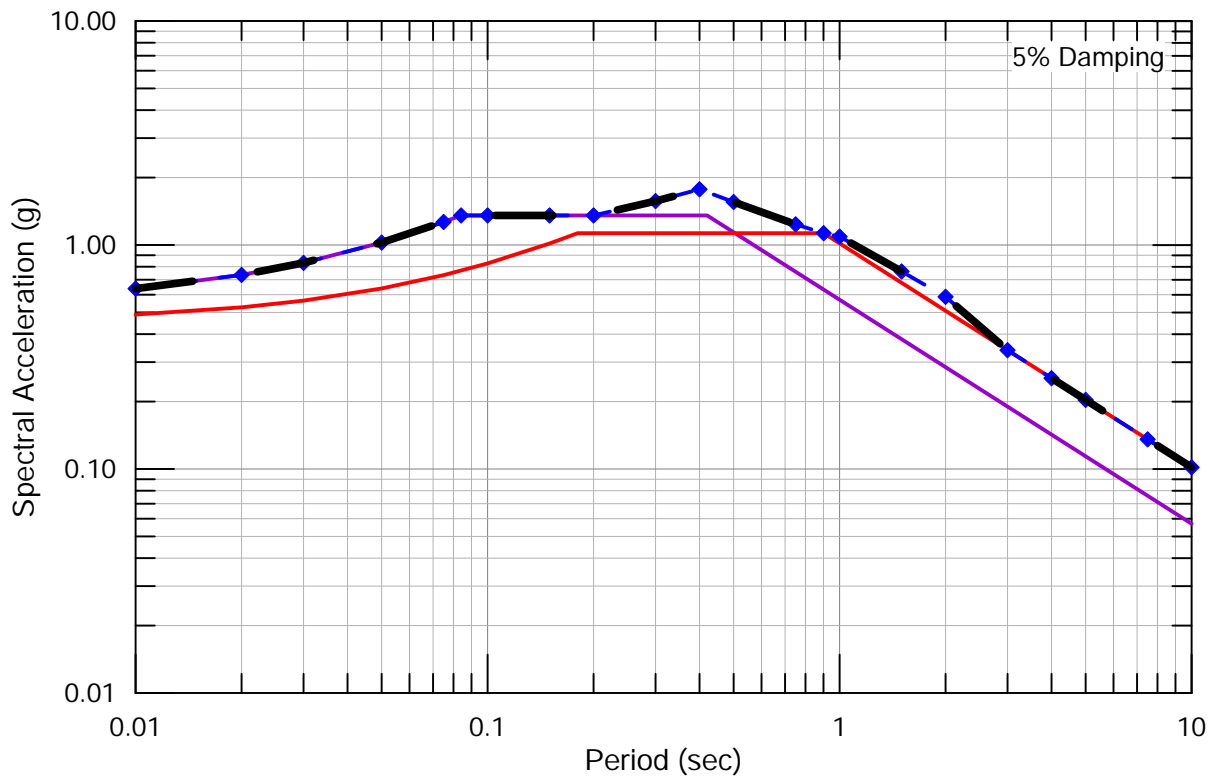
- Deterministic MCE
- Probabilistic MCE_R
- 80% ASCE 7-16 MCE_R, Site Class C (Fa = 1.2, Fv = 1.4)
- 80% ASCE 7-16 MCE_R, Site Class D (Fa = 1.0, Fv = 2.5)
- - Site-Specific MCE_R

**Site-Specific Horizontal MCE_R Spectrum
as per ASCE 7-16, Chapter 21
for Zone 0**

STANFORD UNIVERSITY



Lettis Consultants International, Inc.



- ◆ — 2/3rds Site-Specific MCE_R
- 80% ASCE 7-16 DE - Site Class C (Fa = 1.2, Fv = 1.4)
- 80% ASCE 7-16 DE - Site Class D (Fa = 1.0, Fv = 2.5)
- Site-Specific DE

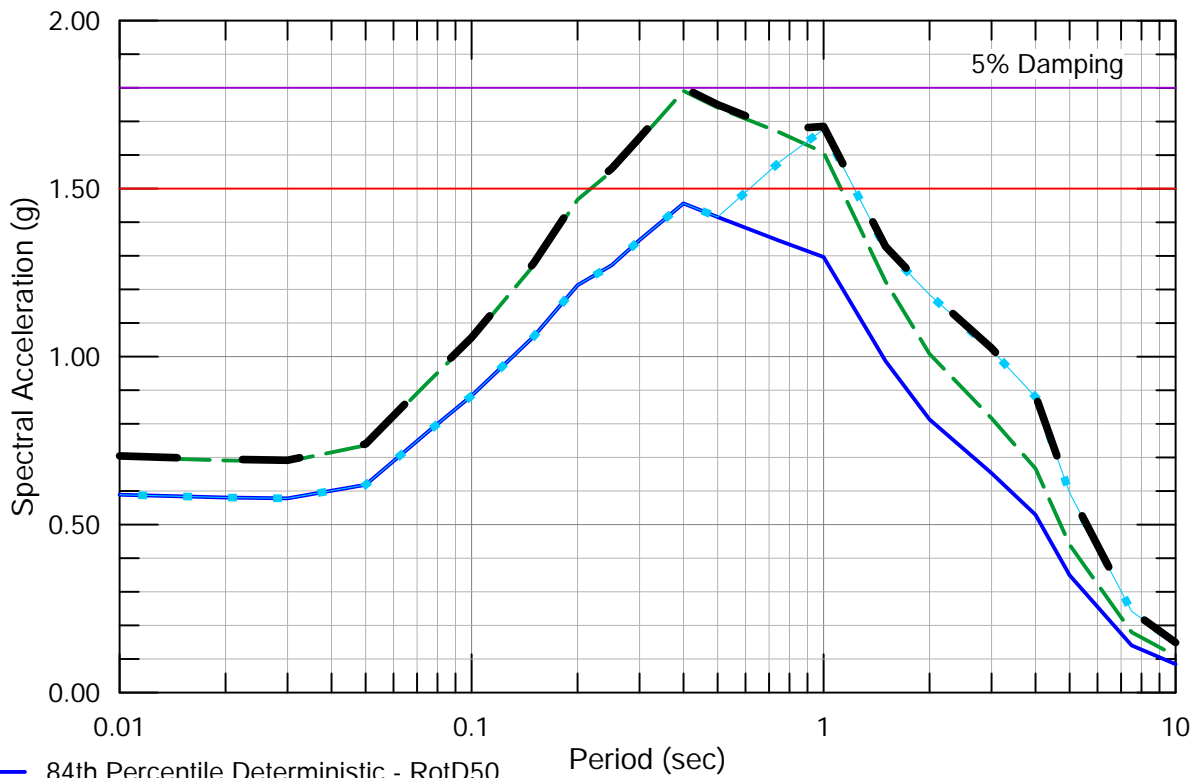
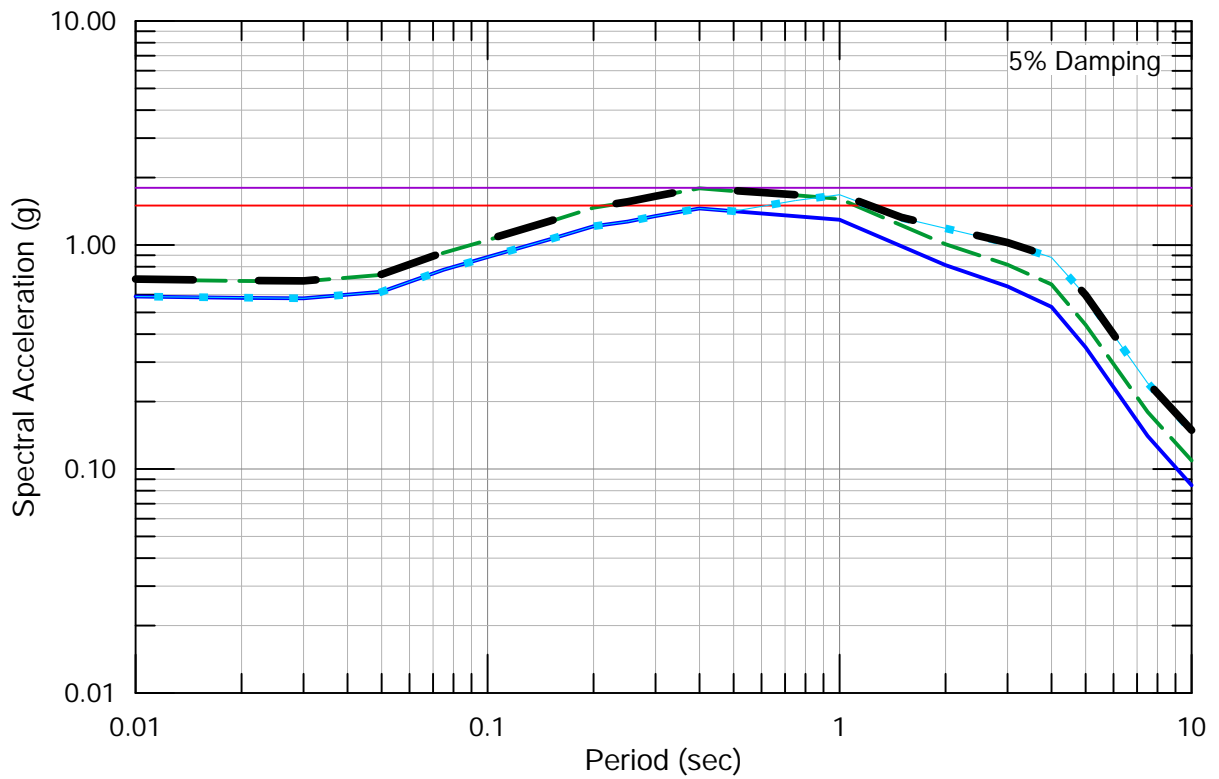
**Site-Specific Horizontal DE Spectrum
as per ASCE 7-16, Chapter 21
for Zone 0**

STANFORD UNIVERSITY



Letis Consultants International, Inc.

Figure 29



- 84th Percentile Deterministic - RotD50
- - - 84th Percentile Deterministic - Maximum Direction
- ■ - 84th Percentile - Fault Normal
- Minimum Deterministic, Site Class C¹
- Minimum Deterministic, Site Class D¹
- Site-Specific Deterministic MCE

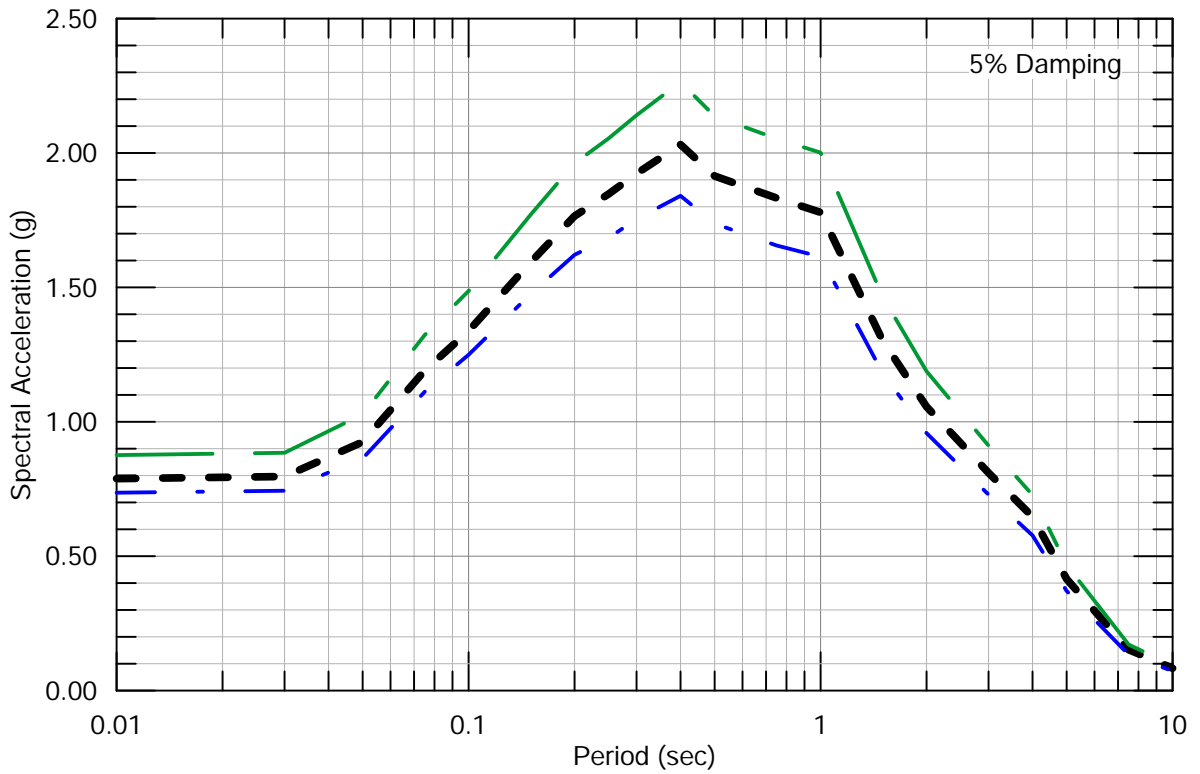
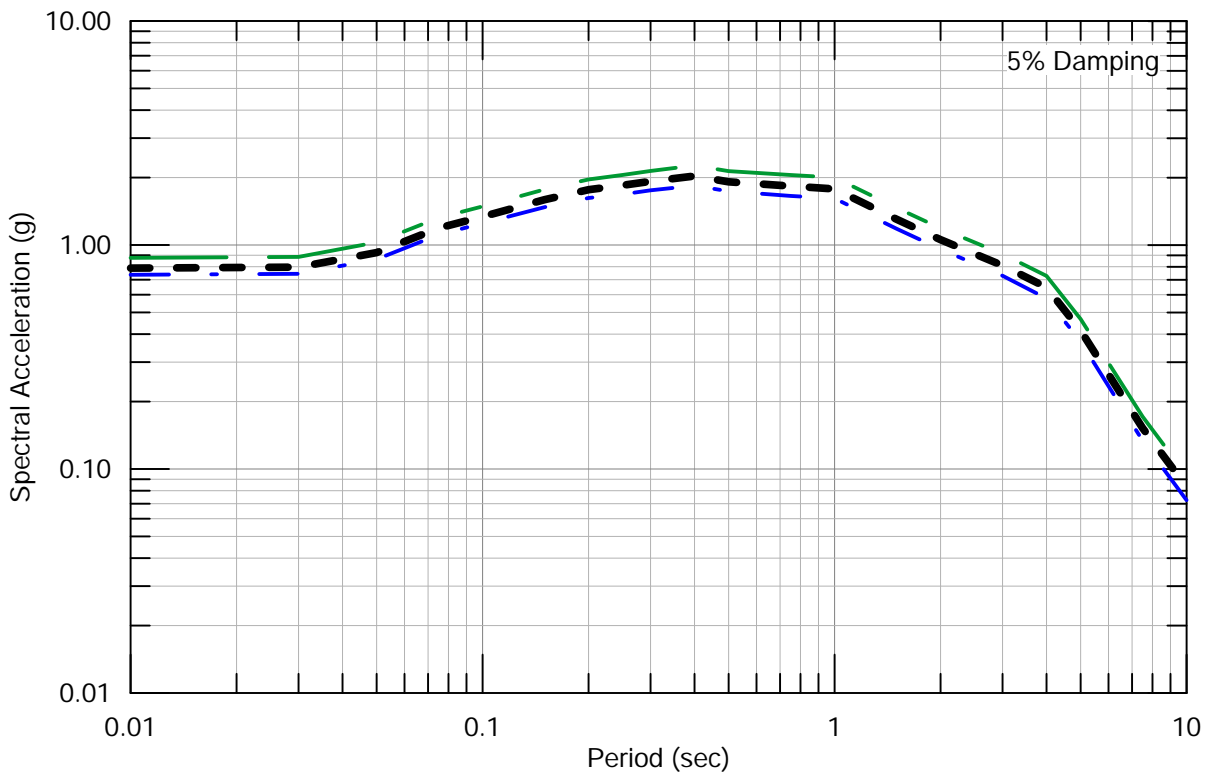
¹As per ASCE 7-16, Supplement 1, largest SA in 84th percentile deterministic spectra must be equal or greater to 1.5*Fa

Calculation of Site-Specific Deterministic Horizontal MCE Spectrum as per ASCE 7-16, Chapter 21 for Zone 1

STANFORD UNIVERSITY



Lettis Consultants International, Inc.



- · — 2,475-yr UHS - RotD50
- 2,475-yr UHS - Maximum Direction
- - · - - Site-Specific Probabilistic MCE_R -
= Maximum Direction, Risk-Targeted UHS

Note:
Risk coefficients $C_{RS} = 0.900$, $C_{R1} = 0.889$ from
USGS Website

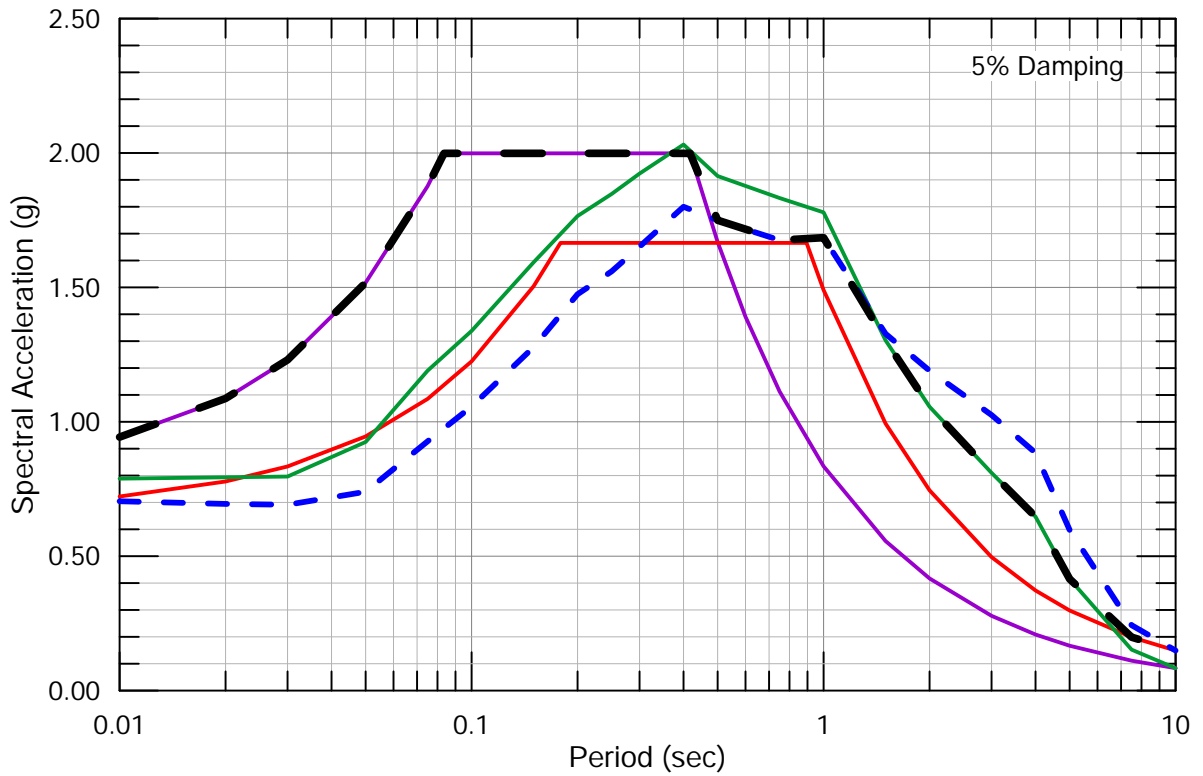
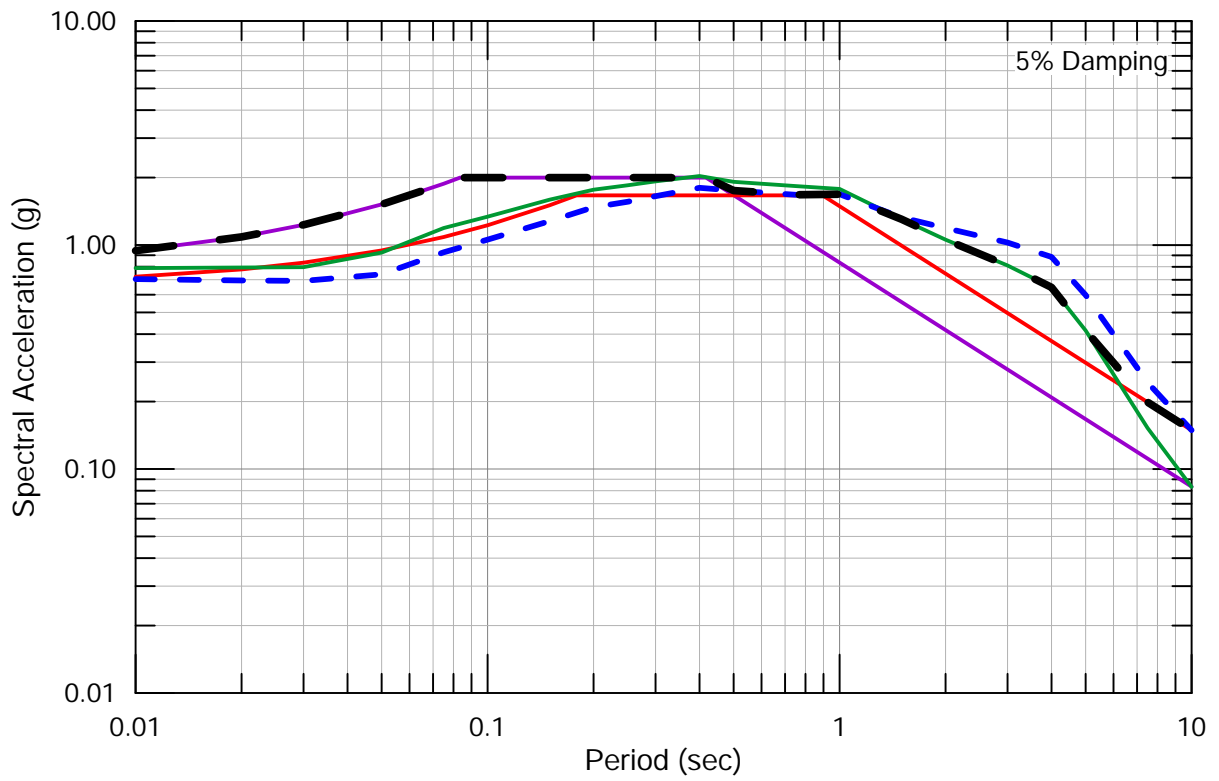
**Calculation of Site-Specific Probabilistic
Horizontal MCE_R Spectrum as per ASCE 7-16,
Chapter 21 for Zone 1**

STANFORD UNIVERSITY



Lettis Consultants International, Inc.

Figure 31



- Deterministic MCE
- Probabilistic MCE_R
- 80% ASCE 7-16 MCE_R, Site Class C (Fa = 1.2, Fv = 1.4)
- 80% ASCE 7-16 MCE_R, Site Class D (Fa = 1.0, Fv = 2.5)
- Site-Specific MCE_R

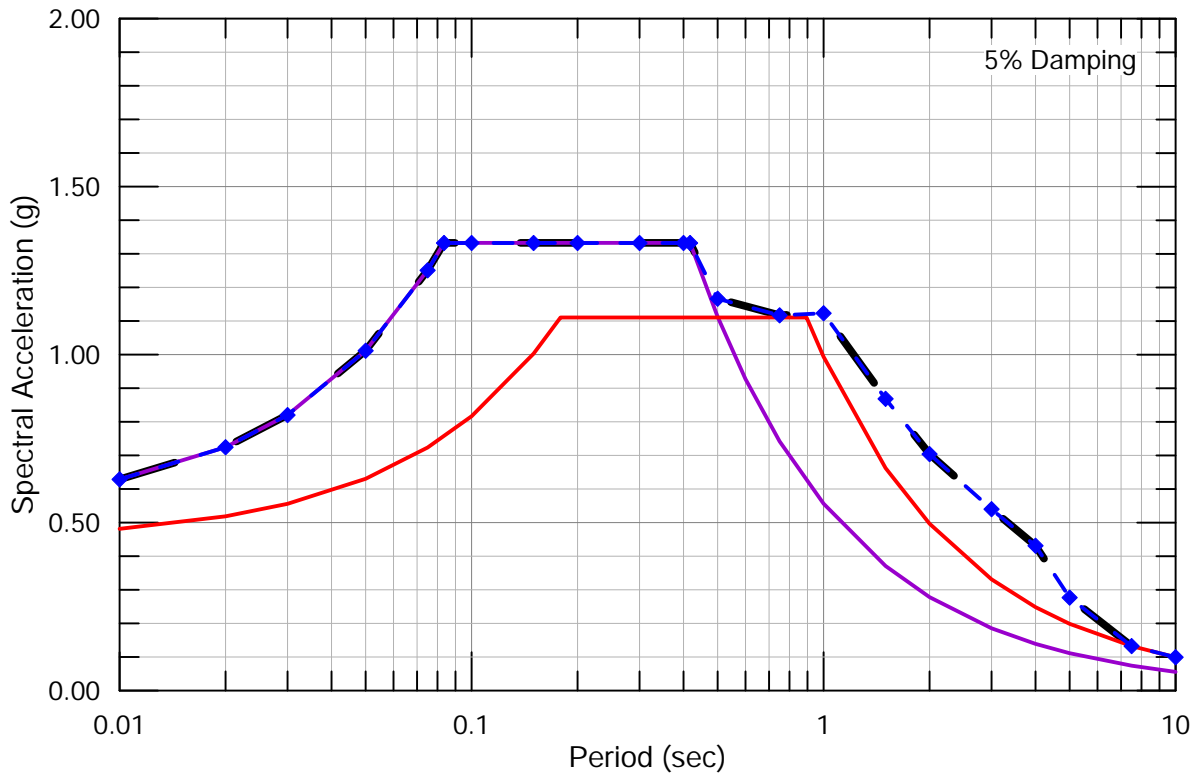
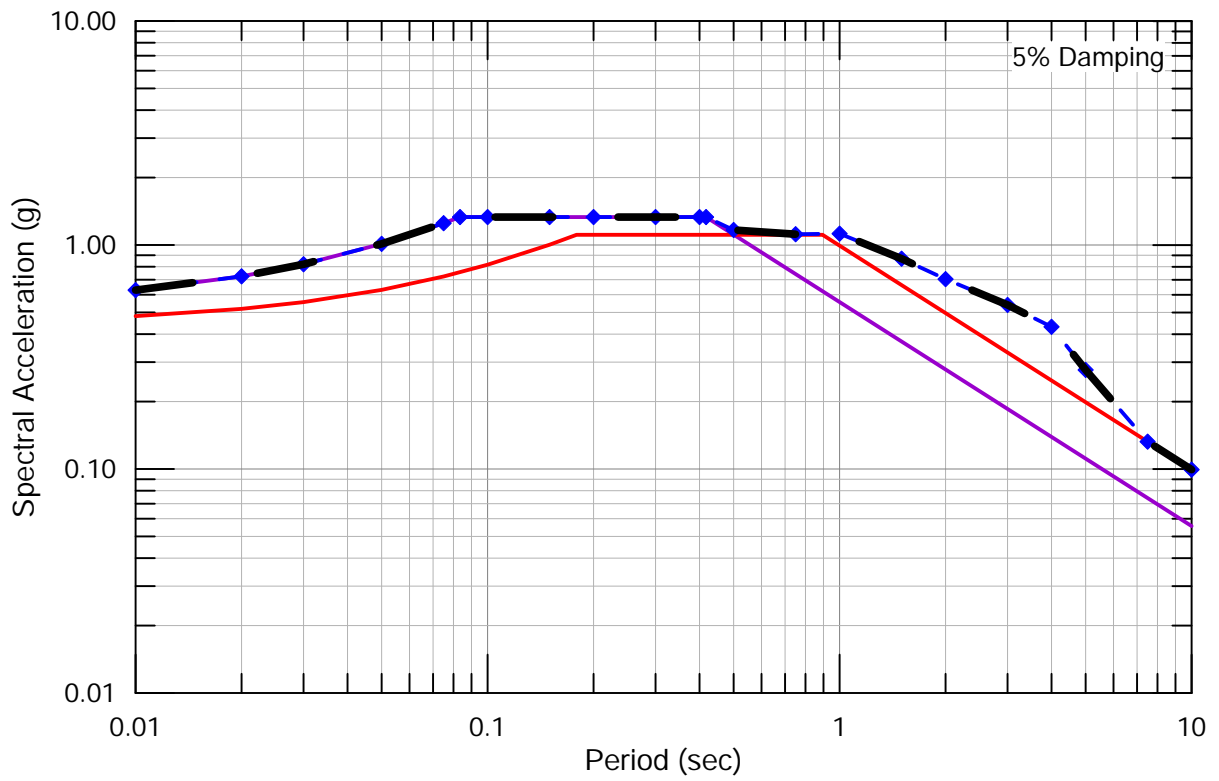
**Site-Specific Horizontal MCE_R Spectrum
as per ASCE 7-16, Chapter 21
for Zone 1**

STANFORD UNIVERSITY



Lettis Consultants International, Inc.

Figure 32



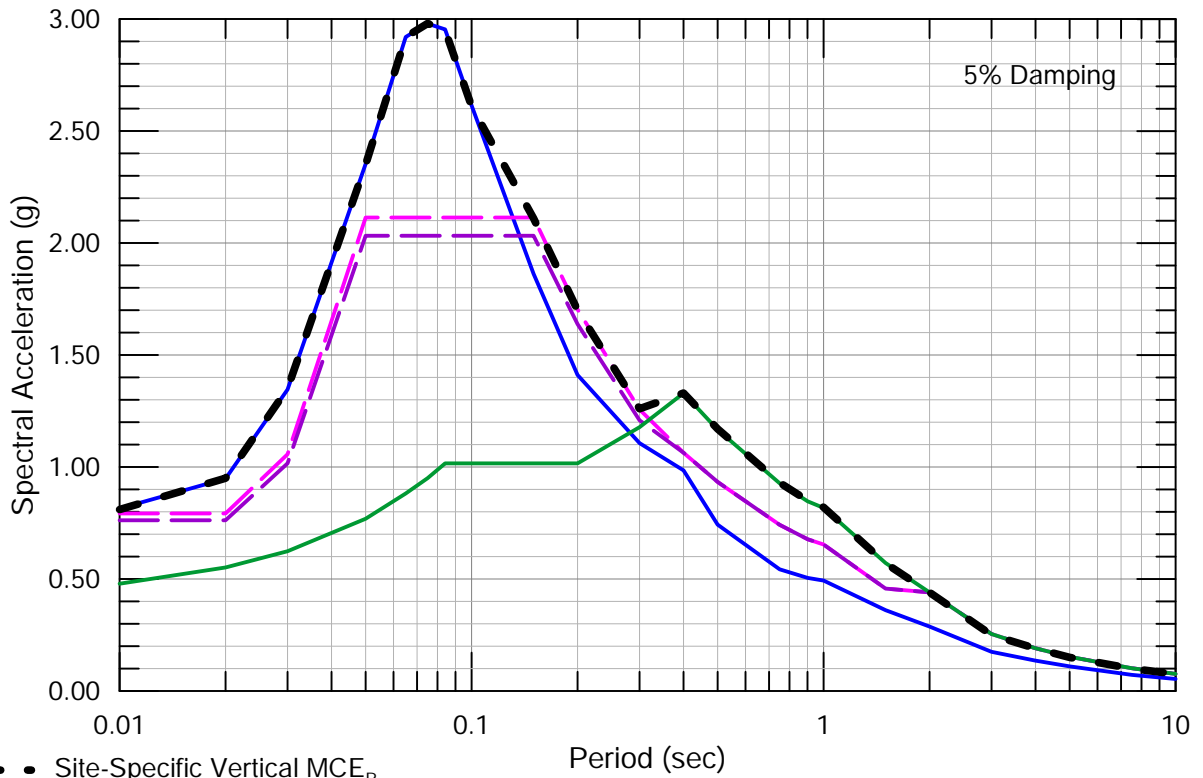
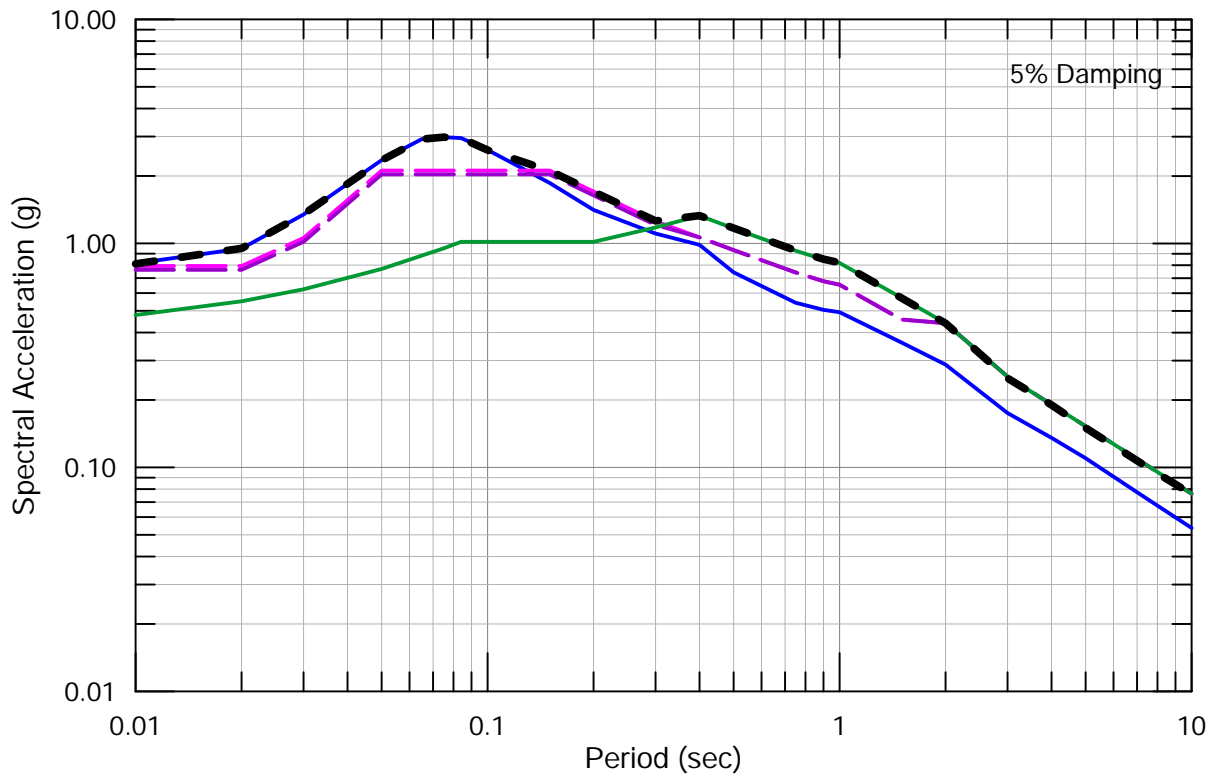
- ◆ — 2/3rds Site-Specific MCE_R
- 80% ASCE 7-16 DE - Site Class C (Fa = 1.2, Fv = 1.4)
- 80% ASCE 7-16 DE - Site Class D (Fa = 1.0, Fv = 2.5)
- Site-Specific DE

**Site-Specific Horizontal DE Spectrum
as per ASCE 7-16, Chapter 21
for Zone 1**

STANFORD UNIVERSITY



Lettis Consultants International, Inc.



- Site-Specific Vertical MCE_R
- Vertical MCE_R using site-specific V/H factors
- 80% ASCE 7-16 Vertical MCE_R , Site Class C
- 80% ASCE 7-16 Vertical MCE_R , Site Class D
- $0.5 \times$ Site-Specific Horizontal MCE_R

Note: ASCE 7-16 Vertical MCE_R spectrum defined per Section 11.9 (site class C: $S_{MS} = 2.54$, $C_v = 1.3$; site class D: $S_{MS} = 2.12$, $C_v = 1.5$) for $T \leq 2$ sec.

For $T > 2$ sec, vertical MCE_R defined as site-specific horizontal $MCE_R \times \min(\text{site-specific V/H factors}, 0.5)$

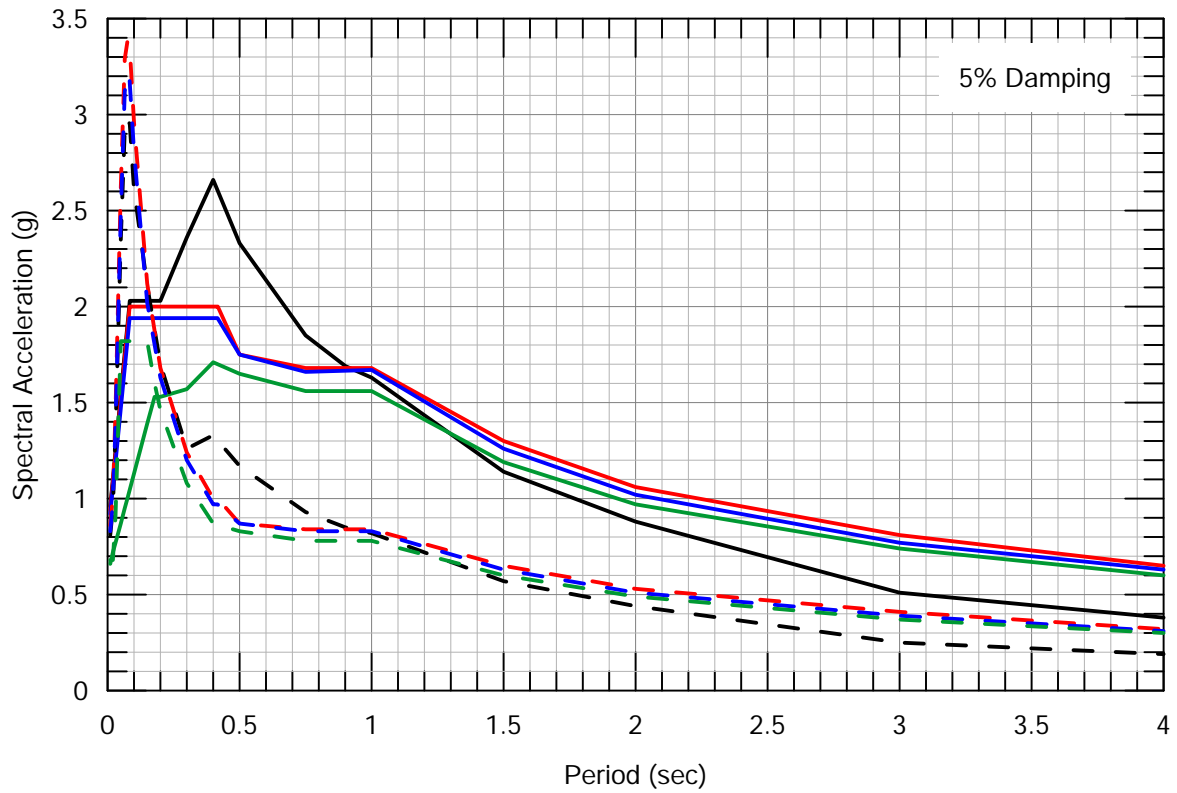
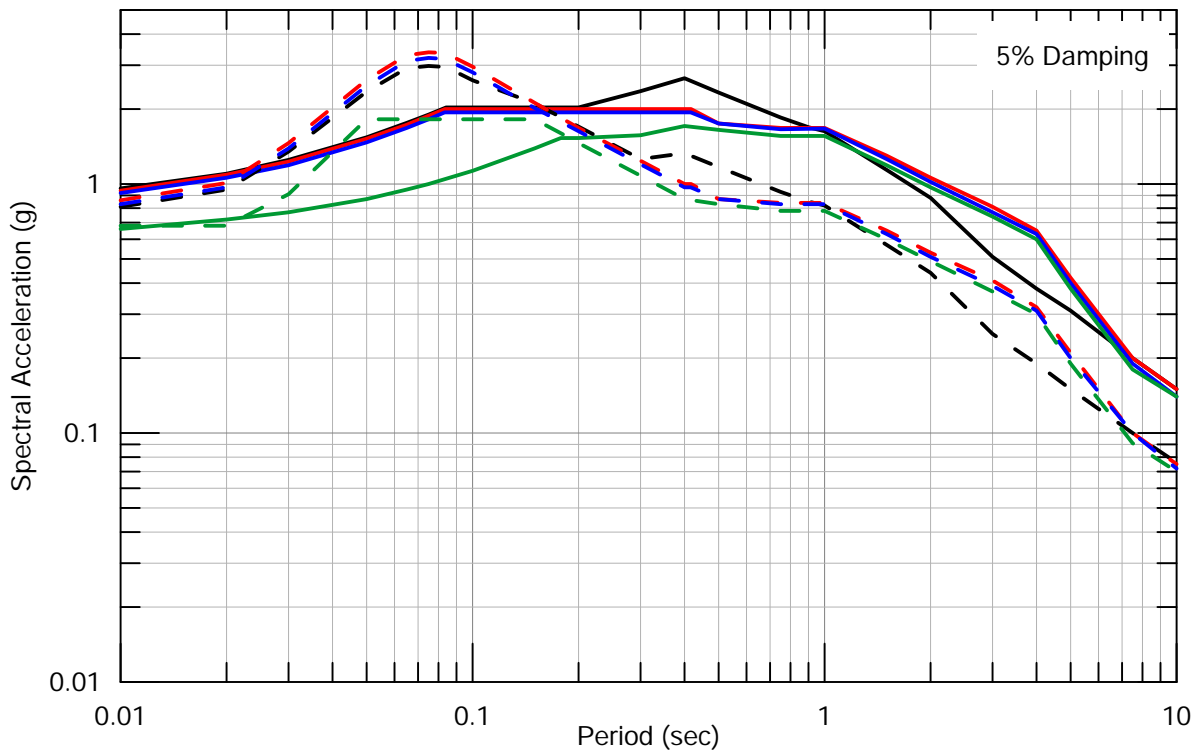
Calculation of Site-Specific Vertical MCE_R for Zone 0

STANFORD UNIVERSITY



Lettis Consultants International, Inc.

Figure 34



MCE_R Spectra

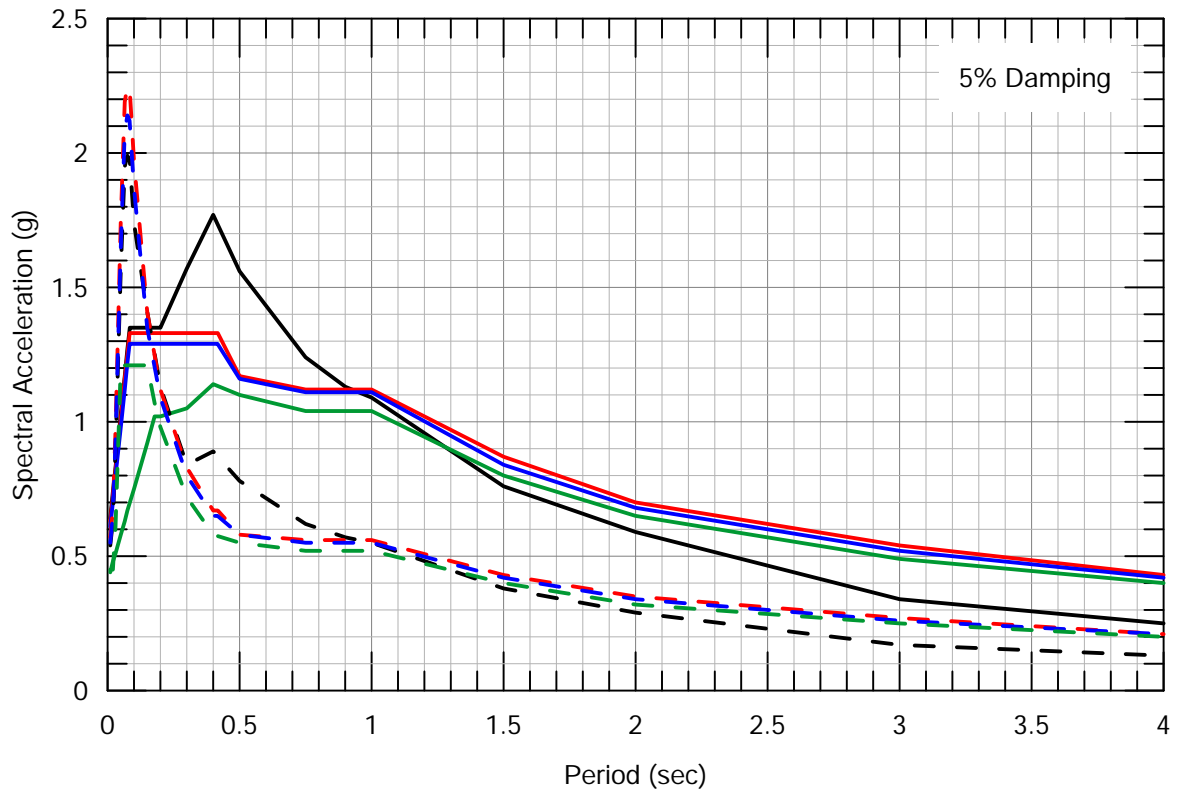
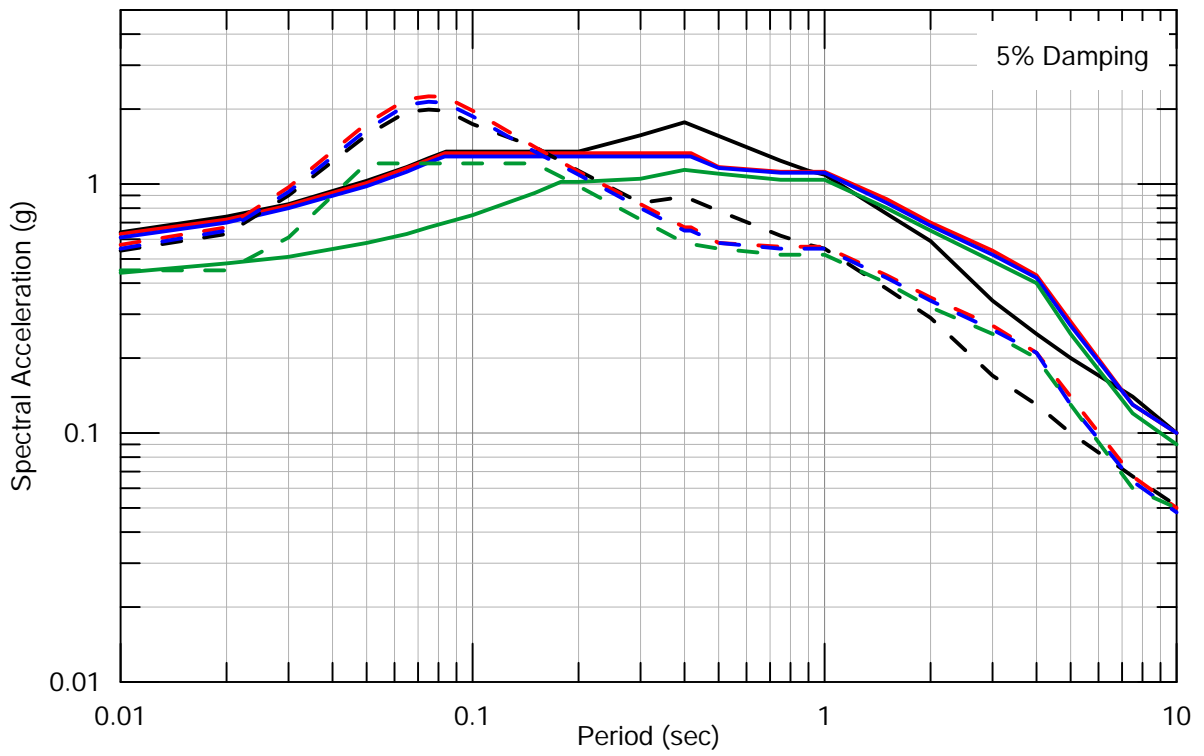
- | | |
|-----------------------|-----------------------|
| — Zone 0 - Horizontal | - - Zone 0 - Vertical |
| — Zone 1 - Horizontal | - - Zone 1 - Vertical |
| — Zone 2 - Horizontal | - - Zone 2 - Vertical |
| — Zone 3 - Horizontal | - - Zone 3 - Vertical |

Site-Specific Horizontal and Vertical MCE_R Response Spectra for Zones 0, 1, 2 and 3

STANFORD UNIVERSITY



Lettis Consultants International, Inc.



DE Spectra

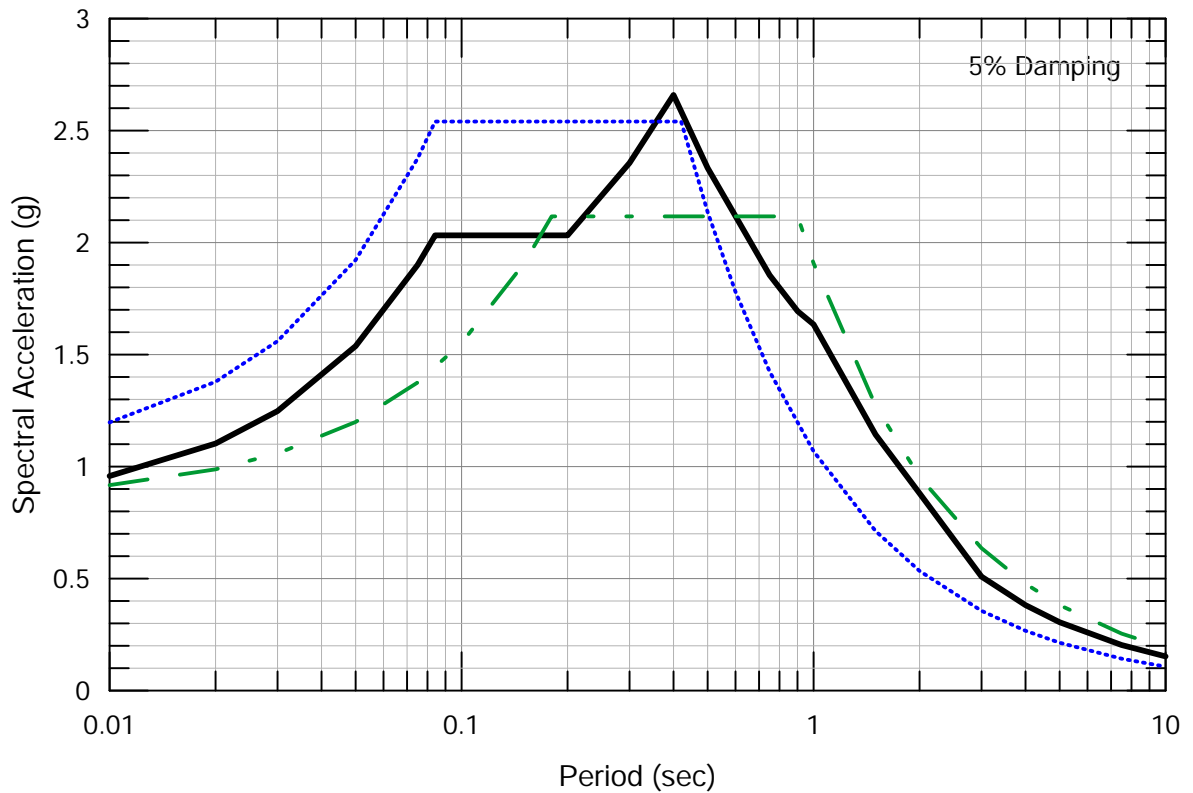
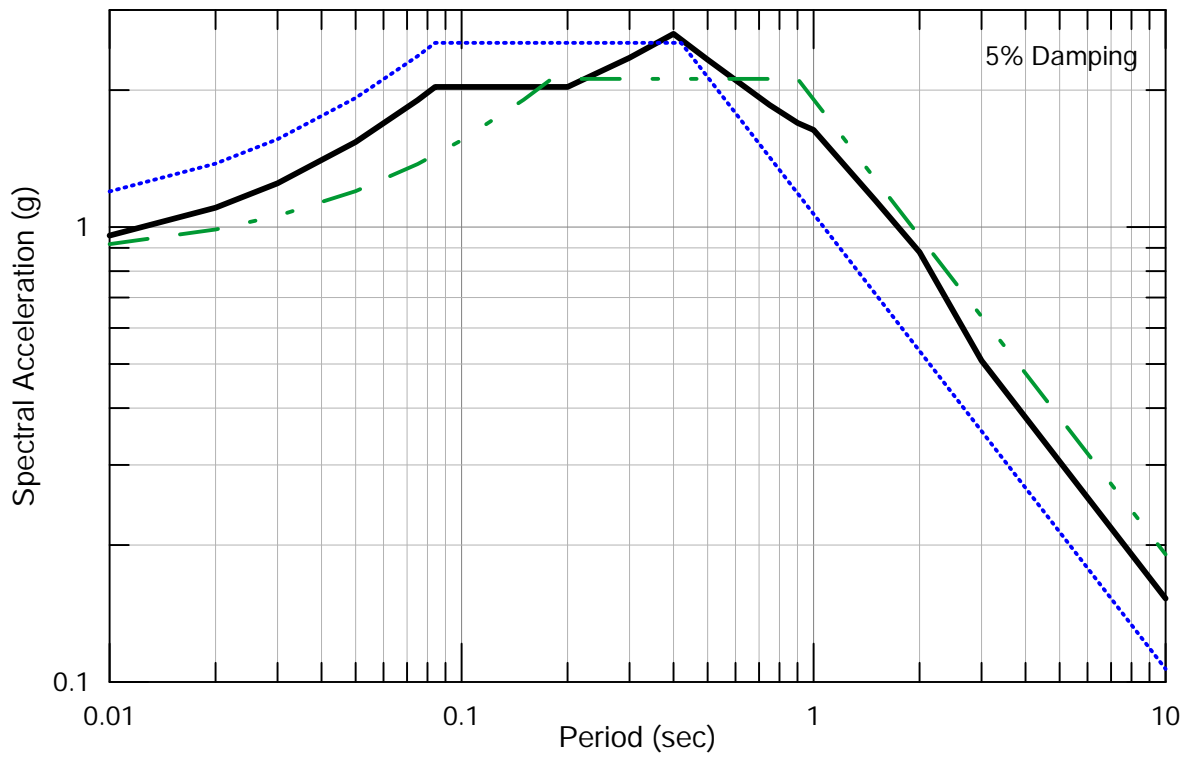
— Zone 0 - Horizontal	- - Zone 0 - Vertical
— Zone 1 - Horizontal	- - Zone 1 - Vertical
— Zone 2 - Horizontal	- - Zone 2 - Vertical
— Zone 3 - Horizontal	- - Zone 3 - Vertical

Site-Specific Horizontal and Vertical DE Response Spectra for Zones 0, 1, 2 and 3

STANFORD UNIVERSITY



Lettis Consultants International, Inc.



Zone 0 MCE_R Spectra

- Site-Specific
- ⋯ ASCE 7-16 Site Class C
- - ASCE 7-16 Site Class D

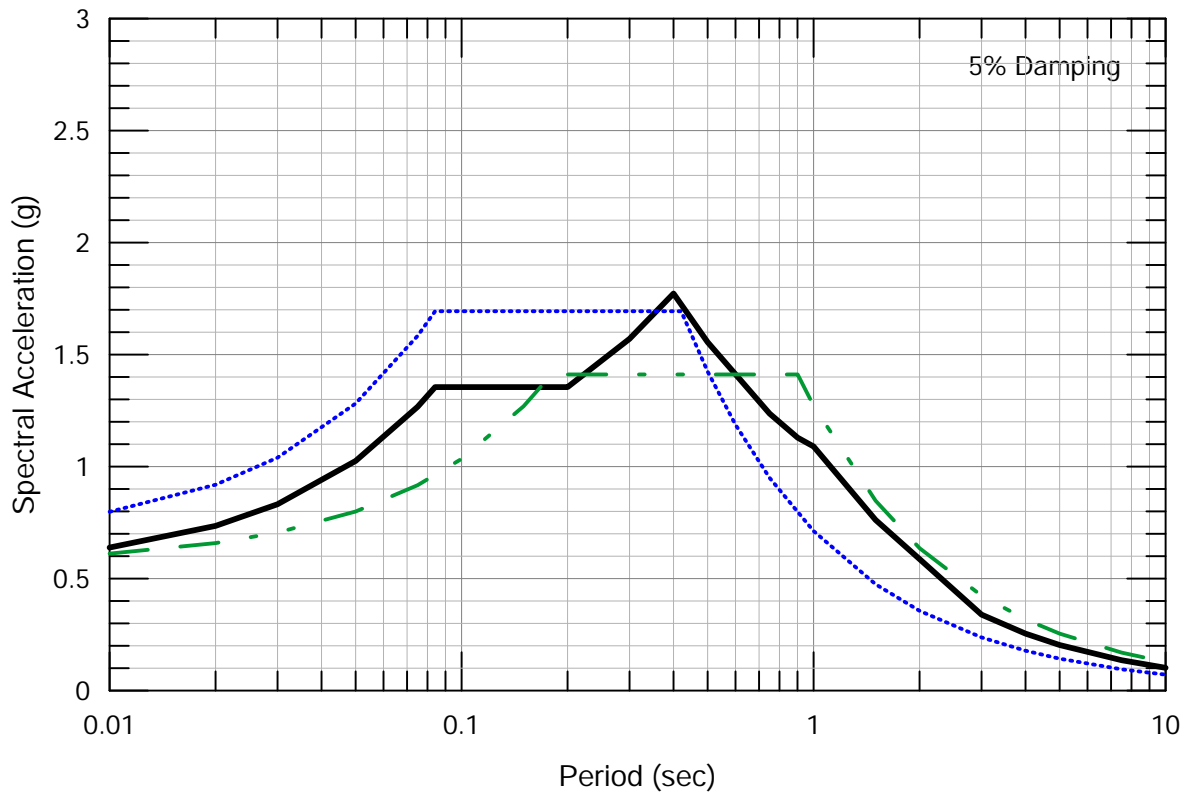
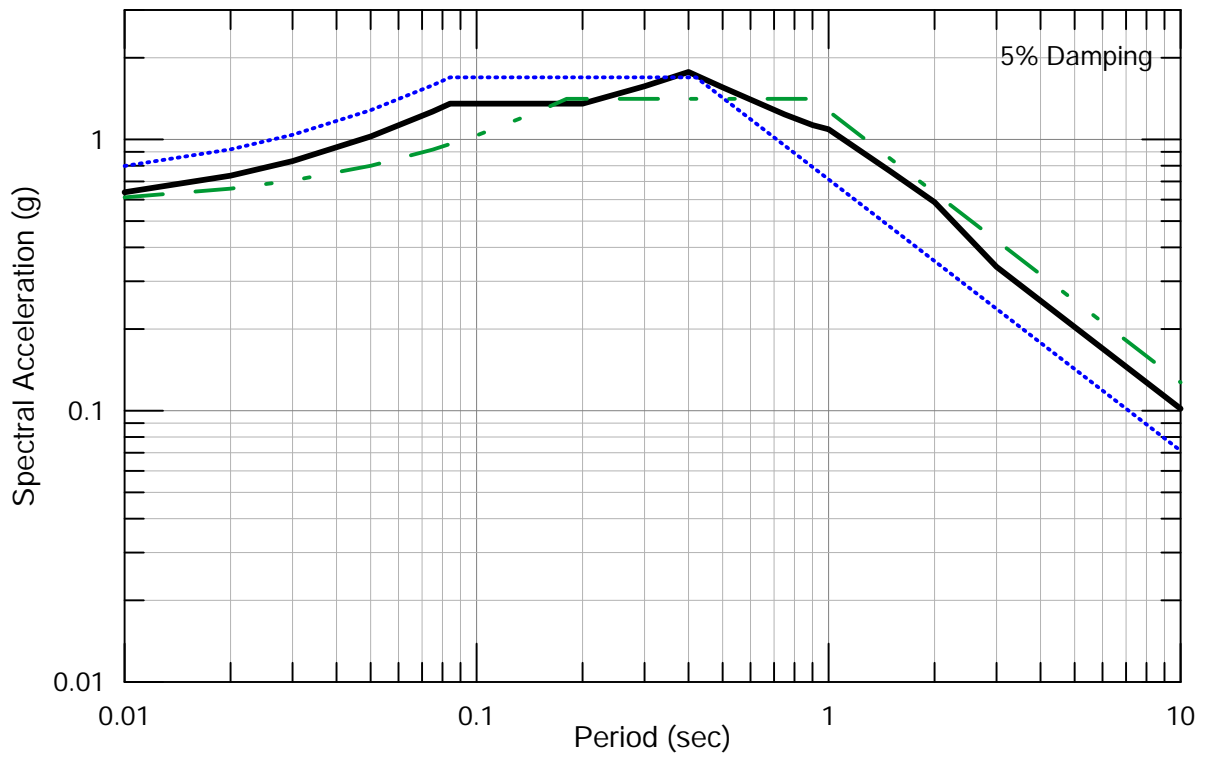
**Comparison of Site-Specific Horizontal MCE_R
for Zone 0 with ASCE 7-16 MCE_R
for Site Classes C and D**

STANFORD UNIVERSITY



Lettis Consultants International, Inc.

Figure 37



Zone 0 DE Spectra

- Site-Specific
- ⋯ ASCE 7-16 Site Class C
- - ASCE 7-16 Site Class D

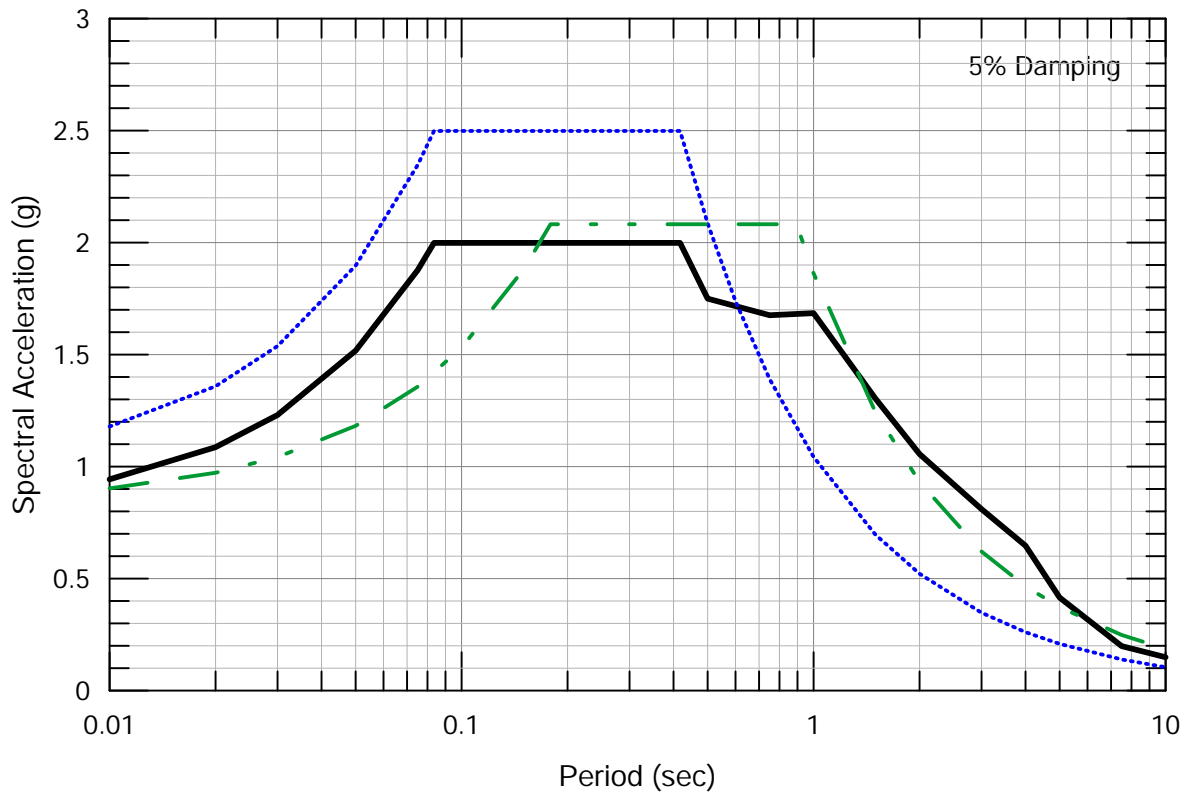
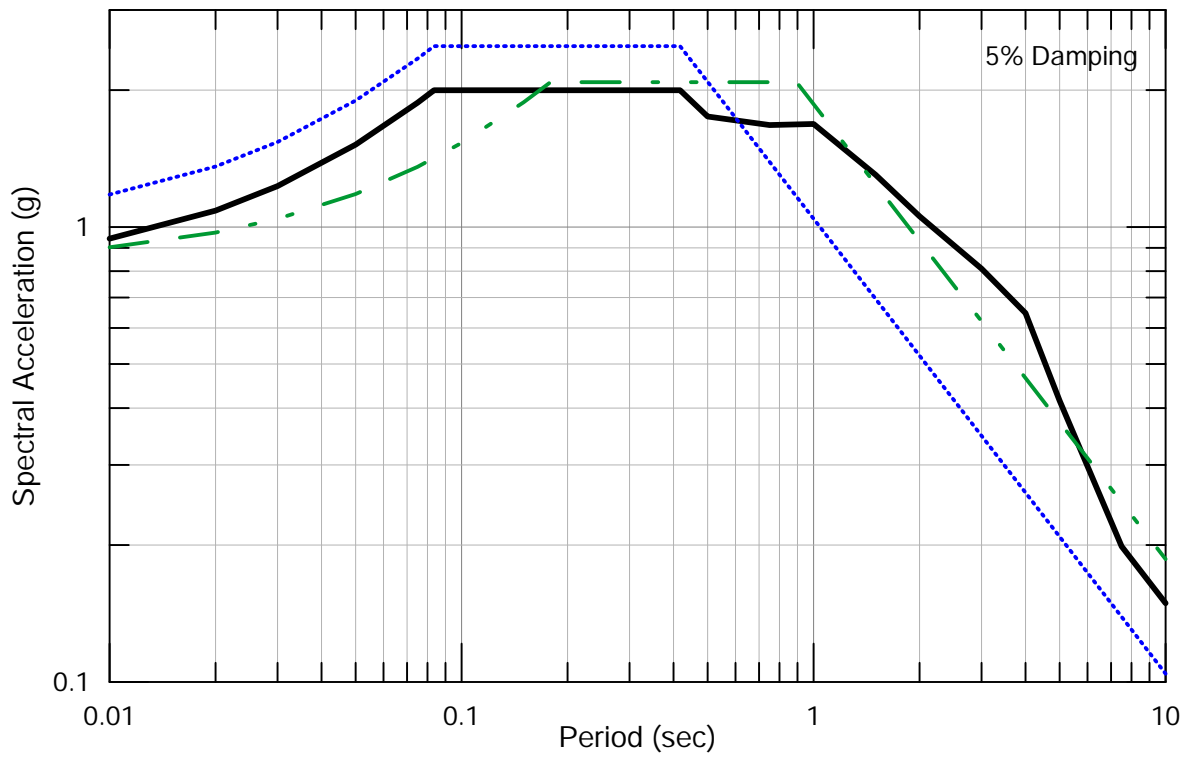
**Comparison of Site-Specific DE Spectrum
for Zone 0 with ASCE 7-16 DE
for Site Classes C and D**

STANFORD UNIVERSITY



Lettis Consultants International, Inc.

Figure 38



Zone 1 MCE_R Spectra

- Site-Specific
- ⋯ ASCE 7-16 Site Class C
- - - ASCE 7-16 Site Class D

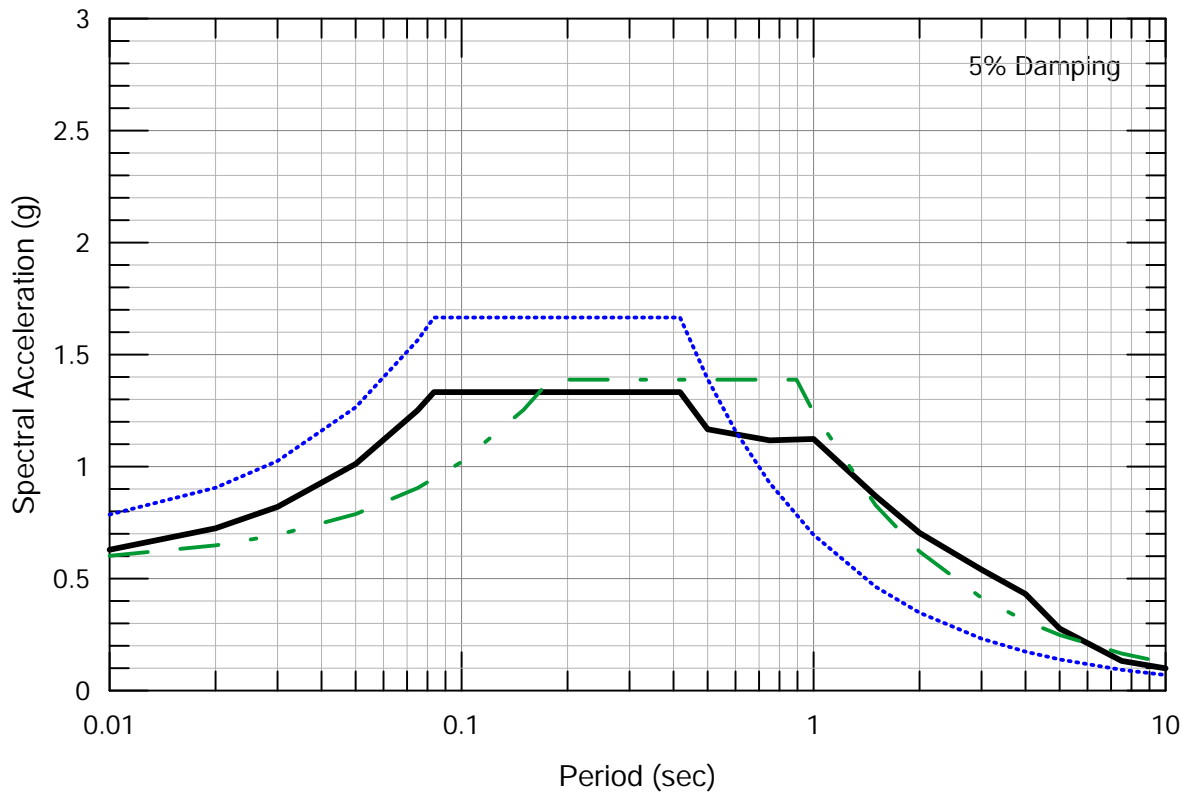
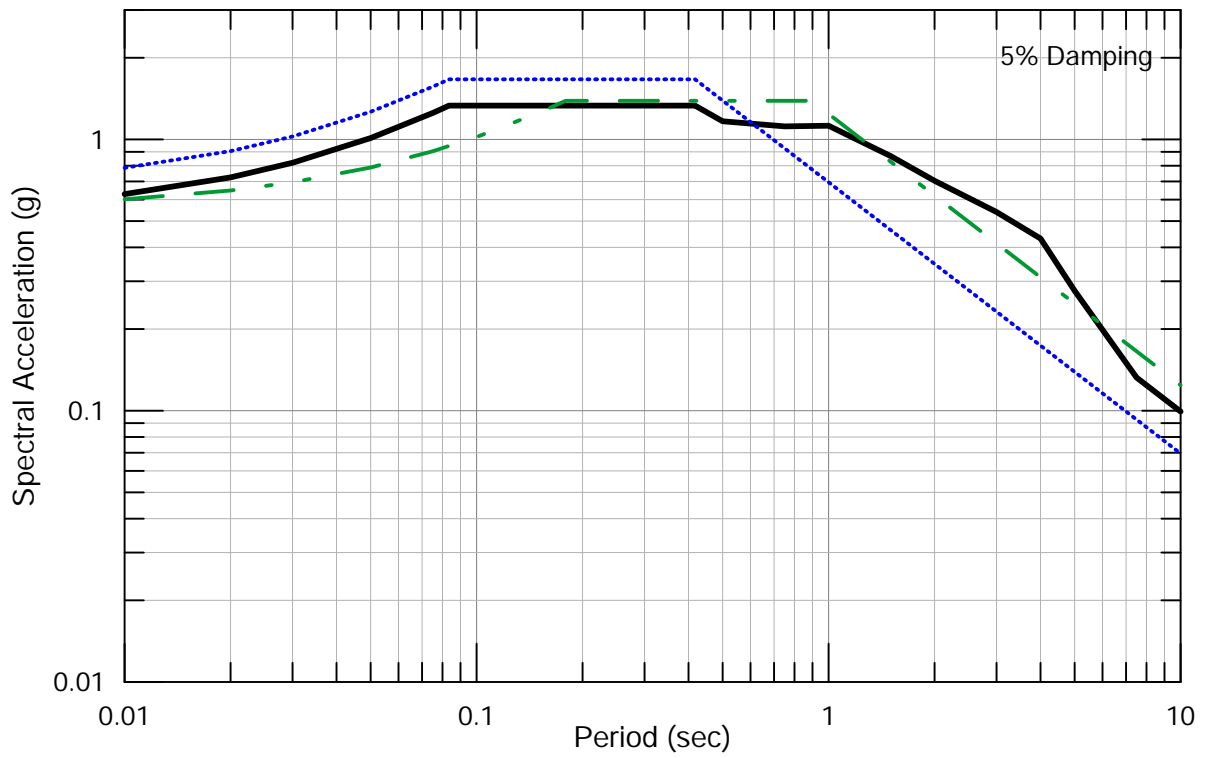
**Comparison of Site-Specific Horizontal MCE_R
for Zone 1 with ASCE 7-16 MCE_R
for Site Classes C and D**

STANFORD UNIVERSITY



Lettis Consultants International, Inc.

Figure 39



Zone 1 DE Spectra

- Site-Specific
- ⋯ ASCE 7-16 Site Class C
- - ASCE 7-16 Site Class D

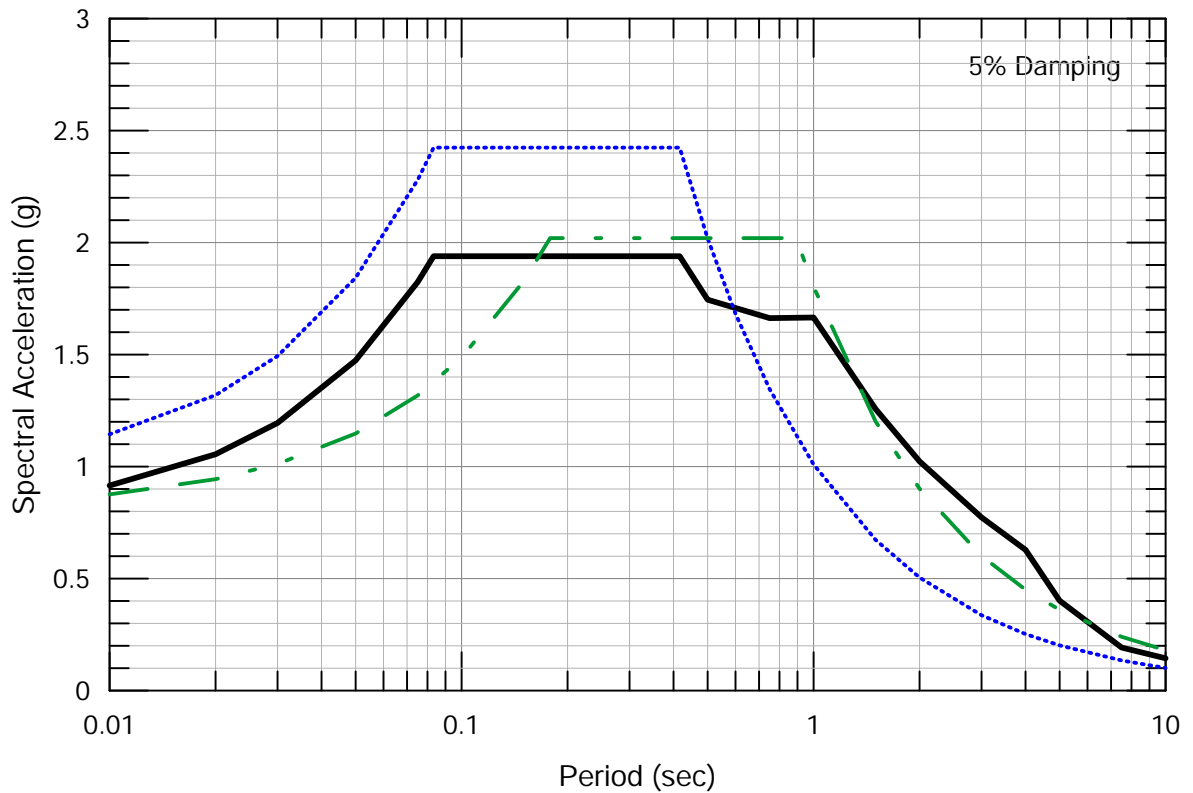
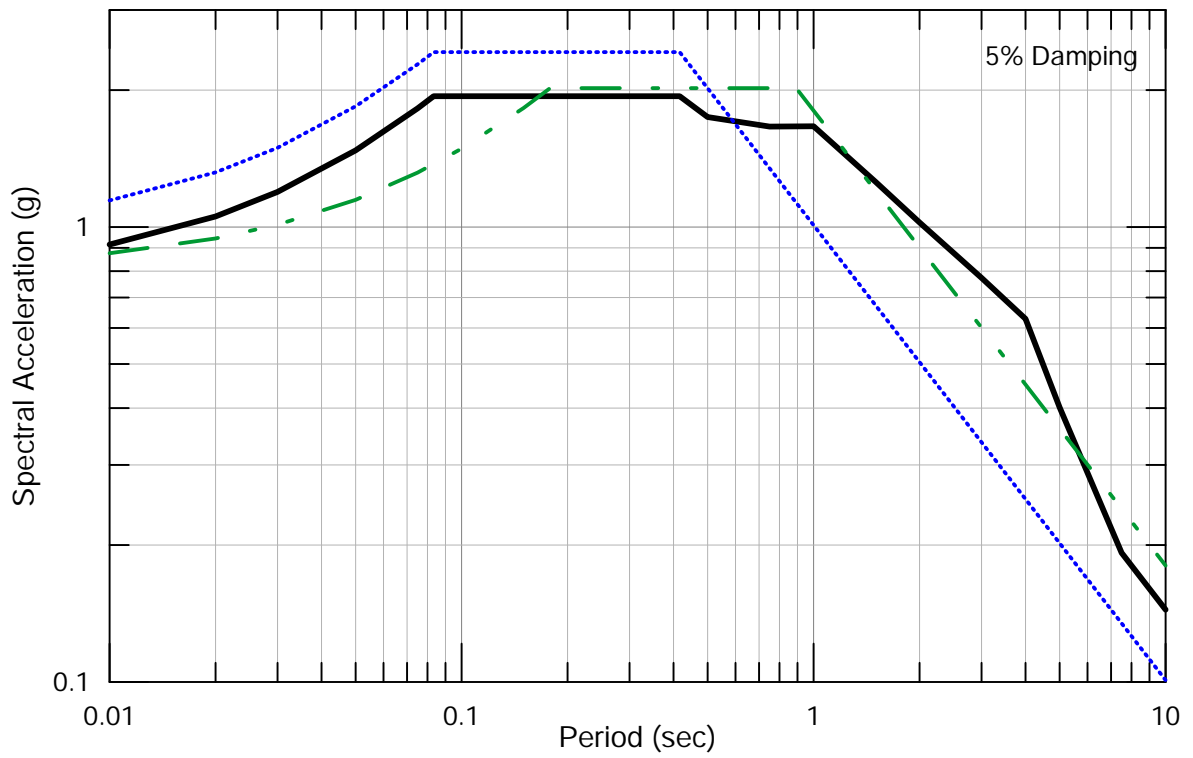
**Comparison of Site-Specific DE Spectrum
for Zone 1 with ASCE 7-16 DE
for Site Classes C and D**

STANFORD UNIVERSITY



Lettis Consultants International, Inc.

Figure 40



Zone 2 MCE_R Spectra

- Site-Specific
- ⋯ ASCE 7-16 Site Class C
- - ASCE 7-16 Site Class D

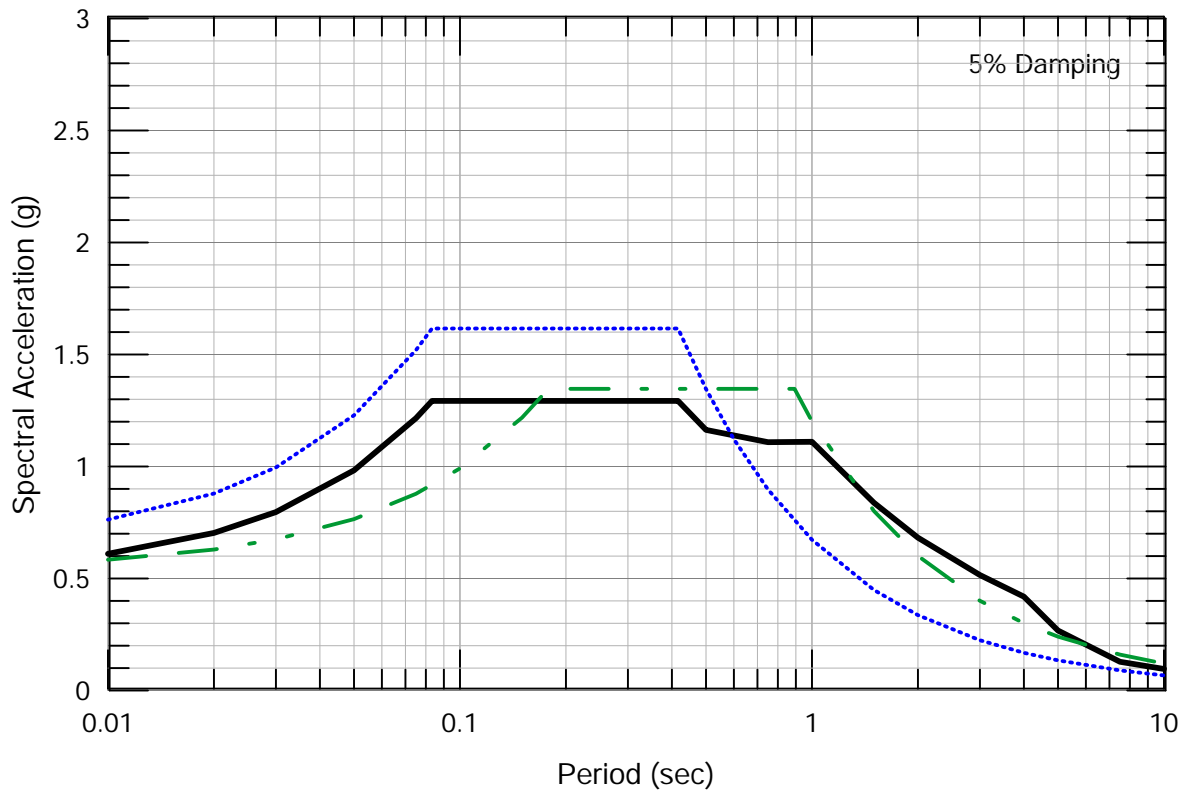
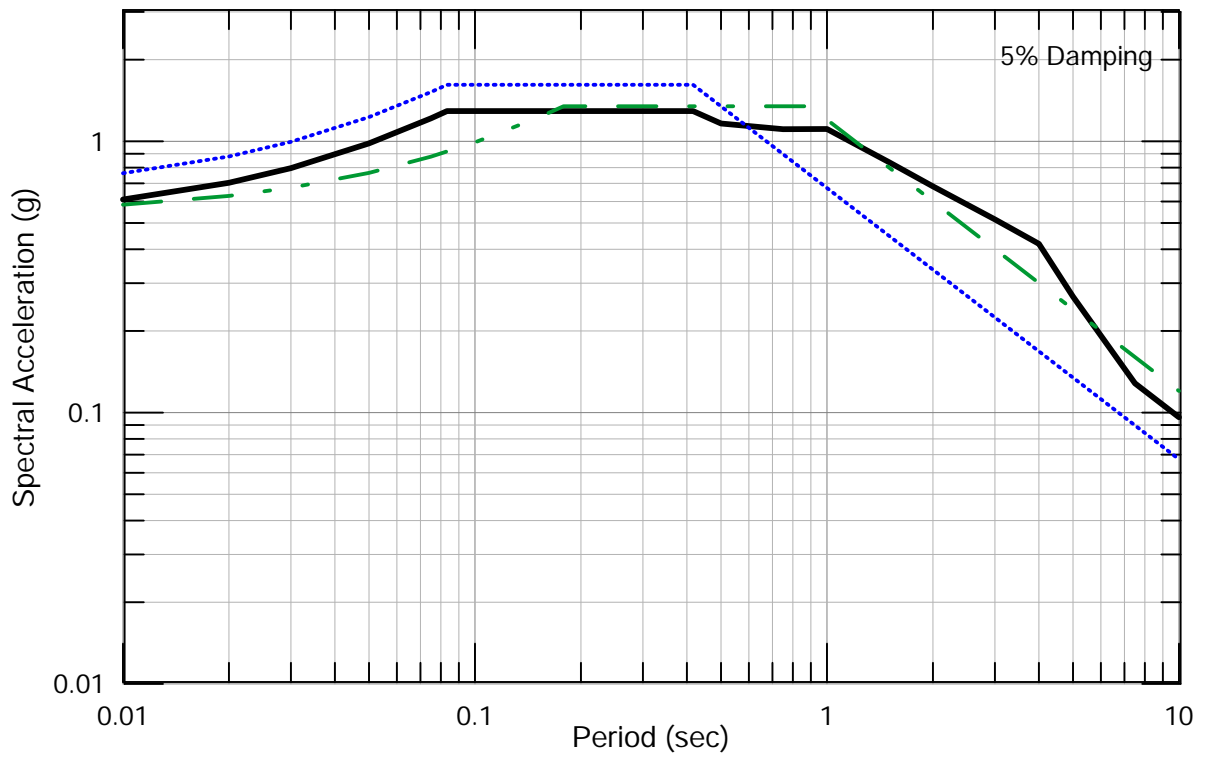
**Comparison of Site-Specific MCE_R Spectrum
for Zone 2 with ASCE 7-16 MCE_R
for Site Classes C and D**

STANFORD UNIVERSITY



Lettis Consultants International, Inc.

Figure 41



Zone 2 DE Spectra

- Sie-Specific
- ⋯ ASCE 7-16 Site Class C
- - - ASCE 7-16 Site Class D

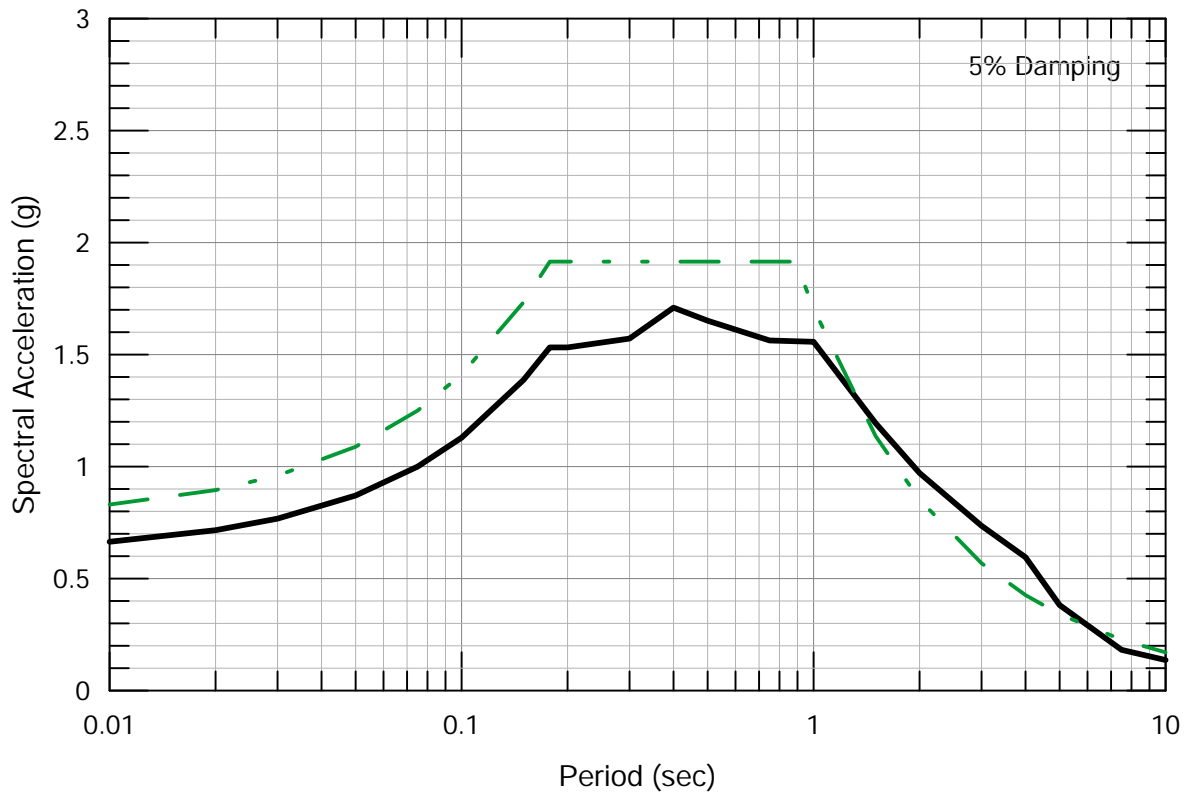
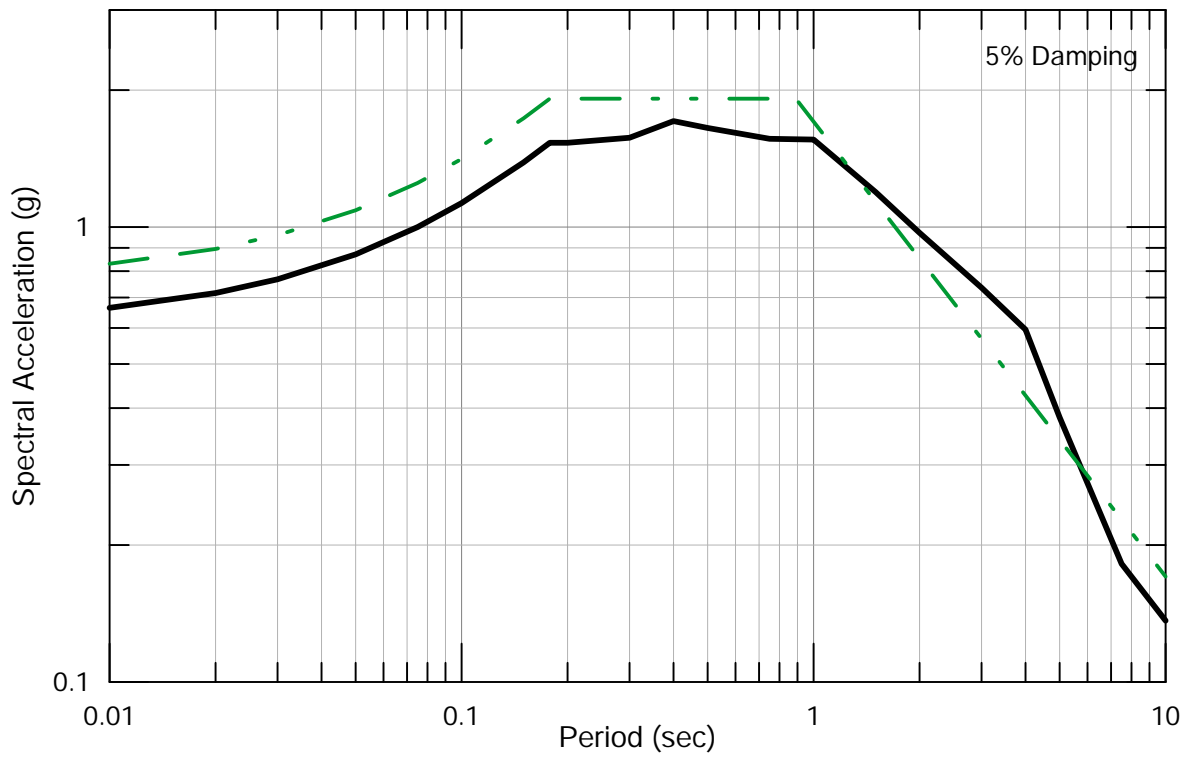
**Comparison of Site-Specific DE Spectrum
for Zone 2 with ASCE 7-16 DE
for Site Classes C and D**

STANFORD UNIVERSITY



Lettis Consultants International, Inc.

Figure 42



Zone 3 MCE_R Spectra

- Site-Specific
- - ASCE 7-16 Site Class D

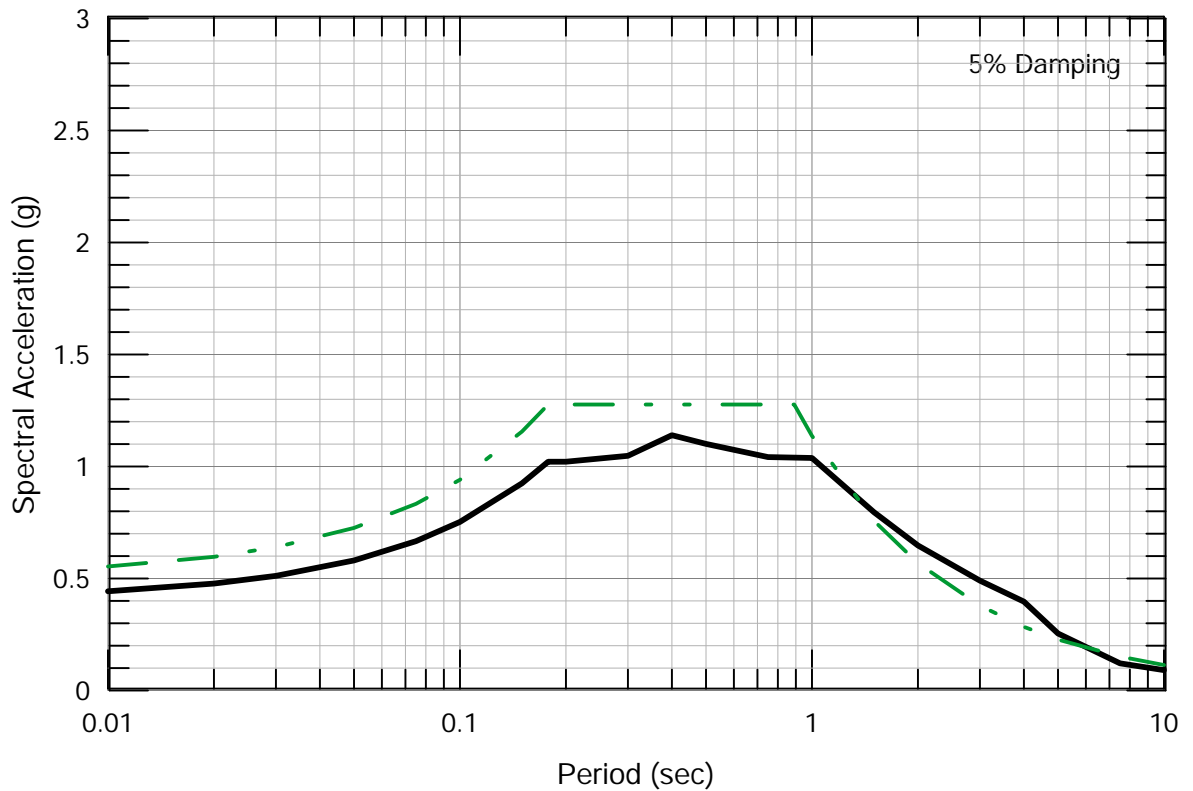
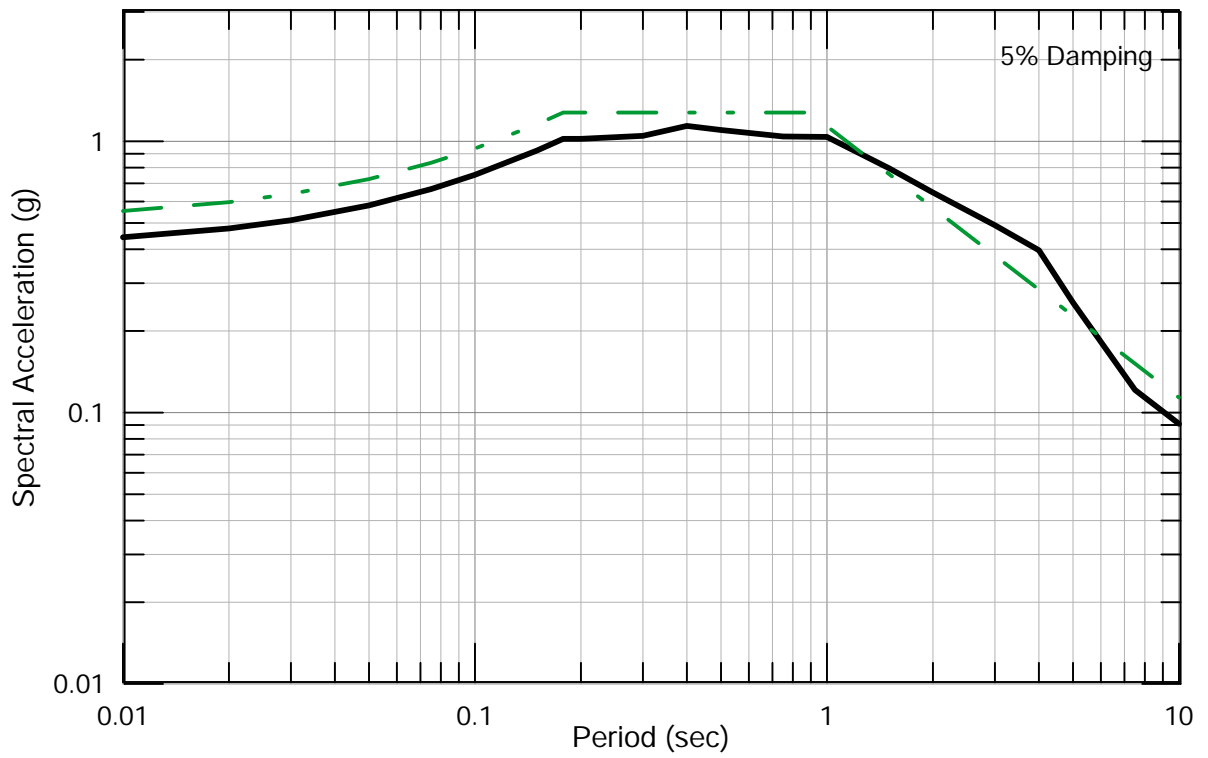
**Comparison of Site-Specific MCE_R Spectrum
for Zone 3 with ASCE 7-16 MCE_R
for Site Class D**

STANFORD UNIVERSITY



Lettis Consultants International, Inc.

Figure 43



Zone 3 DE Spectra

- Site-Specific
- - ASCE 7-16 Site Class D

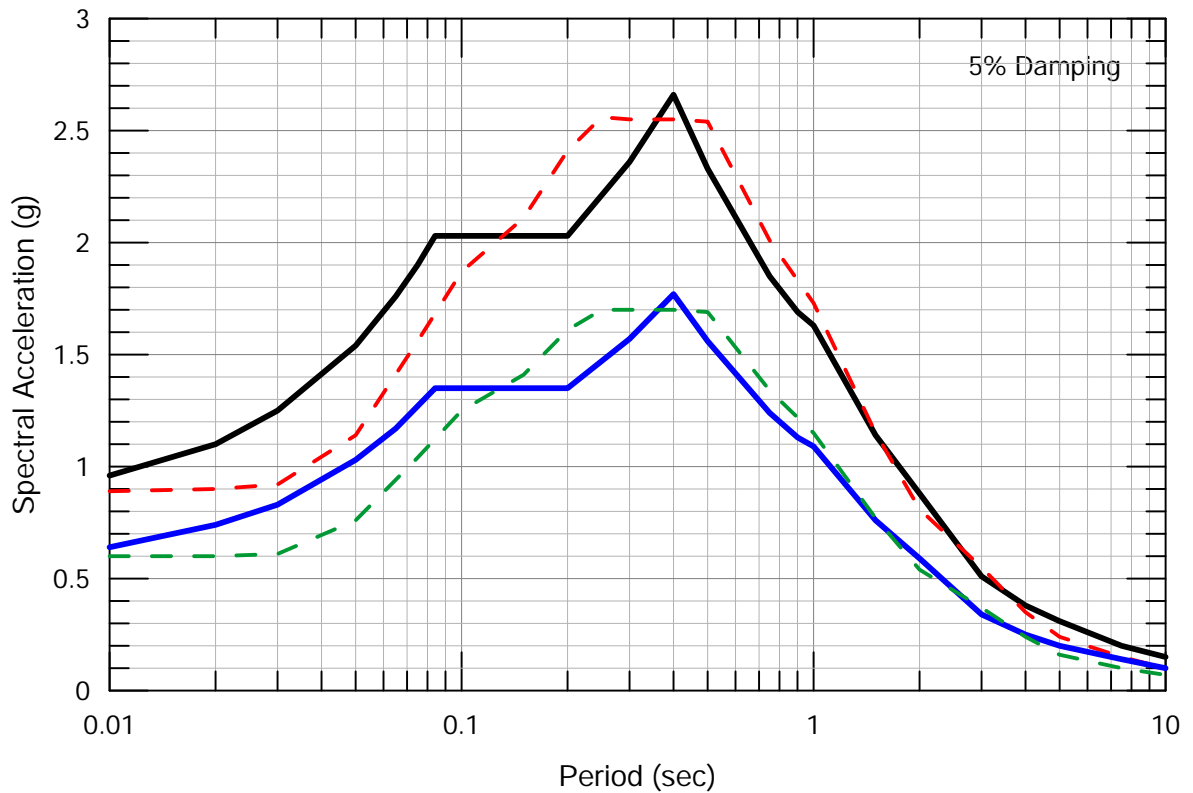
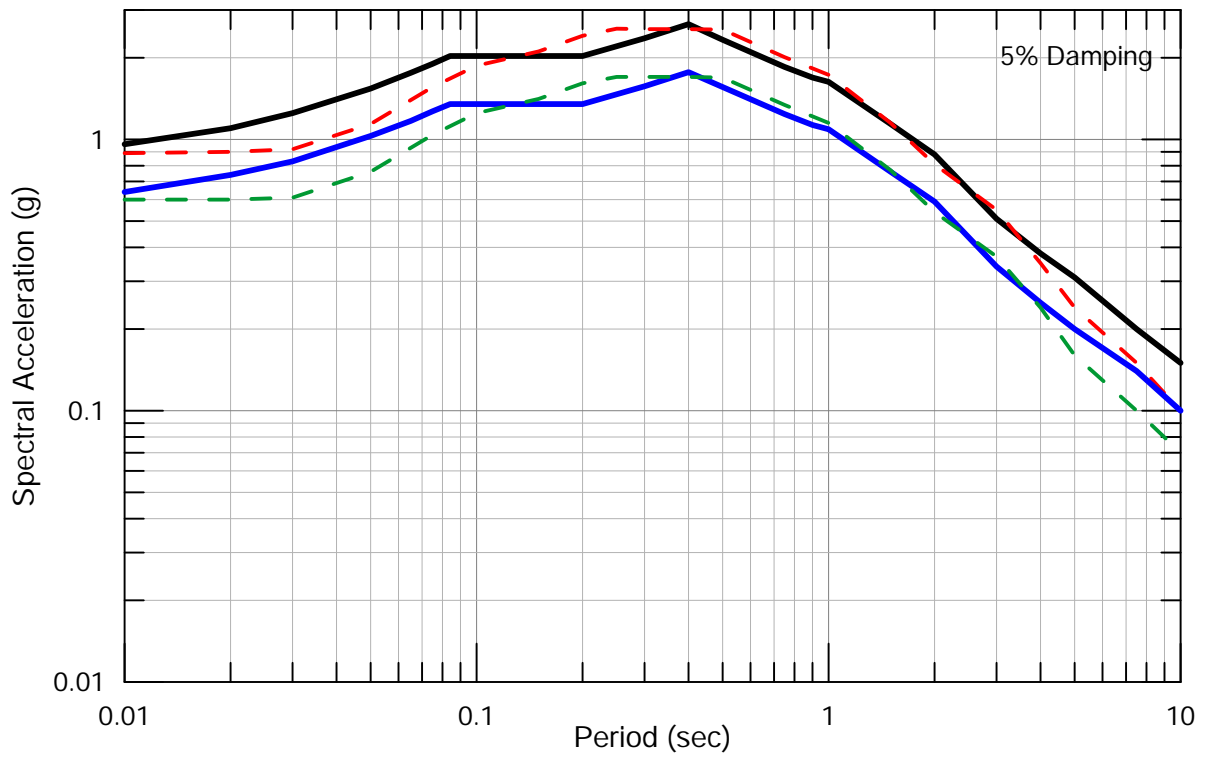
**Comparison of Site-Specific DE Spectrum
for Zone 3 with ASCE 7-16 DE
for Site Class D**

STANFORD UNIVERSITY



Lettis Consultants International, Inc.

Figure 44



Zone 0 Site-Specific Design Spectra

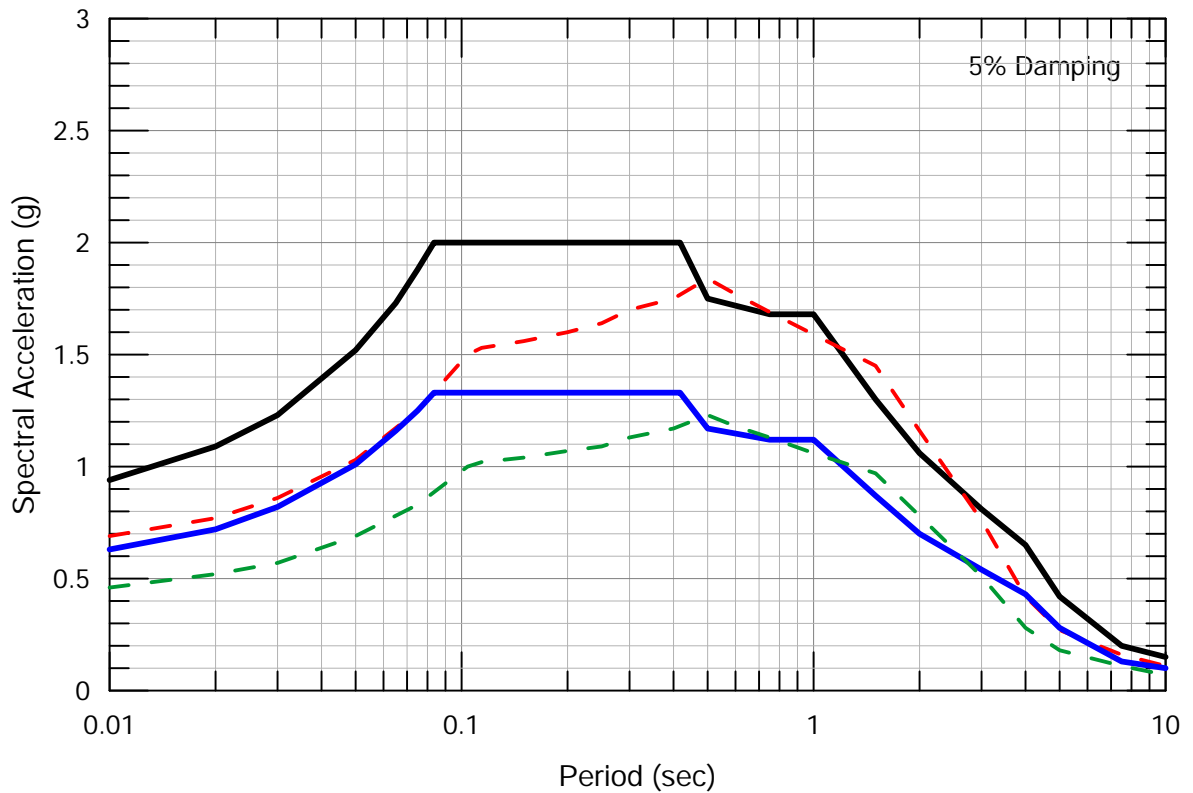
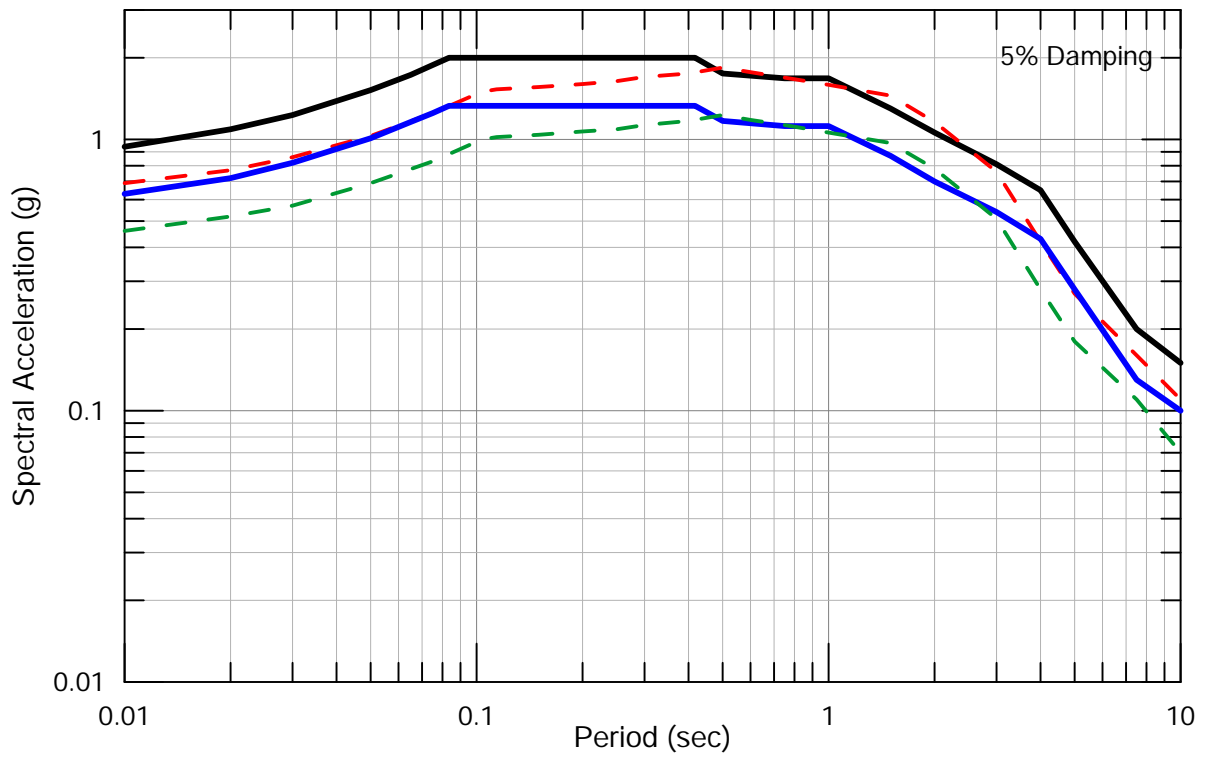
- MCE_R
- DE
- - - 2013 MCE_R
- - - 2013 DE

Comparison of Site-Specific Horizontal MCE_R and DE Spectra for Zone 0 with 2013 Site-Specific MCE_R and DE Spectra

STANFORD UNIVERSITY



Lettis Consultants International, Inc.



Zone 1 Site-Specific Design Spectra

- MCE_R
- DE
- - - 2013 MCE_R
- - - 2013 DE

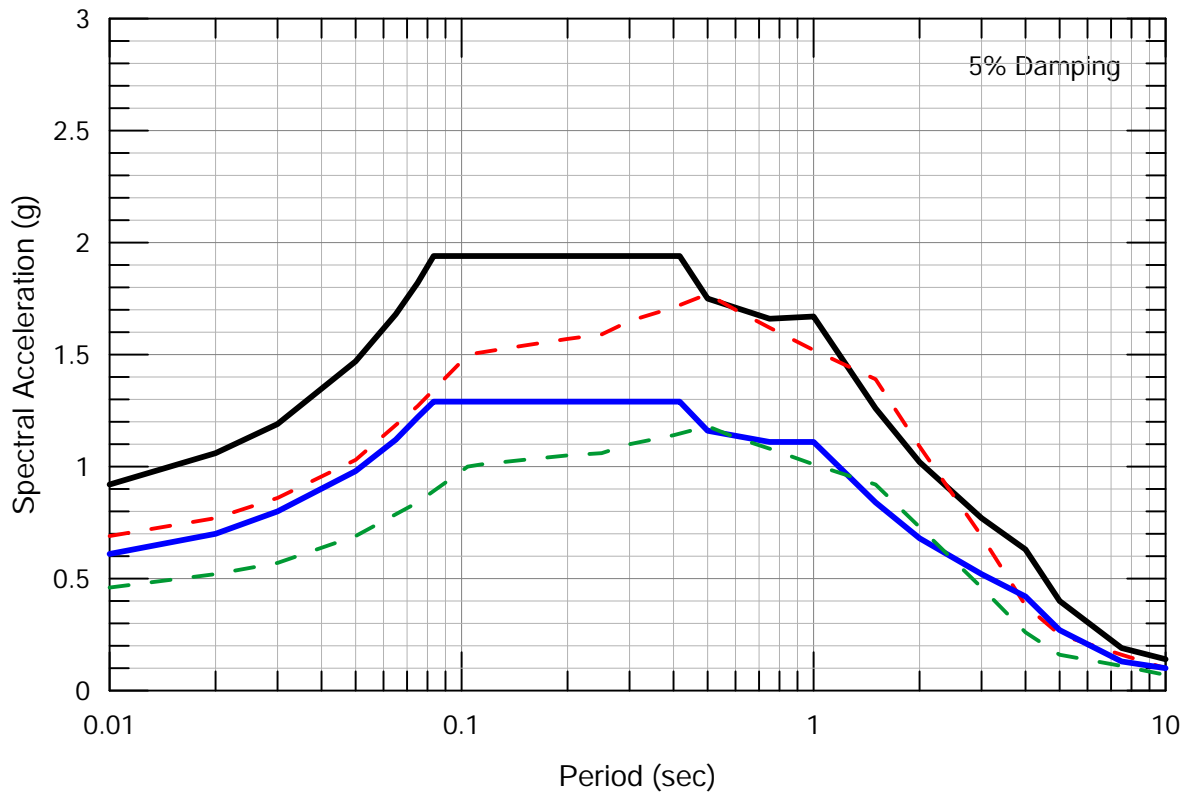
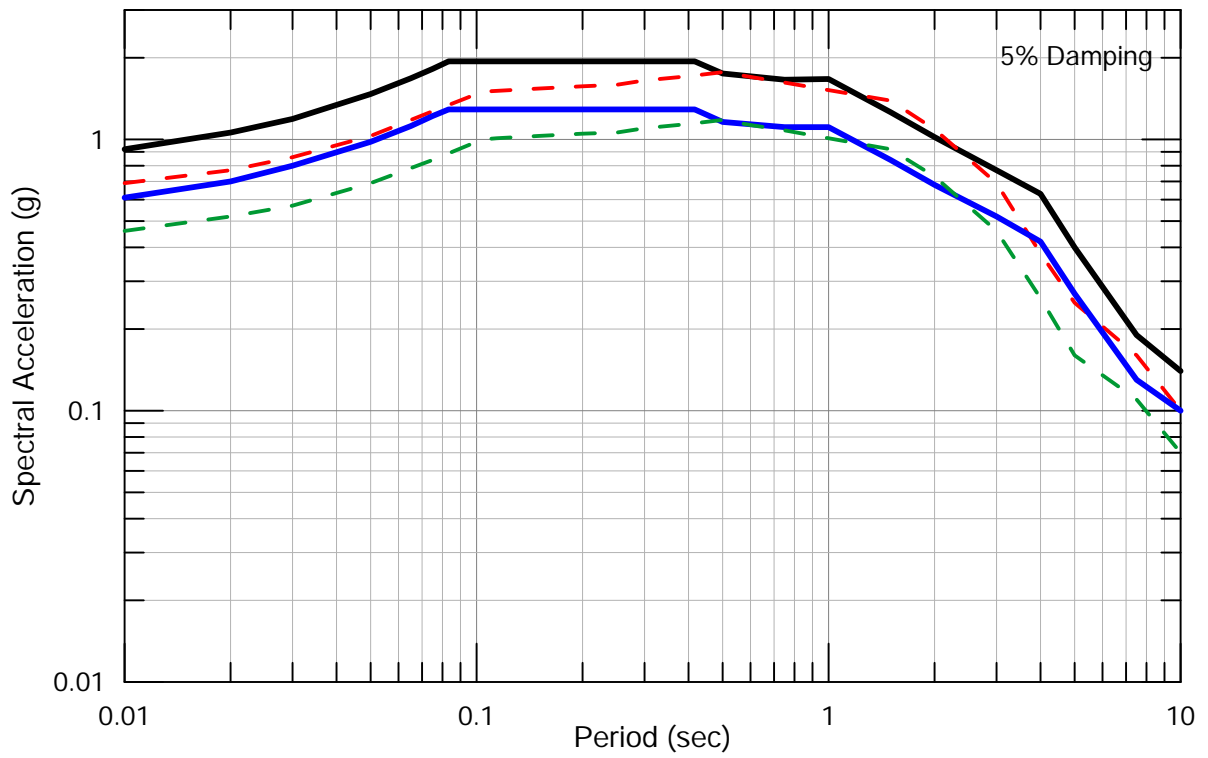
Comparison of Site-Specific Horizontal MCE_R and DE Spectra for Zone 1 with 2013 Site-Specific MCE_R and DE Spectra

STANFORD UNIVERSITY



Lettis Consultants International, Inc.

Figure 46



Zone 2 Site-Specific Design Spectra

- MCE_R
- DE
- - - 2013 MCE_R
- - - 2013 DE

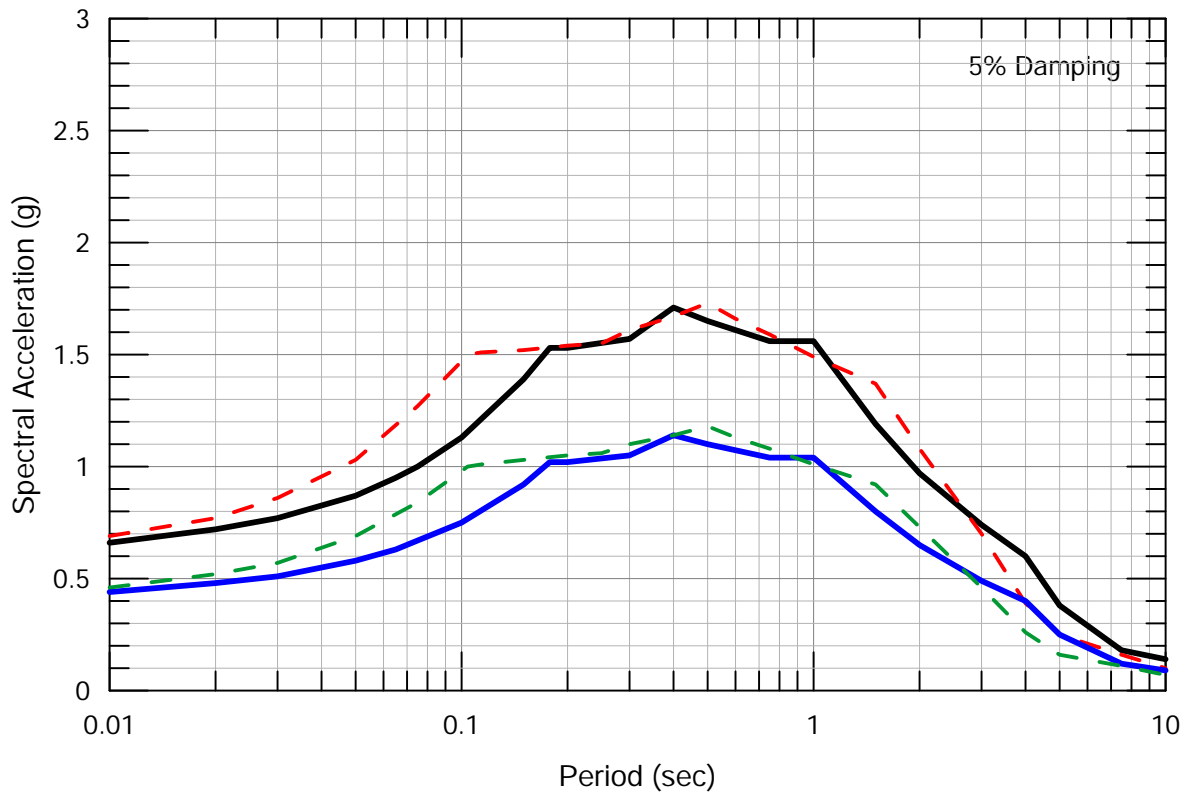
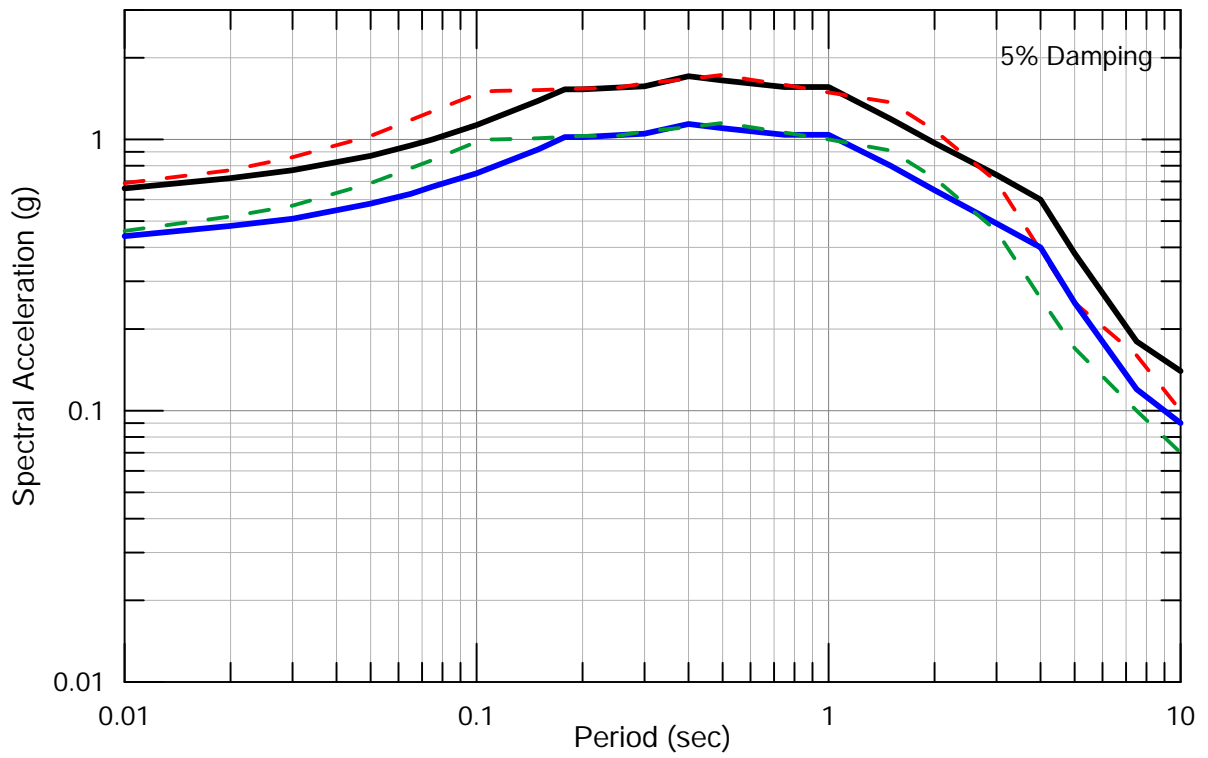
**Comparison of Site-Specific Horizontal
MCE_R and DE Spectra for Zone 2 with
2013 Site-Specific MCE_R and DE Spectra**

STANFORD UNIVERSITY



Lettis Consultants International, Inc.

Figure 47



Zone 3 Site-Specific Design Spectra

- MCE_R
- DE
- - - 2013 MCE_R
- - - 2013 DE

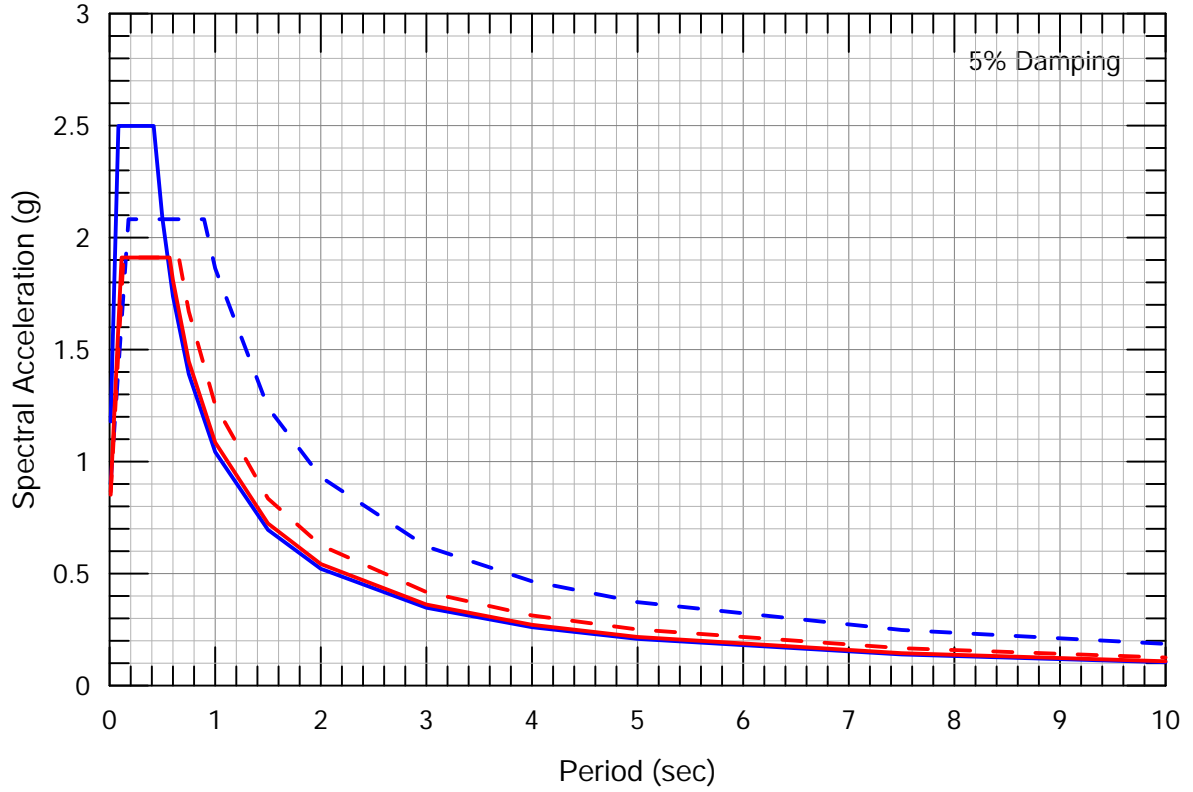
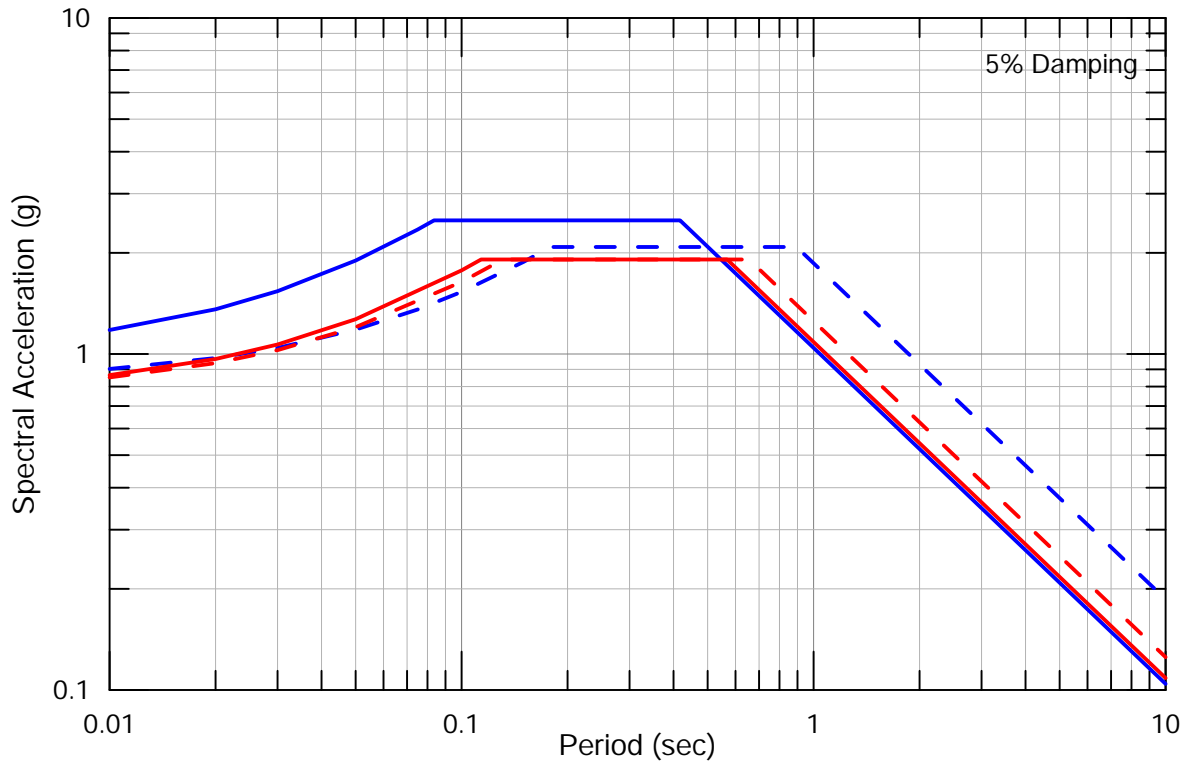
**Comparison of Site-Specific Horizontal
MCE_R and DE Spectra for Zone 3 with
2013 Site-Specific MCE_R and DE Spectra**

STANFORD UNIVERSITY



Lettis Consultants International, Inc.

Figure 48



- ASCE 7-16 Site Class C
- ASCE 7-10 Site Class C
- - ASCE 7-16 Site Class D
- - ASCE 7-10 Site Class D

**Comparison of MCE_R Spectra
for Site Classes C and D for Zone 1
using ASCE 7-10 and ASCE 7-16**

STANFORD UNIVERSITY

Lettis Consultants International, Inc.

Figure 49